



1200 Discovery Drive, Suite 500  
Bakersfield, CA 93309

---

March 10, 2025

Special Projects Section  
County of Los Angeles Department of Regional Planning  
320 West Temple Street  
Los Angeles, CA 90012  
Attn: Christina Nguyen

RE: CSD Section 22.310, 050.D.5  
Accumulated Ground Movement Study – Year 2024  
Baldwin Hills Community Standards District (CSD)

Dear Christina,

Submitted electronically for your review is one set of three reports pursuant to CSD Section 22.310, 050.D.5. The reports cover the 12-month time interval from July 2023 through June 2024. The CSD requires that the Accumulated Ground Movement Study (AGMS) be conducted by the following experts:

- A California-licensed surveyor. For this year, Viridien Group handled these responsibilities (name changed from CGG to Viridien). Viridien utilized InSAR (Interferometric Synthetic Aperture Radar) data to quantify surface deformation for analysis by the other experts.
- A Certified Engineering Geologist. For this year, Langan again handled these responsibilities.
- A Registered Geotechnical Engineer. For this year, Langan again handled these responsibilities.
- A California-registered Professional Petroleum Engineer. For this year, Evans and Walker took over these responsibilities for the retired engineer from 2H.

This submittal contains the following reports:

***Baldwin Hills and LA Basin, InSAR Monitoring, Viridien Group***

InSAR data was acquired by Viridien to quantify surface deformation measurements for the Inglewood Field and for the wider Los Angeles Basin from July 2023 to June 2024. InSAR has been approved for use by LA County Public Works in lieu of land survey data for 2024 and 2026. Per the approval, land survey data will be used in 2025 and 2027 by a California-licensed surveyor, and the data gathering process will be reevaluated again in 2027.

***Baldwin Hills CSD Inglewood Oil Field, Surface Monitoring Program, Evaluation of 2023-24 Survey and Production Data, Evans & Walker***

This report summarizes analysis of InSAR data and oilfield activities such as liquid production/injection and pressure data as they pertain to changes in horizontal and vertical positioning for the production period.

***Geotechnical and Engineering Geology Evaluation, Baldwin Hills Community Standards District, 2024 Annual Ground Movement Survey, Inglewood Oil Field 2023 Production Year, Langan***

This report summarizes the interpretation of vertical and horizontal surface movements that occurred during the production period.

Evaluation of property damage claims is also a CSD requirement. Evaluations are due immediately after the results of the AGMS are available. For the past production period, no property damage claims were received.

Should you have any questions or comments regarding these reports, please contact me at [dbudy@sentinelpeakresources.com](mailto:dbudy@sentinelpeakresources.com) or (661) 395-5471.

Respectfully,

A handwritten signature in blue ink, appearing to read 'David Budy', with a large, sweeping loop at the end.

David Budy  
EH&S Manager  
Sentinel Peak Resources California LLC

cc      Greg Johnson, LAC DPW  
         Steven Jareb, LAC Planning  
         Miriam Thompson, LAC Planning  
         Luis Perez, MRS  
         Dean Dusette, MRS



**EVANS & WALKER**

Consulting Petroleum Engineers

---



**Sentinel Peak Resources**

**Baldwin Hills Community Standards District**

**Inglewood Oil Field**

Surface Monitoring Program

Evaluation of 2023-24 Survey and Production Data

January 29, 2025

Thomas Walker

California PE (Petroleum) 1686

## Contents

<b>1</b>	<b>Executive Summary .....</b>	<b>2</b>
<b>2</b>	<b>Introduction .....</b>	<b>4</b>
<b>3</b>	<b>Monuments .....</b>	<b>5</b>
<b>4</b>	<b>InSAR Results.....</b>	<b>6</b>
<b>5</b>	<b>Oilfield Causes of Ground Movement .....</b>	<b>7</b>
<b>6</b>	<b>Ground Movement and Comparison to Previous Years .....</b>	<b>8</b>
<b>7</b>	<b>Ground Movement and Oilfield Operations.....</b>	<b>9</b>
<b>8</b>	<b>Summary and Recommendations.....</b>	<b>12</b>
<b>9</b>	<b>References.....</b>	<b>13</b>



# 1 Executive Summary

This report summarizes Evans & Walker's (formerly InterAct PMTI / 2H Offshore California) analysis of satellite data and oilfield activities such as liquid injection/production, individual oil producing zones, and pressure data as it pertains to vertical and horizontal elevation change in and around the Baldwin Hills Community Standards District (BHCSO) measured during the production period from June 2023 through July 2024. The satellite data analysis used in this report was sourced directly from Viridien, while the production data and fluid level data used to calculate reservoir pressure was provided by Sentinel Peak Resources (SPR) the operator of the Inglewood oil field (IOF).

Analysis of ground movement as it relates to the BHCSO began in Year 2010 with a baseline study (Accumulated Ground Movement Study, or AGMS). Each year since, oilfield operations in the IOF have been evaluated regarding ground movement data. The area of investigation extends approximately one mile in all directions from the field boundary and includes 57 active monuments as shown in Figure 1. The AGMS has transitioned from a field survey of these monuments to the satellite acquisition of ground movement over a 25-square-mile area centering the IOF.

We specifically analyzed the Interferometric Synthetic Aperture Radar surveys (InSAR; cumulative June 25, 2023 through July 1, 2024), the IOF production/injection data from the Vickers Rindge (V/R) oil sands (both cumulative since initial production from the IOF in 1924 through June 30, 2024 and annual from July 1, 2023 through June 30, 2024), and the reservoir pressure in the V/R oil sands, estimated from static fluid levels taken on June 25, 2024 by SPR. The V/R reservoir sands are the focus of the study because they comprise about 94% of field liquids production and are also highly porous with shallow burial depths.

We find that:

1. The transition from ground surveys to InSAR is a transition from an analysis of movement at individual points (somewhere in the BHCSO) to an analysis of the overall field (everywhere in the BHCSO). That said, data is still reported based on the existing 57 monuments, and there were no monument changes over the 12-month period.
2. The transition from ground surveys to InSAR replaces the need to account for local secondary effects with the need to account for atmospheric effects and potential inaccuracies in the modeled satellite orbits.
3. Ten monument locations as recorded by the InSAR moved more than 0.6 inches vertically, the threshold as specified in the BHCSO ordinance.
  - Monuments 128, 303, 50004, and 106 showed negative vertical movement (subsidence) of -0.8390", -0.7020", -0.6620", and -0.6120", respectively. Note that monument 303 is the twin of monument 5004.

- Monuments 50002, 307, 126, 50000, 308, and 50003 showed positive vertical movement (uplift) of +1.1390", +1.0230", +0.8220", +0.8180", +0.6540", and +0.6170", respectively. Note that monument 307 is the twin of monument 50002, and monument 308 is the twin of monument 50000.
  - Average vertical elevation change for the 57 monuments was +0.1511" (uplift).
4. Nine monument locations as recorded by the InSAR moved more than 0.6 inches horizontally, the threshold as specified in the BHCSD ordinance.
    - Monuments 302, 101, 50003, 304, 102, 116, 301, 117, and 126 showed positive (easterly) horizontal movement of +1.0490, +1.0220, +1.0010, +0.7490, +0.6720, +0.6620, +0.6570, +0.6370, respectively. Note that monument 301 is the twin of monument 102, monument 302 is the twin of monument 50003, and monument 304 is the twin of monument 116.
    - No monuments showed negative (westerly) horizontal movement.
    - Average horizontal movement for the 57 monuments was +0.1764" (easterly).
  5. The overall IOF voidage replacement ratio (VRR) was 102% for the V/R reservoirs from July 1, 2023 through June 30, 2024. This indicates that fluid injection and withdrawal are essentially balanced.
  6. The average V/R reservoir pressure in 2024, based on the static fluid level data supplied by SPR is 867 pounds per square inch (psi), slightly higher than the 852 psi calculated in 2023. This indicates that the overall subsurface pressure is being maintained by injection activities in the field. The average reservoir pressure of 866 psi over the last three years is very close to the original reservoir pressure historically measured at 880 psi.
  7. There was a poor correlation between ground movement and operations at the BHCSD, IOF, and regional levels.
  8. The ground movements observed in the current and past Annual Ground Movement Surveys (AGMS) are relatively small and, taken in context with overall Los Angeles Basin ground movement, are not considered unusual or excessive. Ground movements also show significant variations in displacement (both magnitude and direction) from year to year. Field operations alone cannot account for this variation as they are essentially stable, suggesting several independent factors are involved in observed ground motion.

The 2023/24 survey data can be found in the report from Viridien; the results are incorporated in this report.

## 2 Introduction

The BHCSO survey monitoring program began in 2010 and requires the operator to conduct ground movement surveys, including both vertical and horizontal surveys, once every 12 months. A variance was granted for the 12-month period to be extended to 18 months in 2020 due to the COVID-19 pandemic. The operator received permission to transition from ground movement surveys to InSAR data for the 2024 report, which covers the ~12-month period from June 25, 2023, to July 1, 2024. The reporting time frame has now permanently shifted from calendar year to the July- June time frame, adjusted slightly to account for the satellite orbits closest to July 1, 2023 and June 30, 2024.

The survey results are analyzed in relation to oil field activities, taking into consideration individual oil producing zones, production and injection volumes, and reservoir pressure. The intent of this program is to monitor vertical displacement and where damage due to vertical displacement is found to be caused by oil operations, to adjust operations accordingly.

Evans & Walker's (formerly InterAct's and 2H Onshore California's) report prepared by a Registered Professional Engineer (Petroleum). The inclusion of InSAR data by Viridien constitutes SPR's current AGMS of the IOF, as required under the guidelines established by the BHCSO Environmental Impact Report (EIR) (Marine Research Specialists, 2008).

### **3 Monuments**

Reference locations used for the AGMS include 57 actively monitored monuments both within and outside of the field boundaries. (See Figure 1). Five monuments are older historical monuments (the 50000 series monuments). Thirty-five of the monuments were established by Psomas in 2010 both in and around the BHCS D (the 100 series monuments). Five monuments were established by Psomas in 2010 as benchmarks outside the BHCS D (the 200 series monuments). The twelve monuments installed in 2014 (the 300 series monuments) were driven to refusal to serve as twin monuments to those that could be unduly influenced by surface features such as hill slopes, tree roots, or other factors unrelated to actual ground movement.

The transition from ground surveys to InSAR replaces the need to account for local secondary effects with the need to account for atmospheric effects and potential inaccuracies in the modeled satellite orbits. No monument changes have occurred during the 12-month interval of this study; the 57 monuments used this year are intact from last year.

## 4 InSAR Results

The Viridien analysis of the 12-month vertical displacement over 2023 – 2024 shows an uplift trend in the center of the CSD and a subsidence trend on the eastern edge of the CSD, in contrast with the dominating subsidence trend seen in the previous report. This vertical uplift displacement from June 2023 to July 2024 reaches a maximum of approximately 1.75 inches. The vertical subsidence to the East reaches a maximum of -0.75 inches.

From June 2023 to July 2024, East-West displacement generally corresponds with the deformation features seen in the vertical results. Specifically, contraction aligns with the center of the subsidence feature on the eastern edge of the CSD and the outward movement aligns with the center of the uplift feature within the CSD. The maximum rates are approximately 0.53 inches in the westerly direction and 0.96 inches in the easterly direction over the one-year period.

Further away from the CSD, around the boundaries of the AOI, there are several low-magnitude wide-scale variations in displacement. These may relate to other natural or anthropogenic processes such as groundwater variations, groundwater abstraction and pumping, and oil field production activity. There is the possibility that some of these low-magnitude signals may represent residual atmospheric artefacts.

The CSD has set a deformation threshold of  $\pm 0.6$  inches. This threshold has been applied to the 2023 – 2024 vertical and East-West results, with the resulting graphic (Figure 2) depicting areas within the IOF AOI that exceed this threshold. Areas experiencing displacement more than -0.6 inches (subsidence or westerly displacement) are styled in red and areas experiencing displacement more than +0.6 inches (uplift or easterly displacement) are styled in blue.

Note that these results are examined for a 12-month interval (summer-summer), rather than the 18-month report for 2019-2020 and winter-winter 12-month intervals prior to that.

InSAR data, just like data from any other measurement technique, has associated uncertainties. These uncertainties are assumed to be normally distributed and quantified using standard deviation. This means that the true value will be within three standard deviations 99.7% of the time. Three standard deviations equate to a vertical accuracy of  $\pm 0.48$  inches and a horizontal accuracy of  $\pm 0.30$  inches for the 12-month period (June 2023, to July 1, 2024).

Details on InSAR data acquisition, processing, and interpretation are given in Viridien's 2024 report filed separately.

## 5 Oilfield Causes of Ground Movement

From the 1924 field discovery until the waterflood began in the 1950's, the Inglewood V/R interval was dominated by solution-gas drive (primary recovery), causing high reservoir pressure depletion and causally related ground subsidence. Once the waterflood began, ground movement due to oilfield causes declined accordingly. Relative to the five to ten feet of subsidence recorded in the early years of field development (and clearly attributed to oilfield operations), the cumulative ground movements observed in the 2010-2023 AGMS have been small, highly variable, and do not correlate well with field operational parameters. The relationship between the two has been examined at two different levels: regional (east of the Newport – Inglewood Fault and west of the Newport – Inglewood Fault), and fieldwide.

Production from and injection into the V/R interval in the IOF from 1924 through 2023 is shown in Figure 3. Fluid production is the sum of oil production, water production, and natural gas production. The production and injection volumes were converted to reservoir barrels. This figure shows that production from the V/R interval in the IOF peaked in the early 2010's and is now on the decline.

Figure 3 also shows the annual and cumulative voidage replacement ration (VRR) for the V/R interval in the IOF. Yearly injection volume first reached a balance with yearly fluid production volume in the early 1970's. The annual VRR has averaged 1.0 from 1975 through 2023. The cumulative VRR through 2023 is 0.88. It has been demonstrated in previous AGMS reports that this increase in net injection since the 1950's has reversed annual and cumulative subsidence caused by underbalanced production prior to that period. Since balance was permanently achieved in 1995, ground movement has been much smaller than in the early years of field development, and annual displacement has generally stabilized such that measurements tend to lie in a range comparable to the level of accuracy of the tools used to record them.

The 2017 engineering report (Minner Engineering, Inc., 2017) states that the original reservoir pressure gradient in the V/R was normal at 0.44 psi/foot subsea. When the large-scale installation of the waterflood was started in 1957, it was estimated that the pore pressure had dropped from the original 880 psi to 40-160 psi, a pressure gradient of 0.02-0.08 psi/foot (Oefelein, 1963) using a datum of 2000 feet below sea level (subsea). The fieldwide waterflood began in the Inglewood V/R interval to rebuild and stabilize reservoir pressure. The current average reservoir pressure is estimated to be 867 psi at 2000 feet subsea, with a gradient of 0.43 psi/foot, approximately equivalent to the original reservoir pressure conditions, validating that the reservoir pressure has been re-established through water injection. Figure 4 shows the average reservoir pressure over the past three years.

## 6 Ground Movement and Comparison to Previous Years

### **InSAR Horizontal Movement Results**

Vertical ground movement results for 2024 are tabulated in Table 1. The results are sorted by both monument number and magnitude of displacement. Four of the monuments exceeded the 0.6-inch vertical movement in the negative direction (subsidence). Monuments 128, 303, 50004, and 106 showed negative vertical movement (subsidence) of -0.8390", -0.7020", -0.6620", and -0.6120", respectively. Note that monument 303 is the twin of monument 5004. Six of the monuments exceeded the BHCSD 0.6-inch vertical movement threshold in the positive direction (uplift). Monuments 50002, 307, 126, 50000, 308, and 50003 showed positive vertical movement (uplift) of +1.1390", +1.0230", +0.8220", +0.8180", +0.6540", and +0.6170", respectively. Note that monument 307 is the twin of monument 50002, and monument 308 is the twin of monument 50000. The average elevation change for the 57 monuments was +0.1511".

### **InSAR Horizontal Movement Results**

Horizontal ground movement results for 2024 are tabulated in Table 1. The results are sorted by both monument number and magnitude of displacement. Nine monument locations as recorded by the InSAR moved more than 0.6 inches horizontally, the threshold as specified in the BHCSD ordinance. Monuments 302, 101, 50003, 304, 102, 116, 301, 117, and 126 showed positive (easterly) horizontal movement of +1.0490, +1.0220, +1.0010, +0.7490, +0.6720, +0.6620, +0.6570, +0.6370, respectively. Note that monument 301 is the twin of monument 102, monument 302 is the twin of monument 50003, and monument 304 is the twin of monument 116. No monuments showed negative (westerly) horizontal movement. Average horizontal movement for the 57 monuments was +0.1764" (easterly).

## 7 Ground Movement and Oilfield Operations

The historical impact of oilfield operations on ground movement prior to the 1980's, before full volume balance was achieved, is well documented and is not the focus of this analysis. Overall vertical displacement after this point has been mostly stable (less than 0.6 inches per year). Much work has been done on causation in previous years: the focus here is on new observations and conclusions for the 2023-2024 production year. The study has historically included fieldwide, local, and regional perspectives. Each of these perspectives is discussed below to further investigate the potential relationship between oilfield operations and ground movement in the BHCSO.

### **Fieldwide Voidage Replacement Ratio**

Table 2 shows that the fieldwide voidage replacement ratio for the Vickers Rindge zone, as defined by the ratio of the total volume of fluids injected to the total volume of fluids produced (in reservoir barrels), was 1.02 (102%) for the production year ending June 30, 2024. The cumulative fieldwide net injection ratio for the Vickers Rindge zone for the duration of the BHCSO program which began in 2010 is also 1.02 (102%).

A cross-plot of fieldwide yearly net injection volume and average yearly infield monument movement over the period from 2010-2024 shows no correlation, as seen in Figure 5. An infield monument is defined as a monument that has had an active producer or injector within a 1000-foot radius in 2024. The IOF remains in positive volume balance. Therefore, based on historical observations, significant displacement at a fieldwide level above the threshold, due directly to volume imbalance, is considered to be very unlikely.

### **Local Monument Balance**

Table 3 shows the 'local' net injection volume for the cumulative time 2022-2023 for each monument, which is defined as the total V/R waterflood injection volume minus the total V/R liquid production for wells with a bottom hole location within a 1000-foot radius of the monument. The list of monuments is ranked by the magnitude of survey vertical elevation change.

The table also shows the total number of V/R wells (waterflood injection or production) within the 1000-foot radius in the data set. There are 28 monuments with non-zero net injection volumes; the remainder were over 1000 feet from any active well.

Figure 6 also presents a cross-plot of the annualized elevation change of the infield monuments versus their associated net injection volume for the corresponding time frame (July 2023 through June 2024). The data shows that there was essentially no correlation between these two measurements.

These figures suggest that ground movement cannot be explained solely by net injection, since other factors (either real or noise-related) must be present to explain the large amount of scatter observed. At the scale of ground movement observed at IOF, the local annual net injection volume is a poor predictor of local annual vertical displacement.



The relationship between surface displacement and net injection within 1000 feet of monuments observed this year is very similar to that seen in previous years since the beginning of the BHCS D program: there has been no discernable correlation between the two variables.

### **Regional Volume Balance**

The BHCS D was divided into two regions, shown in Figure 1, based on the location of the isolating Newport – Inglewood fault. These regions, East of the Newport – Inglewood fault and West of the Newport – Inglewood Fault, exist at an intermediate or regional level, in between the fieldwide and local levels discussed above. Each region was analyzed, and their associated production and injection figures are shown in Table 2. Data from 599 completions was used in the interpretation.

The East area had a negative net injection (98%) and an average elevation average change of -0.07 inches. The West area had a positive net injection (102%) and an average elevation change of +0.29 inches. Data on both areas is shown in Table 2. A graph of the historical voidage replacement ratio for the East area is included as Figure 7, and a graph of the historical voidage replacement ratio for the West area is included as Figure 8.

We conclude that even at the regional level, other factors apart from field operations must be important contributors to ground movement based on the inconsistent correlation observed between average ground movement and net injection for each region.

### **IOF and the BHCS D in Relation to the Los Angeles Basin**

Figure 9 depicts the InSAR vertical displacement for the Los Angeles Basin from July 2023 through June 2024. Figure 10 depicts the InSAR horizontal displacement for the Los Angeles Basin for this same time period. Figure 11 depicts the cumulative InSAR vertical displacement for the Los Angeles Basin from July 2010 – July 2024. These figures indicate that there is no correlation between the location of Los Angeles Basin oil fields and either vertical or horizontal displacement in the Los Angeles Basin.

### **Summary of Ground Movement and Oilfield Operations Analysis**

Evaluation of surface survey results relative to the V/R net injection volume balance and reservoir pressure does not indicate a quantitative relationship exists between ground movement and oilfield operations at the fieldwide, local, or regional level. At the scale of ground movement observed in recent years, any relationship between field operations and subsidence, if it does exist, appears to be masked by other factors. Our conclusions are summarized below:

1. Similar to previous years, there is low confidence in using the monument displacement trends to provide clear guidance for fieldwide, local, or regional replacement ratio targets.
2. There are significant mechanisms not directly related to volume balance affecting ground movement at the scales analyzed.

3. There is no relationship discernible with survey measurements between the yearly fieldwide net injection ratio and the number of monuments that cross the 0.6 inches elevation change threshold and/or their movement direction.

## **8 Summary and Recommendations**

The amount of movement observed in the BHCS D is relatively small and not unique. It is recognized that significant ground movement occurred due to oilfield operations prior to the start of the waterflood in 1954, but since the maintenance of net injection near or above 100% was established in 1995, the ground movement on average has been relatively stable (<0.6 inches/year) on a fieldwide basis.

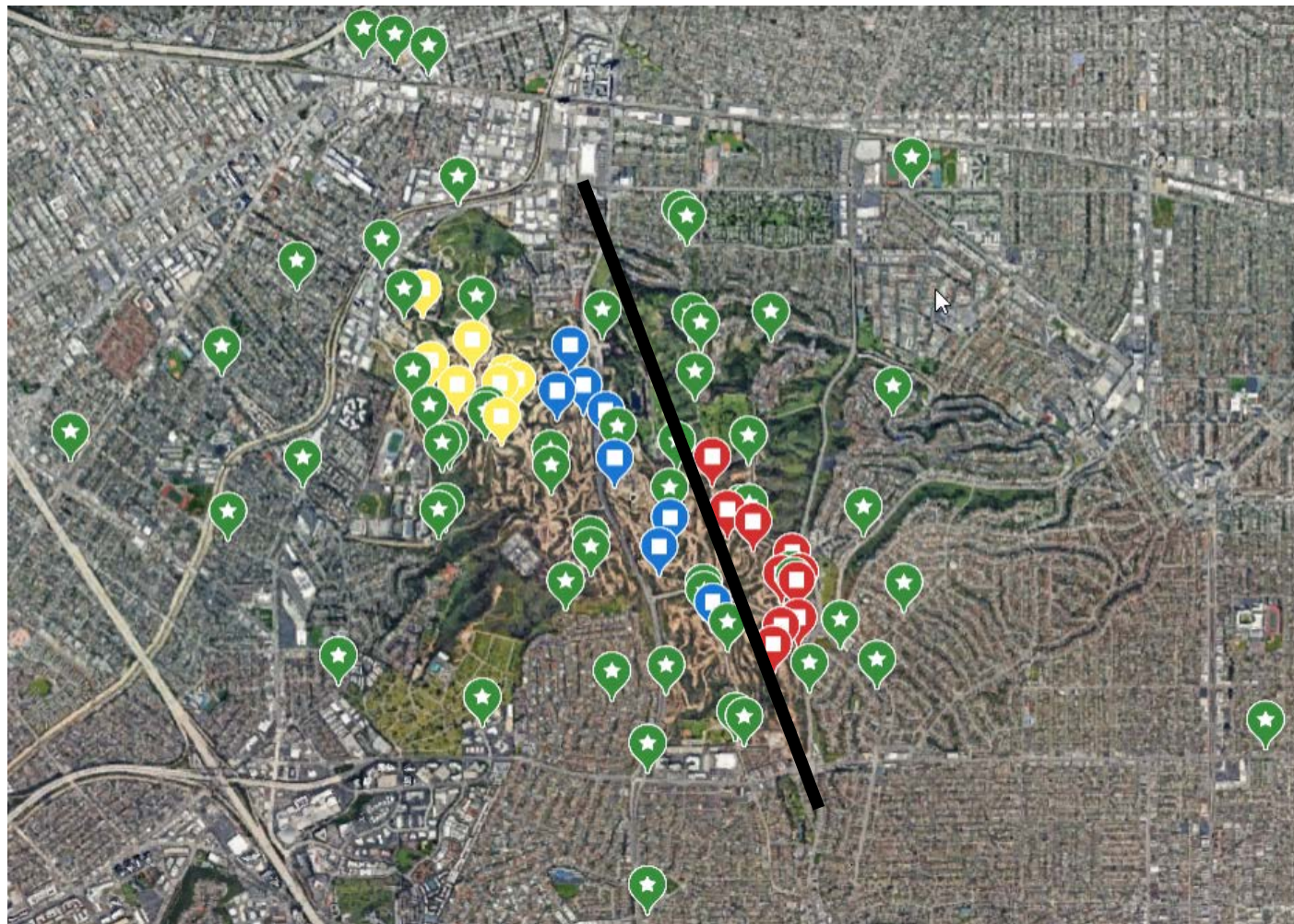
There does not appear to be a consistent relationship between the yearly waterflood injection ratio and vertical displacement observed in the InSAR data. No significant trends were identified in the annualized 2024 monument elevation changes plotted against the fieldwide, local (1000-foot radius), or regional net waterflood injection volumes. The lack of a simple connection between the net injection volume and surface monument movement is likely due to more than one mechanism impacting the surface survey results at the current scale of ground movement under volume balanced conditions. Other possible contributors to ground movement are discussed in the LANGAN report. Additionally, the amount of displacement at near volume balance conditions may be at the limit of tool resolution, and both random and systematic noise are probably also impacting the measurements.

It is recommended that SPR continue its practice of 100% net injection ratio and monitoring of the BHCS D as outlined in the EIR. The 14 years of data gathered during the period of the AGMS (since 2010) has proven the good correlation between the twin monuments and the original monuments.

## **9      References**

References used are the same as those listed in the 2018 report, updated as appropriate.

Figure 1 - AMS Monument Network and Idle Wells Analyzed for Reservoir Pressure



- Monuments
- Idle Vickers Rindge Wells – West of Newport - Inglewood Fault (West of Trace Fault)
- Idle Vickers Rindge Wells – West of Newport - Inglewood Fault (East of Trace Fault)
- Idle Vickers Rindge Wells – East of Newport - Inglewood Fault
- Approximate Location - Newport - Inglewood Fault



Figure 2 - Localized InSAR Vertical and Horizontal Displacement from July 2023 through June 2024

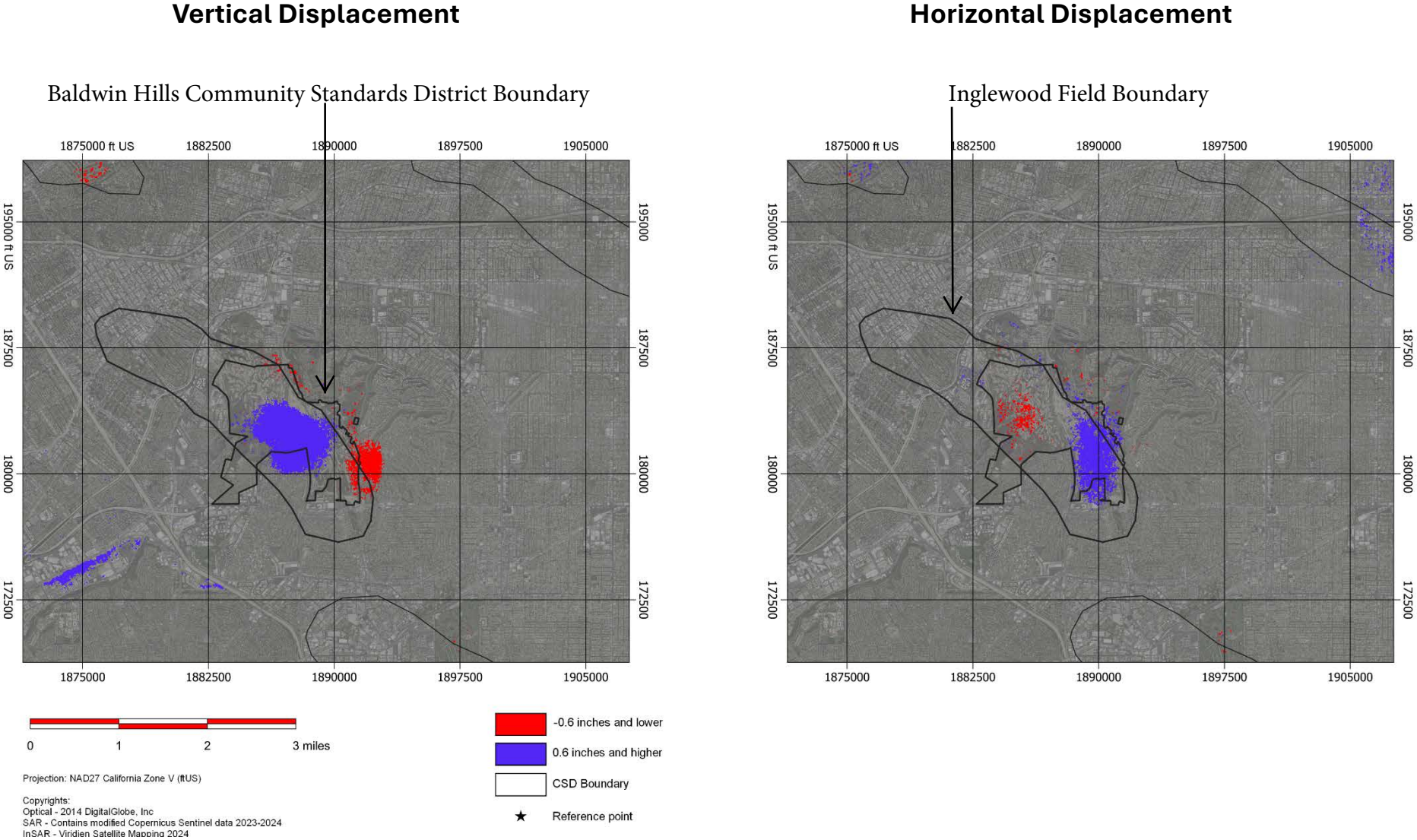
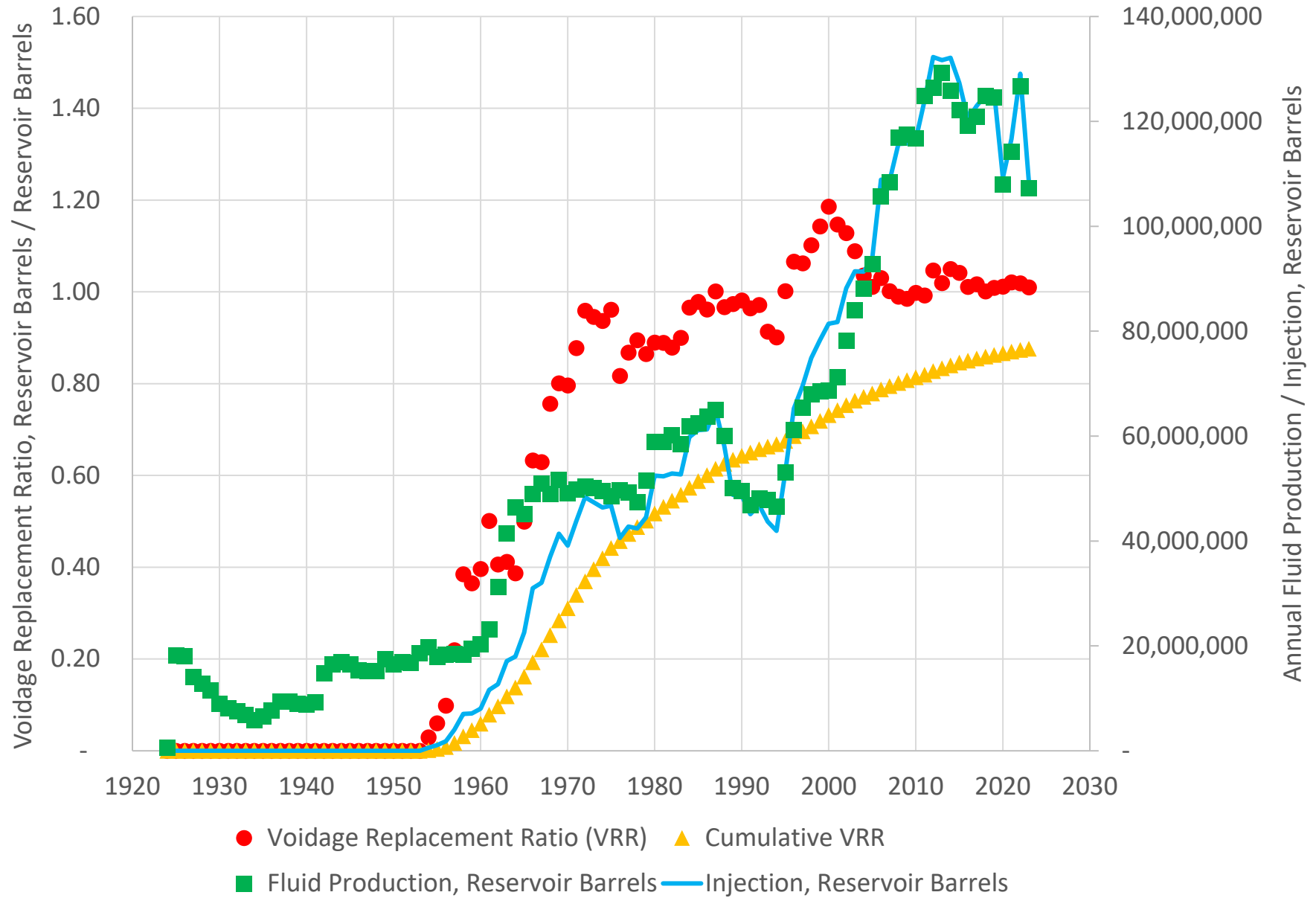


Figure 3 - Vickers Rindge (Total) Voidage Replacement Ratio



**Figure 4 - Vickers Rindge Reservoir Pressure**  
(Static Fluid Levels - Measured at Mid Point of Completion Interval)





# Table 1

2023 - 2024 Ground Movement									
Vertical (Negative = Subsidence, Positive = Uplift)					Horizontal (Negative = West, Positive = East)				
Sorted by Monument					Sorted by Monument				
Number		Sorted by Movement			Number		Sorted by Movement		
101	0.1780	128	(0.8390)		101	1.0220	129	(0.4680)	
102	(0.0400)	303	(0.7020)		102	0.6720	105	(0.4180)	
103	(0.2920)	50004	(0.6620)		103	(0.2710)	128	(0.3320)	
104	0.1290	106	(0.6120)		104	(0.0920)	50000	(0.2790)	
105	(0.5620)	105	(0.5620)		105	(0.4180)	103	(0.2710)	
106	(0.6120)	129	(0.4570)		106	(0.0970)	308	(0.2690)	
107	0.3870	103	(0.2920)		107	0.3220	309	(0.2490)	
108	(0.1410)	108	(0.1410)		108	(0.0710)	111	(0.2410)	
109	0.0310	301	(0.0930)		109	0.0800	311	(0.1890)	
110	(null)	111	(0.0530)		110	0.3900	130	(0.1170)	
111	(0.0530)	311	(0.0500)		111	(0.2410)	106	(0.0970)	
112	0.3410	102	(0.0400)		112	0.0710	104	(0.0920)	
113	0.2040	121	(0.0240)		113	0.2290	50002	(0.0900)	
114	0.2570	130	(0.0240)		114	0.2440	108	(0.0710)	
116	0.2280	309	0.0050		116	0.6620	205	(0.0540)	
117	0.1670	131	0.0100		117	0.6550	307	(0.0530)	
118	0.3730	109	0.0310		118	0.5910	50010	(0.0390)	
120	0.1970	312	0.0730		120	0.0420	306	(0.0330)	
121	(0.0240)	139	0.0750		121	0.3030	123	0.0030	
122	0.1400	50010	0.0770		122	0.2580	305	0.0300	
123	0.5910	306	0.0940		123	0.0030	132	0.0340	
126	0.8220	132	0.1170		126	0.6370	120	0.0420	
127	0.2610	204	0.1220		127	0.4120	310	0.0600	
128	(0.8390)	305	0.1220		128	(0.3320)	202	0.0630	
129	(0.4570)	104	0.1290		129	(0.4680)	112	0.0710	
130	(0.0240)	122	0.1400		130	(0.1170)	131	0.0720	
131	0.0100	304	0.1530		131	0.0720	109	0.0800	
132	0.1170	134	0.1620		132	0.0340	204	0.1070	
133	0.2340	117	0.1670		133	0.1640	206	0.1330	
134	0.1620	205	0.1680		134	0.2600	203	0.1480	
135	0.2360	101	0.1780		135	0.2060	137	0.1500	
136	0.3000	120	0.1970		136	0.1770	138	0.1610	
137	0.3780	113	0.2040		137	0.1500	312	0.1620	
138	0.2950	203	0.2190		138	0.1610	133	0.1640	
139	0.0750	116	0.2280		139	0.4040	136	0.1770	
201	0.2340	133	0.2340		201	0.2640	135	0.2060	
202	0.3570	201	0.2340		202	0.0630	113	0.2290	
203	0.2190	135	0.2360		203	0.1480	114	0.2440	
204	0.1220	206	0.2400		204	0.1070	122	0.2580	
205	0.1680	114	0.2570		205	(0.0540)	134	0.2600	
206	0.2400	127	0.2610		206	0.1330	201	0.2640	
301	(0.0930)	138	0.2950		301	0.6570	121	0.3030	
302	0.5910	136	0.3000		302	1.0490	107	0.3220	
303	(0.7020)	112	0.3410		303	0.4770	110	0.3900	
304	0.1530	310	0.3440		304	0.7490	139	0.4040	
305	0.1220	202	0.3570		305	0.0300	127	0.4120	
306	0.0940	118	0.3730		306	(0.0330)	50004	0.4720	
307	1.0230	137	0.3780		307	(0.0530)	303	0.4770	
308	0.6540	107	0.3870		308	(0.2690)	118	0.5910	
309	0.0050	123	0.5910		309	(0.2490)	126	0.6370	
310	0.3440	302	0.5910		310	0.0600	117	0.6550	
311	(0.0500)	50003	0.6170		311	(0.1890)	301	0.6570	
312	0.0730	308	0.6540		312	0.1620	116	0.6620	
50000	0.8180	50000	0.8180		50000	(0.2790)	102	0.6720	
50002	1.1390	126	0.8220		50002	(0.0900)	304	0.7490	
50003	0.6170	307	1.0230		50003	1.0010	50003	1.0010	
50004	(0.6620)	50002	1.1390		50004	0.4720	101	1.0220	
50010	0.0770	110	(null)		50010	(0.0390)	302	1.0490	
Average	0.1511	Average	0.1511		Average	0.1764	Average	0.1764	

## Table 2

Reservoir Fluid Properties:		
Bo	1.0620	Reservoir Barrels / Stock Tank Barrels
Rs	130	Standard Cubic Feet / Stock Tank Barrels
Bg	0.0021	Reservoir Barrels / Standard Cubic Feet
Bw	1.0100	Reservoir Barrels / Stock Tank Barrels

Voidage Replacement Ratio - <b>Vickers Rindge</b> - July 1, 2023 through June 30, 2024			
Fluid / Area	East	West	Total
Oil Production, Stock Tank Barrels	286,252	863,634	1,149,886
Gas Production, MSCF	129,036	285,454	414,490
Water Production, Stock Tank Barrels	14,995,810	68,196,067	83,191,877
Injection, Stock Tank Barrels	15,234,241	71,170,336	86,404,577
Oil Production, Reservoir Barrels	304,000	917,179.31	1,221,178.93
Solution Gas, MSCF	37,213	112,272	149,485
Free Gas, MSCF	91,823	173,182	265,005
Free Gas, Reservoir Barrels	192,829	363,681	556,510
Water Production, Reservoir Barrels	15,145,768	68,878,028	84,023,796
Fluid Production, Reservoir Barrels	15,642,597	70,158,888	85,801,485
Injection, Reservoir Barrels	15,386,583	71,882,039	87,268,623
<b>Voidage Replacement Ratio</b>	<b>0.98</b>	<b>1.02</b>	<b>1.02</b>
<b>Avg Monument Movement, Inches</b>	<b>(0.0742)</b>	<b>0.2927</b>	<b>0.1511</b>

Voidage Replacement Ratio - <b>Vickers Rindge</b> - January 1, 2010 through June 30, 2024			
Fluid / Area	East	West	Total
Oil Production, Stock Tank Barrels	6,753,938	20,333,535	27,087,483
Gas Production, MSCF	2,269,977	5,459,136	7,729,112
Water Production, Stock Tank Barrels	326,040,415	1,350,680,646	1,676,721,061
Injection, Stock Tank Barrels	349,959,204	1,394,778,432	1,744,737,626
Oil Production, Reservoir Barrels	7,172,682	21,594,214.52	28,766,907.44
Solution Gas, MSCF	878,012	2,643,360	3,521,373
Free Gas, MSCF	1,391,965	2,815,776	4,207,740
Free Gas, Reservoir Barrels	2,923,126	5,913,129	8,836,253
Water Production, Reservoir Barrels	329,300,819	1,364,187,452	1,693,488,272
Fluid Production, Reservoir Barrels	339,396,628	1,391,694,796	1,731,091,432
Injection, Reservoir Barrels	353,458,796	1,408,726,216	1,762,185,002
<b>Voidage Replacement Ratio</b>	<b>1.04</b>	<b>1.01</b>	<b>1.02</b>

Voidage Replacement Ratio - <b>Vickers Rindge</b> - Initial Production (1924) - June 30, 2024			
Fluid / Area	East	West	Total
Oil Production, Stock Tank Barrels	65,097,698	262,725,734	327,823,442
Gas Production, MSCF	17,830,888	78,145,277	95,976,164
Water Production, Stock Tank Barrels	920,966,996	3,813,908,486	4,734,875,482
Injection, Stock Tank Barrels	977,036,571	3,590,129,120	4,567,165,681
Oil Production, Reservoir Barrels	69,133,755.41	279,014,729.86	348,148,495.89
Solution Gas, MSCF	8,462,701	34,154,345	42,617,048
Free Gas, MSCF	9,368,187	43,990,931	53,359,117
Free Gas, Reservoir Barrels	19,673,193	92,380,955	112,054,146
Water Production, Reservoir Barrels	930,176,666	3,852,047,571	4,782,224,237
Fluid Production, Reservoir Barrels	1,018,983,614	4,223,443,256	5,242,426,878
Injection, Reservoir Barrels	986,806,937	3,626,030,411	4,612,837,338
<b>Voidage Replacement Ratio</b>	<b>0.97</b>	<b>0.86</b>	<b>0.88</b>

Figure 5 - Fieldwide Net Injection vs. Average Infield Monument Vertical Displacement

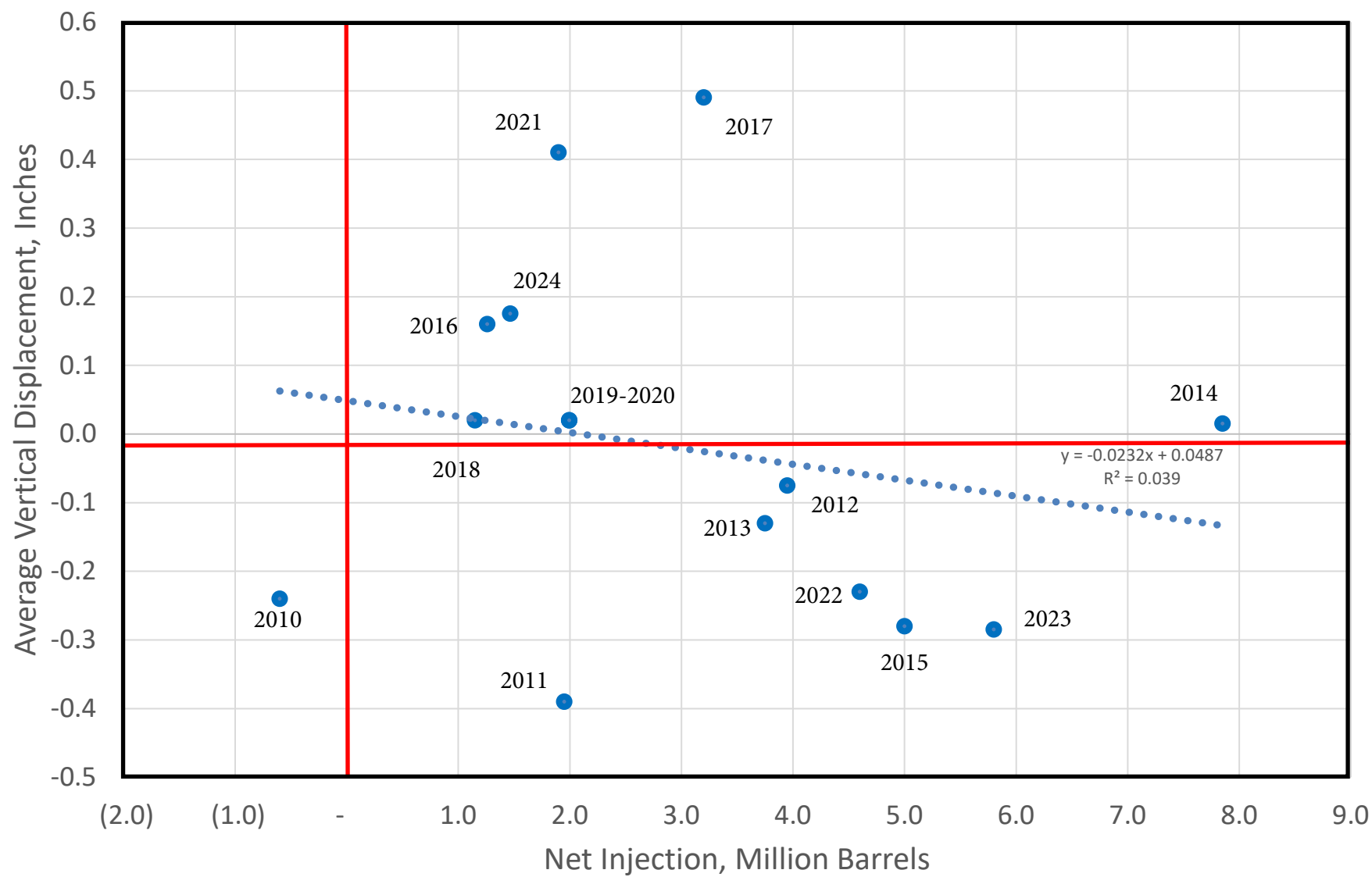


Table 3

Monument	Wells within 1,000' of Monument	Vickers Rindge Net Injection W/I 1,000', 1,000 Reservoir Barrels	2023 - 2024 Vertical Ground Movement, Inches (Negative = Subsidence, Positive = Uplift)
110	69	(456)	(null)
50002	26	1,252	1.1390
307	19	716	1.0230
126	70	968	0.8220
50000	52	2,006	0.8180
308	62	(1,445)	0.6540
50003	54	426	0.6170
123	2	539	0.5910
302	47	1,186	0.5910
116	34	546	0.2280
120	3	1,117	0.1970
101	55	336	0.1780
117	44	(192)	0.1670
304	30	1,404	0.1530
122	11	(1,174)	0.1400
139	5	884	0.0750
312	6	646	0.0730
109	26	(3,399)	0.0310
309	41	1,594	0.0050
121	10	(119)	(0.0240)
311	6	2,260	(0.0500)
111	47	(208)	(0.0530)
108	6	519	(0.1410)
105	1	(14)	(0.5620)
106	34	509	(0.6120)
50004	27	996	(0.6620)
303	28	703	(0.7020)
128	14	415	(0.8390)

Figure 6 - 07/23 - 06/24 Net Injection within 1,000' Radius of Monument vs. Vertical Displacement of

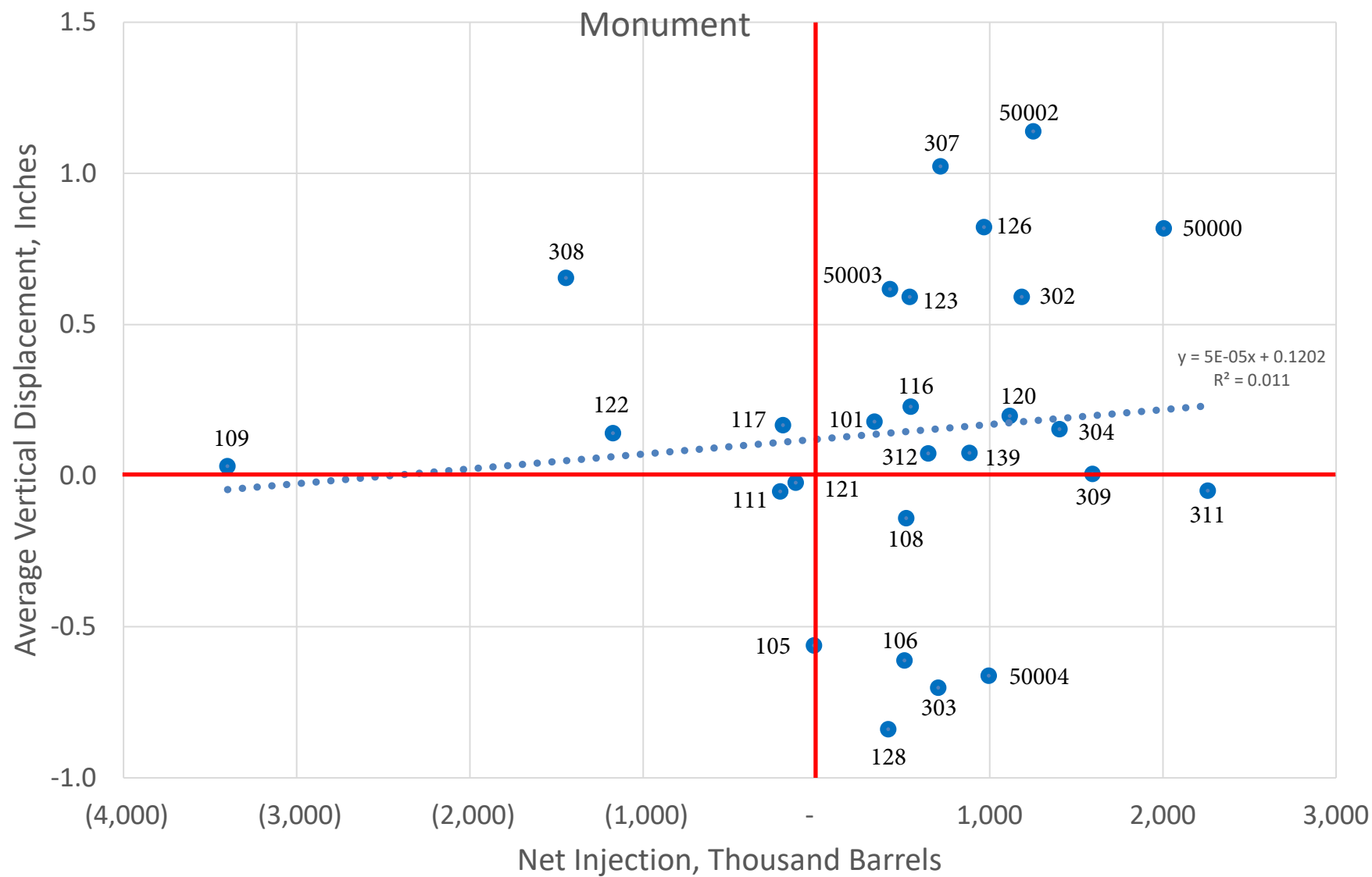


Figure 7 - Vickers Rindge (East) Voidage Replacement Ratio



**Figure 8 - Vickers Rindge (West) Voidage Replacement Ratio**



**Figure 9 - Regional InSAR Vertical Displacement from July 2023 through June 2024**  
(Los Angeles Basin oil fields outlined in black)

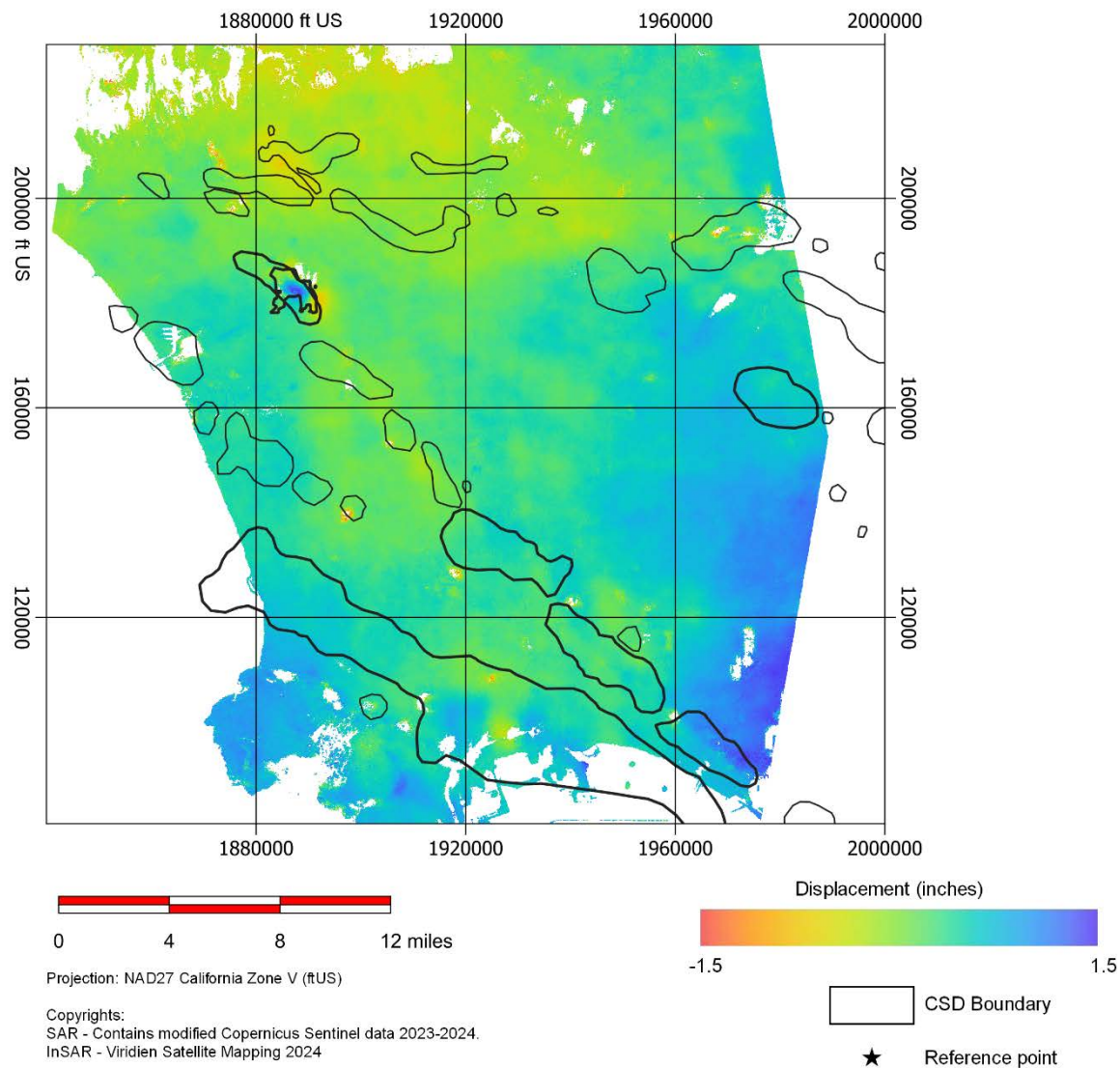




**Figure 10 - Regional InSAR Horizontal (East-West) Displacement from July 2023 through June 2024 (Los Angeles Basin oil fields outlined in black)**

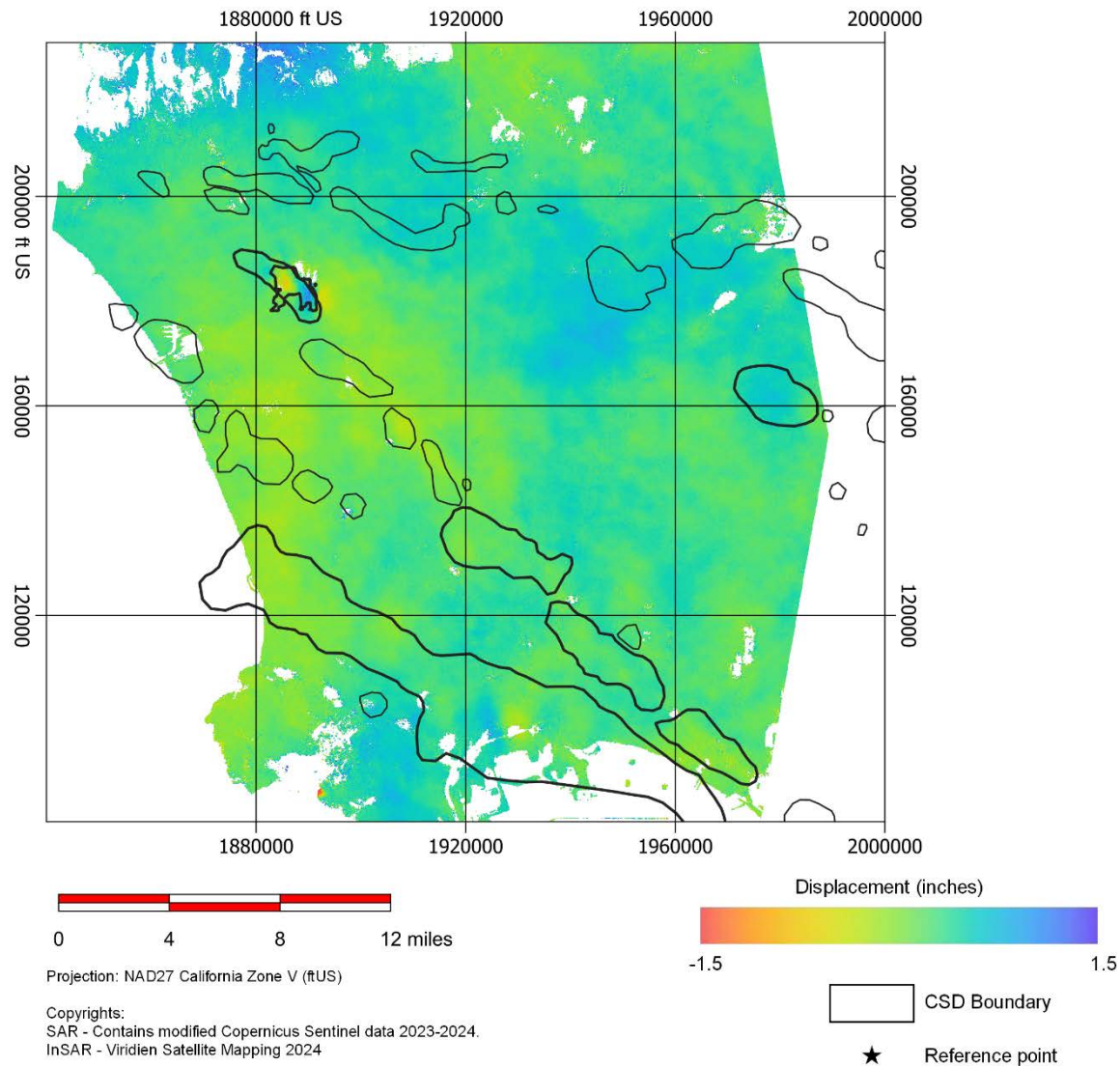
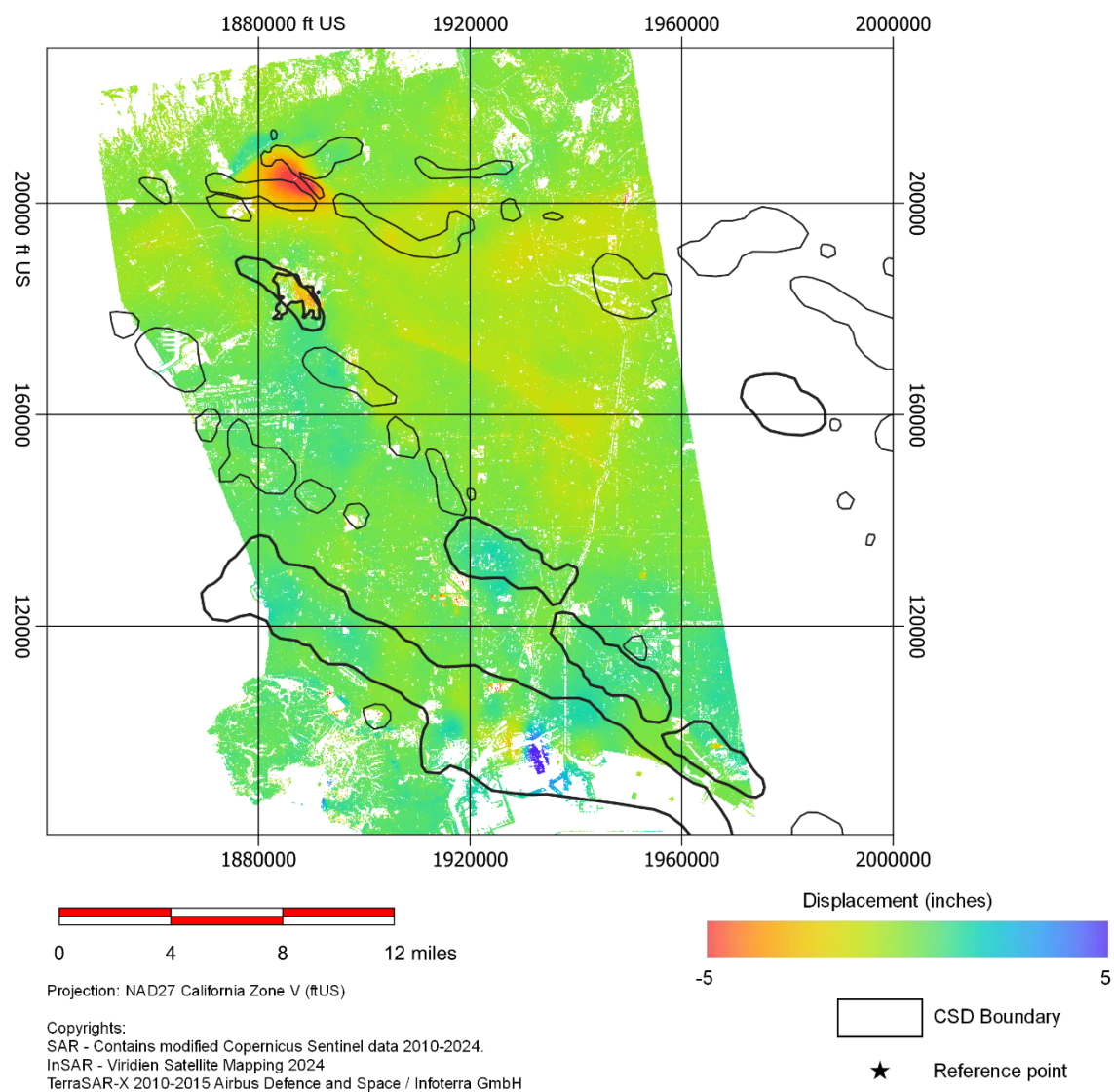


**Figure 11 - Regional InSAR Vertical Displacement - Cumulative from June 2010 - July 2024 (Los Angeles Basin oil fields outlined in black)**



19 February 2025

Mr. David Budy  
Sentinel Peak Resources  
1200 Discovery Drive, Suite 500  
Bakersfield, California 93309

**Re: Geotechnical and Engineering Geologic Evaluation  
Baldwin Hills Community Standards District  
2024 Annual Ground Movement Survey  
Inglewood Oil Field 2023 Production Year  
Langan Project No.: 721049201**

Dear Mr. Budy,

In accordance with our 9 June 2024 proposal, and subsequent authorization by Sentinel Peak Resources, Langan CA, Inc. (LANGAN) has prepared this letter report to summarize our interpretation of the 2024 annual ground movement survey of the Baldwin Hills Community Standards District (BHCSO), an unincorporated area of Los Angeles County, California (Project).

The production season for this campaign includes July 2023 to June 2024 (2023 production year). Our interpretation of the 2024 annual ground movement survey is based on our analysis of Interferometric Synthetic Aperture Radar (InSAR) satellite data provided by Viridien and analyzed by Langan. For the 2023-2024 period our analysis is based on the observations captured via satellite monitoring ground movement in the BHCSO.

## PROJECT OVERVIEW

The BHCSO was adopted in 2008 and provides a site-specific set of regulations for the Inglewood Oil Field. As part of the BHCSO requirements, surface ground movement monitoring has been performed typically every year since a benchmark survey was performed in 2010 for most of the surveyed monuments. The survey data is collected to identify ground surface movement in the BHCSO and to evaluate the direction and magnitude of the movement. As of the 2022 production year, the survey data included monitoring of fifty-seven (57) survey monuments and discretionary collection of InSAR elevation and east-west deformation data. Starting with the 2023 production year, Los Angeles County agreed to amending the surface ground movement monitoring to use only the InSAR data in 2024 and 2026, and the land survey monitoring points would be incorporated in 2025 and 2027. The data is reviewed each year by a licensed petroleum engineer, a certified engineering geologist, and a licensed geotechnical engineer to evaluate the potential cause of any movement that meets or exceeds the BHCSO threshold of 0.6 inches of vertical or horizontal movement. We reviewed the summary report by the petroleum engineer as part of our evaluation.

In addition to evaluating if the BHCSO threshold is met based on the surficial ground movement survey data, the operator is required to review and analyze any "claim or complaint of subsidence damage" that was submitted to the operator or county in the prior twelve months. The reporting period for the current 2023 production period includes July 2023 through June 2024. The InSAR measurements for this production season were collected between 25 June 2023 and 1 July 2024.

## DATA METHODS

Interferometric Synthetic Aperture Radar (InSAR) data, capturing vertical and horizontal (East-West) movement, was provided by Viridien in raster format which we used to calculate displacement values at each survey monument for the referenced period. All data extraction processes were completed in ArcGIS Pro, where each of the previously monitored survey monuments was plotted according to its precise coordinates and buffered by 175 feet to define the area for averaging. For continuity during this transition period of survey techniques, we have included the 57 survey monument locations on our figures, though the monuments were not directly surveyed this year, as described above.

Using the Zonal Statistics to Table tool, an average displacement was calculated within the 175-foot buffer around each monument, based on InSAR raster centroid values within those buffers. These averaged displacement values are used in this report to assess movement for the referenced period. "No data" values within the buffer were excluded from calculations.

The client provided well locations and proprietary fault data from the Inglewood oil field, which were analyzed in relation to each survey monument. Using automated geoprocessing tools in ArcGIS Pro, proximity and identification details for wells and fault lines within a 350-foot radius of each monument were extracted, with all distances recorded in feet.

Additionally, Quaternary-aged faults, with locations provided by the United States Geological Survey (USGS) in 2020, were downloaded and similarly analyzed in ArcGIS Pro to assess proximity and relevant identifiers in relation to each survey monument.

## DATA TRENDS

### Vertical Trends

Based on the 2023-2024 Viridien InSAR data, there were observed changes in elevation greater than the 0.6-inch BHCSO threshold near nine survey monument locations. The following table, Table 1, lists the eight survey monuments that increased in elevation more than 0.6 inch, and one survey monument that decreased in elevation more than 0.6 inch.

**Table 1 – Summary of Survey Monument Locations  
with Vertical Movement Exceeding 0.6 Inch**

<b>Monument<sup>1,2</sup></b>	<b>Vertical Movement (in/yr)</b>	<b>Approximate Monument Location (Longitude, Latitude)</b>
123	0.77	Southern-central, just outside of BHCSO (W -118.3753, N 33.9972)
126	0.86	East side of BHCSO (W -118.3682, N 34.0025)
128	-0.74	Southeast, outside of BHCSO (W -118.3565, N 33.9950)
302	0.71	Southeast side of BHCSO, twin of 50003 (W -118.3659, N 33.9967)
307	1.08	Southern-central of BHCSO, twin of 50002 (W -118.3736, N 33.9992)
308	0.82	Middle of BHCSO, twin of 50000 (W -118.3765, N 34.0047)



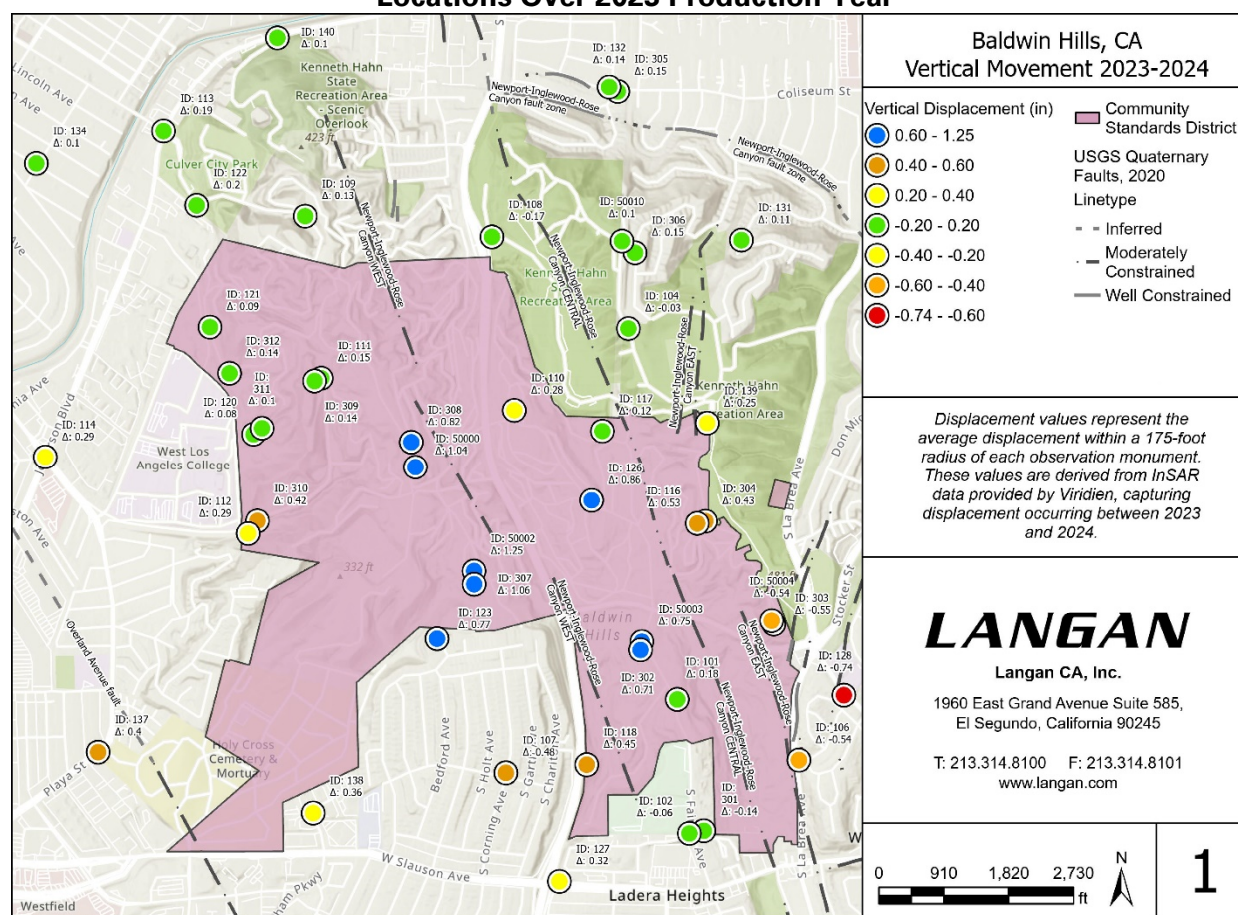
50000	0.97	Middle of BHCS D, twin of 308 (W -118.3763, N 34.0038)
50002	1.21	Southern-central of BHCS D, twin of 307 (W -118.3736, N 33.9998)
50003	0.75	Southeast side of BHCS D, twin of 302 (W -118.3658, N 33.9970)

**Notes:**

1. Survey monuments 302 and 50003, 307 and 50002, and 308 and 50000, are twin markers.
2. Vertical movements averaged over 175-foot radius around each monument location.

Summarized vertical movement trend and magnitudes are provided for each of the survey monument locations on Figure 1. An overview of the vertical movements across the BHCS D based on the InSAR data is shown on Figure 2. The InSAR data presented on Figure 2 indicates that the central and southern portion of the district experienced uplift of 0.6 to 1.45 inches while the southeastern edge of the district experienced subsidence of -0.6 to -0.75 inches.

**Figure 1 – Vertical Movements of the Survey Monument Locations Over 2023 Production Year**



**Notes:**

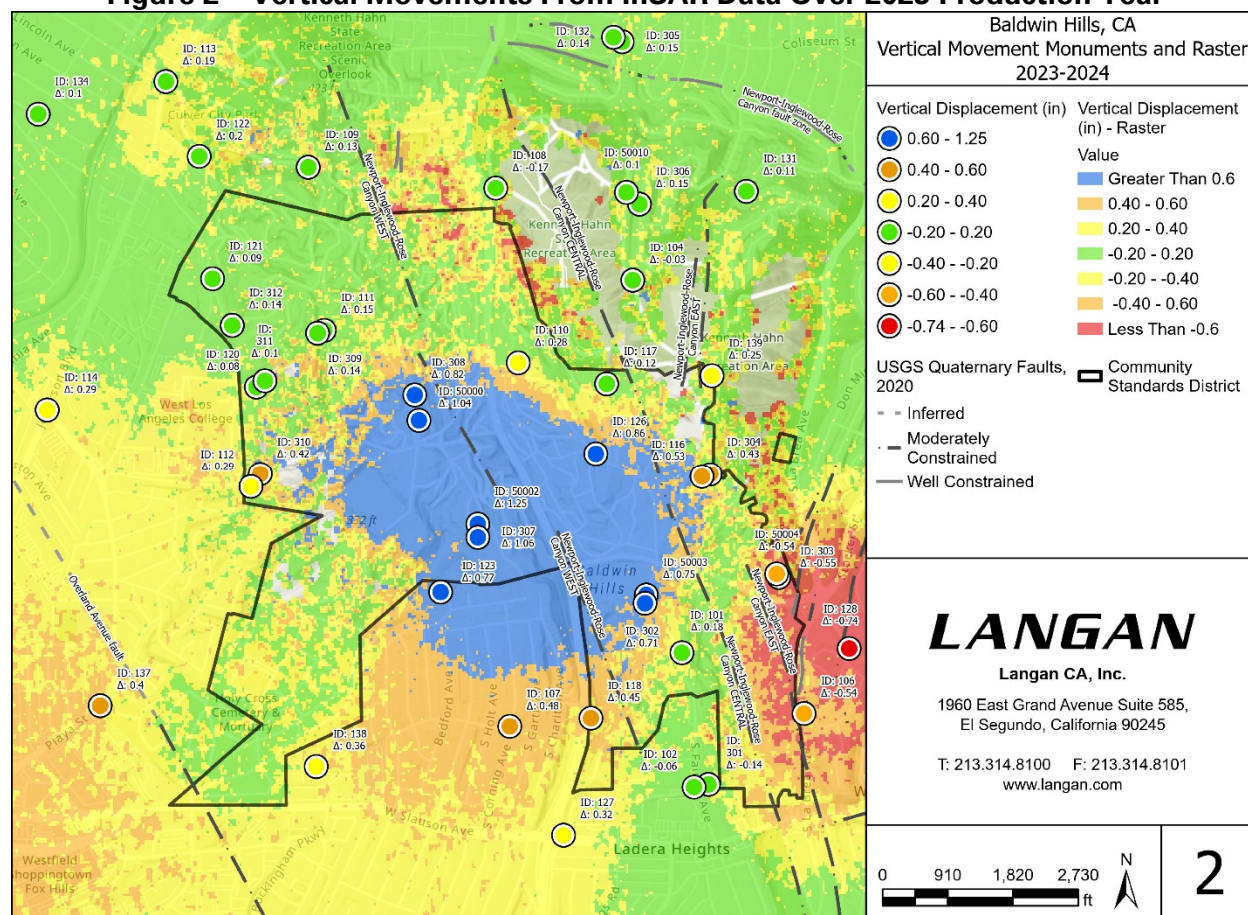
1. Vertical movements averaged over 175-foot radius around each monument location.
2. Negative values indicate a subsidence trend while positive values indicate an uplift trend.

## Faults

The USGS has mapped several active and potentially active faults near the BHCS. Most of the mapped fault segments are associated with the Newport-Inglewood-Rose Canyon (NIRC) fault system. The Quaternary Fault and Fold database, hosted by USGS, indicates that there are three primary northwest-trending fault segments of the NIRC. The eastern two northwest-trending fault segments are anticipated to have experienced surface deformation in Latest Quaternary time (approximately the last 15,000 years). The western segment of the northwest-trending NIRC is anticipated to have experienced surface deformation in Late Quaternary time (approximately the last 130,000 years). The NIRC also has several, shorter, northeast-trending fault segments mapped on the eastern side of the BHCS. These fault segments show surface deformation is historic time (approximately the last 150 years).

The Overland Avenue fault, located on the western side of the BHCS is anticipated to have experienced surface deformation in Late Quaternary time.

**Figure 2 – Vertical Movements From InSAR Data Over 2023 Production Year**



## Notes:

1. Negative values indicate a subsidence trend while positive values indicate an uplift trend.
2. Background shows Viridian InSAR raster symbolized to show exceedances of 0.6 inches in subsidence (red) or uplift (blue).

The approximate location of the Newport-Inglewood fault (USGS Quaternary Faults) as shown on the figures is provided by the United States Geological Survey (USGS).

Based on a review of the Viridien report, uplift reached a maximum of approximately 1.75 inches in the south-central portion of the BHCS D. Subsidence on the southeastern edge reached a maximum of -0.75 inches. The reason for the slight difference between the calculated vertical movement noted by us and by Viridien are discussed later in this report.

#### Horizontal Trends

Over the same period, the Viridien data indicates that seven survey monument locations experienced horizontal movement over the BHCS D 0.6-inch threshold, all in an eastward direction. The following table, Table 2, lists the seven survey monument locations that moved horizontally more than 0.6 inch.

**Table 2 – Summary of Survey Monument Locations  
with Horizontal Movement Exceeding 0.6 Inch**

<b>Monument</b>	<b>Horizontal Movement (in/yr)<sup>1,2</sup></b>	<b>Approximate Monument Location (Longitude, Latitude)</b>
101	0.90	Southeast side of BHCS D (W -118.3642 N 33.9948)
102 <sup>3</sup>	0.61	Southeast side of BHCS D, twin of 301 (W -118.3636, N 33.9897)
116	0.69	East side of BHCS D, twin of 304 (W -118.3633, N 34.0016)
301	0.61	Southeast side of BHCS D, twin of 102 (W -118.3630, N 33.9898)
302	1.00	Southeast side of BHCS D, twin of 50003 (W -118.3659 N 33.9967)
304	0.62	East side of BHCS D, twin of 116 (W -118.3629, N 34.0017)
50003	0.88	Southeast side of BHCS D, twin of 302 (W -118.3658 N 33.9970)

**Notes:**

1. Only East-West movement was able to be captured using the InSAR data due to the flight path of the satellite.
2. Positive values indicate eastward movement while negative values indicate westward movement.
3. Survey monuments 102 and 301, 116 and 304, and 302 and 50003 are twin markers.

Based on a review of the Viridien report, eastward movement within the BHCS D reached a maximum of approximately 0.96 inches in the southeastern portion of the district. An area of eastward movement approaching the district threshold of 0.6 inches was also observed at the northwestern corner of the district. Westward movement within the BHCS D reached a maximum of 0.83 inches in the west-central portion of the district. For comparison purposes, the maximum eastward movement noted at the survey monument locations in our analysis was 0.997 inches (rounds to 1.00), at monument location 302 while the maximum westward movement noted at the survey monument locations in our analysis was 0.59 inches. An area of westward movement approaching the district threshold of 0.6 inches was also observed just beyond the southeastern edge of the district. The maximum observed westward movement within this area based on our

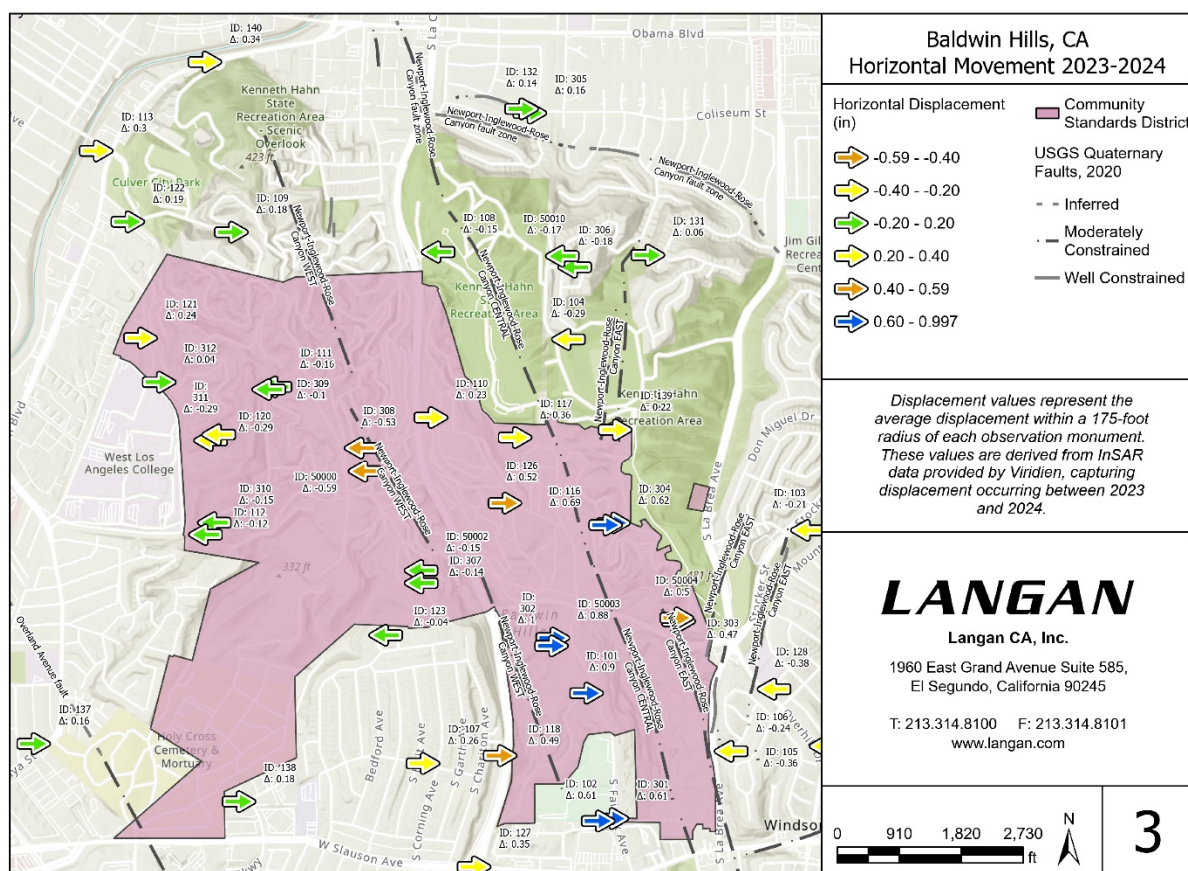


analysis is 0.70 inches. The maximum observed eastward movement within this area based on our analysis is 1.02 inches.

The reason for the disparity between the values reported by Viridien and our numbers/raster plot is a function of the methodology utilized when analyzing the InSAR dataset. Viridien plotted movement trends by averaging data within a 350-foot radius and only included data returns in which the data was acquired consistently over the past 10 years. For our analysis, we averaged data over a 175-foot radius and included all point cloud data that was available in the 2023-2024 dataset. This methodology eliminates clear "edge effects" in the raster data while preserving clustered values indicating movement over threshold in either direction. We reviewed our methodology with Viridien, and they agreed that it was appropriate for our analysis.

Summarized horizontal movement trend and magnitudes are provided for each of the survey monument locations on Figure 3. An overview of the horizontal movements across the BHCSO is shown on Figure 4.

**Figure 3 – Horizontal Movements of the Survey Monument Locations Over 2023 Production Year**

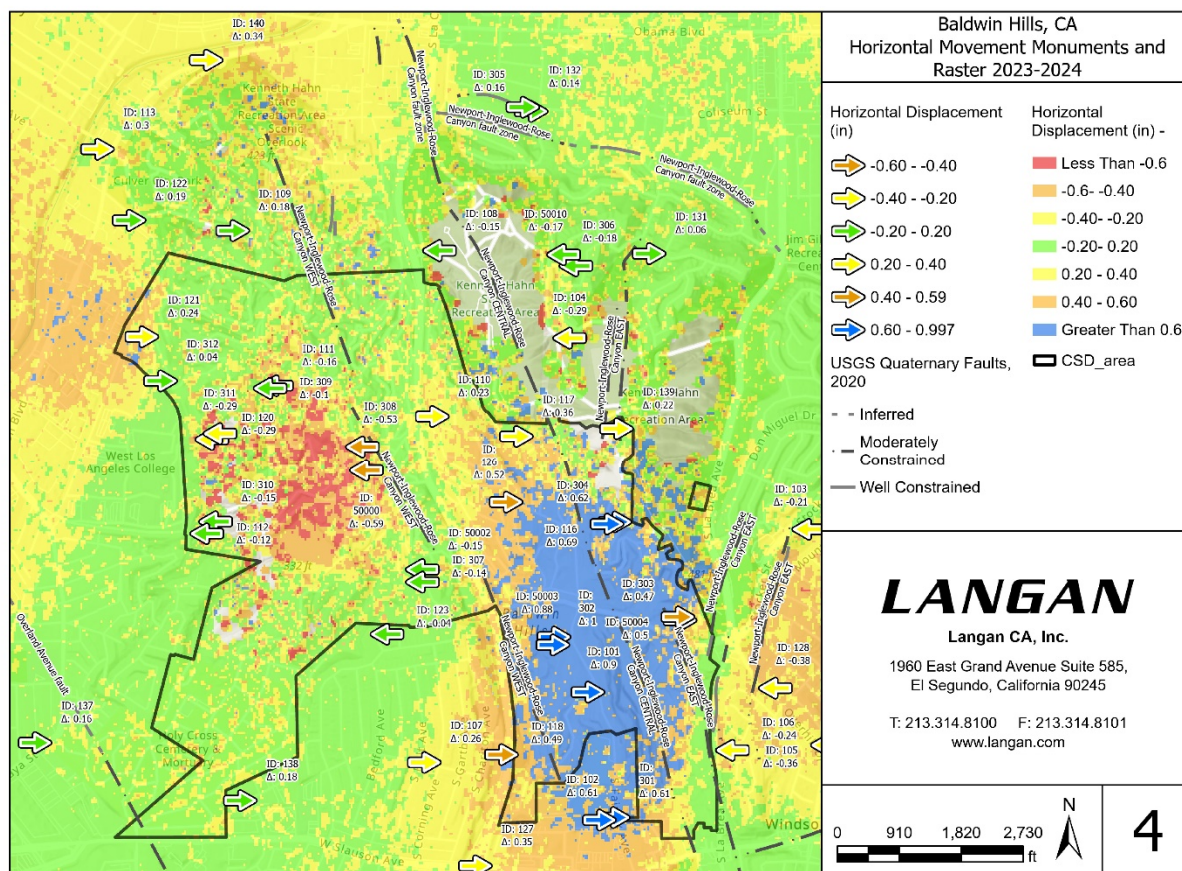


**Notes:**

1. Horizontal movements averaged over 175-foot radius around each monument location.
2. Positive values indicate eastward movement while negative values indicate westward movement.



**Figure 4 – Horizontal Movements From InSAR Data Over 2023 Production Year**



**Notes:**

1. Positive values indicate eastward movement while negative values indicate westward movement.
2. Background shows Viridien InSAR raster symbolized to show exceedances of 0.6 inches as movement to the west (red) or to the east (blue).
3. Arrows on the figure indicate location and magnitude of movement at the survey monuments.

**CONCLUSIONS**

Between July 2023 and June 2024, the area around 9 of the 57 monument locations indicated vertical movement trends that exceeded the BHCSO 0.6-inch threshold. Eight of the locations indicated a subsidence trend while one location indicated an uplift trend. The monument area with the largest uplift trend was monument 50002 with uplift of 1.21 inches located in the southern-central portion of the BHCSO. The monument area with the largest subsidence trend was monument 128 with subsidence of 0.74 inches located on the southeastern side of the BHCSO.

Between July 2023 and June 2024, the area around 7 of the 57 monument locations indicated horizontal movement trends that exceeded the BHCSO 0.6-inch threshold. All seven locations indicated that movement trends were toward the east. The monument area with the largest horizontal trend was monument 302 with an eastward movement of approximately 1.00 inches located on the southeastern side of the BHCSO.

Last year, for the 2022 production year, the southeastern portion of the BHCS D generally showed a subsidence trend of up to approximately 1 inch. Observed horizontal trends corresponded well and trended in the direction of the subsidence feature. Significant areas of uplift were not observed last year.

In comparison, the 2023 production year indicates that the central and southern parts of the district have an uplift trend, with recorded uplift of up to 1.75 inches by Viridien. An area of subsidence with subsidence values of up to -0.75 inches was observed on the southeastern edge of the district (see Figure 2).

Horizontal movement trends indicated that in general, areas of significant eastward movement were in the southeastern portion of the district with recorded eastward movement of up to approximately 1 inch, and at the northwest corner of the district where movement approached the 0.6-inch threshold. Areas of significant westward movement (up to approximately 0.8 inches) were located along the west-central portion of the district and along the southeastern edge of the district, where westward movement approached the 0.6-inch threshold.

The primary movement areas (both vertical and horizontal) are roughly centered on, or bordered by, the primary segments of the Newport-Inglewood-Rose Canyon (NIRC) fault, the approximate location of which is presented on all four figures. This indicates that the observed movements may be at least in part a result of creep (slow, steady movement along an active fault trace) or a build-up of pressure along the fault due to tectonic activity.

In particular, the western segment of the NIRC fault appears to be experiencing uplift in the southern and central portions of the BHCS D. This uplift is likely also represented by the eastward and westward ground surface movement noted in the southeastern and west-central portion of the BHCS D as shown on Figure 4. The observed ground surface movement suggests a compressional tectonic environment for this portion of the NIRC.

Based on our review of the petroleum engineer's report for the 2023 production year, the reservoir pressures for the three primary sections of the oil field were relatively consistent with the 2022 production year pressures. We did not observe any obvious correlations between the observed ground surface movement and the oil field pressure data.

In conclusion, the ground movement trends observed across the study area appear to be associated with compressional tectonic activity along the three northwest-trending segments of the NIRC fault that trend through the central and eastern portions of the district.

## LIMITATIONS

The conclusions provided in this report are based on surface conditions inferred from available survey data and reservoir pressure information, provided by others, as well as project information provided to date.

This report was prepared for Sentinel Peak Resources for their review and submittal to the BHCSD.

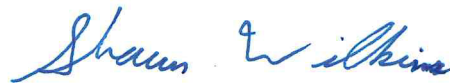
If changes to the survey data are made, we should be notified so that we may review and potentially revise our conclusions.

Sincerely,

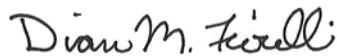
**Langan CA, Inc.**



Carey Johnston  
GIS Analyst



Shaun Wilkins, PG, CEG (2665)  
Senior Project Geologist

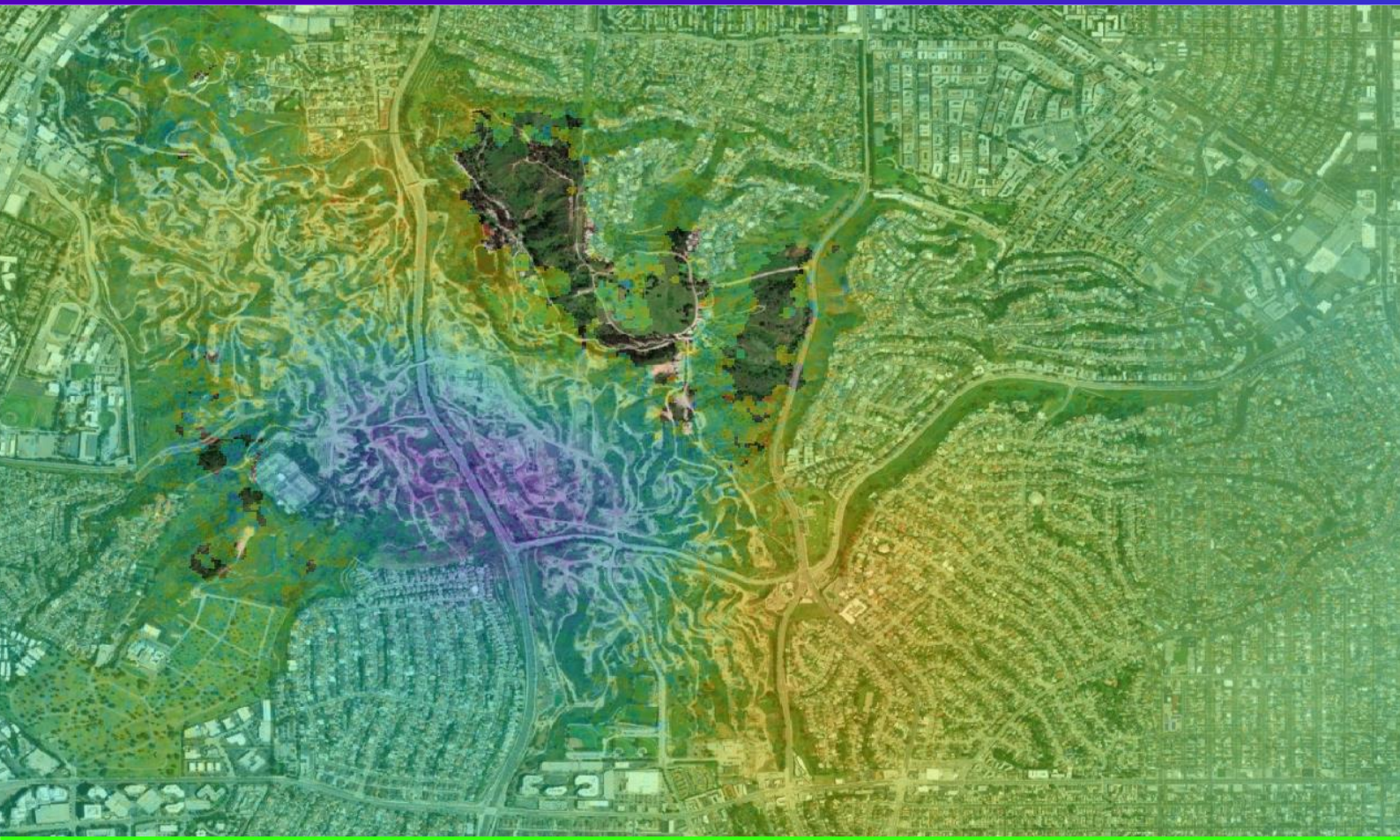


Diane Fiorelli, PE, GE (3042)  
Principal/Vice President

CJ:SHW:DMF

\\Langan.com\data\LAX\data\721049201\Outbound\2025-2-19 - Final 2023 Ground Movement Report\721049201\_2025.02.19\_Geo Report\_cj\_shw\_dmf.docx





# BALDWIN HILLS AND LA BASIN INSAR MONITORING 2010 – 2024

Prepared for Sentinel Peak Resources

Date of issue: 30/08/2024

Version: 1.0

**CONFIDENTIAL**

[viridiengroup.com](http://viridiengroup.com)

SEE THINGS DIFFERENTLY

Confidential - External





Document Change Record			
Revision	Date	Changes	Author(s)
V1.0	30/08/2024	First issue of report	Dr Camille Stock Dr Ben Conway-Jones

**Disclaimer:** The information in this report represents a factual assessment of the information provided and revealed by satellite imagery. With respect to Viridien’s description of ground deformation (InSAR) survey results, use of the terms ‘subsidence’, ‘consolidation’, ‘uplift’ and ‘heave’ are representative of the direction of movement away and towards the satellite sensor respectively, and do not imply the nature or presence of such a hazard being present. Please contact Viridien personnel for assistance in interpreting and analysing the data contained within this report.



## Executive Summary

This report provides satellite InSAR derived surface deformation measurements for the Inglewood Oil Field and wider Los Angeles Basin from June 2023 through July 2024, as well as cumulative measurements from 2010.

### **Inglewood Oil Field**

- From June 2023 to July 2024, vertical displacement is predominantly characterised by uplift reaching approximately 1.45 inches in the center of the Community Standards District (CSD) and by subsidence of approximately -0.75 inches on the easterly edge of the CSD.
- From June 2023 to July 2024, East-West displacement generally corresponds to outward movement along the flanks of the uplift feature and contraction toward the centre of the subsidence feature. The maximum rates are approximately 0.53 inches in the westerly direction and 0.96 inches in the easterly direction.
- In comparison to previous years, displacement regimes have demonstrated a strong uplift trend within the CSD that is a noticeable change from the overall subsidence trend recorded in the 2022 – 2023 report.
- From June 2023 to July 2024, there are no clearly visible discontinuities or abrupt changes in displacement gradient closely associated with mapped faults, although this does not preclude the presence of more subtle fault-related signals.
- Cumulative ascending line of sight displacement from 2010-2024 reaches a maximum of approx. -4.5 inches (predominantly subsidence) from October 2010 to July 2024.

### **Los Angeles Basin**

- For June 2023 to July 2024, complex fault constrained displacement continues near Beverly Hills. Broad uplift trends are observed linked to Santa Ana aquifer (constrained by the Newport-Inglewood fault).
- From October 2010 to July 2024, the greatest displacements are similar to those observed in previous years, including the Santa Ana aquifer constrained along the Newport-Inglewood fault, Long Beach, Baldwin Hills and Beverly Hills.



## Table of Contents

Executive Summary.....	3
1 Background .....	7
1.1 Inglewood Oil Field.....	7
1.2 Los Angeles Basin.....	7
2 Area of interest .....	8
2.1 Inglewood Oil Field.....	8
2.2 Los Angeles Basin.....	9
3 InSAR Data and Processing .....	10
3.1 SAR Data .....	10
3.2 InSAR Processing .....	10
3.2.1 Elevation .....	10
3.2.2 Line-of-sight (LOS).....	10
3.3 Corrections.....	11
3.3.1 Atmospheric Effects .....	11
3.3.2 GPS Trend Removal.....	11
3.4 Uncertainties .....	11
4 Audit Summary .....	12
5 Inglewood Oil Field InSAR Results .....	13
5.1 2023 – 2024 Vertical Results .....	13
5.2 2023 – 2024 East-West Results .....	15
5.3 CSD Threshold.....	16
5.4 Time-Series Analysis.....	17
5.5 Extraction of Point Measurements.....	19
5.6 2010 – 2024 Ascending Results.....	24
5.7 Faulting .....	25
6 Los Angeles Basin InSAR Results.....	27
7 Conclusions.....	31
7.1 Inglewood Oil Field.....	31
7.2 Los Angeles Basin.....	31
8 Deliverables.....	31
8.1 Interpretation .....	32
9 Appendix A: (InSAR Technical Background) .....	33
9.1 SAR.....	33
9.1.1 Amplitude and Phase .....	33
9.2 Interferometry .....	34
9.2.1 Unwrapping.....	35
9.2.2 Coherence .....	35
9.2.3 Atmosphere.....	36
9.2.4 Stable Reference Area.....	36





9.2.5	Line-of-sight (LOS).....	36
-------	--------------------------	----

## Figures

Figure 1 – Optical Satellite image of the Inglewood Oil Field AOI. White polygon = CSD boundary. ....	8
Figure 2 - Total area processed with LA Basin AOI in red and Inglewood Oil Field AOI in white.....	9
Figure 3 – Vertical displacement for IOF AOI with contours at 0.25-inch intervals (June 2023 – July 2024). The black star represents the chosen reference point (NOPK). ....	14
Figure 4 – East-West displacement with arrows indicating direction and magnitude of displacement (June 2023 – July 2024). The black star represents the chosen reference point (NOPK).....	15
Figure 5 – The regions with vertical (left panel) or East-West (right panel) displacement magnitudes greater than 0.6 inches (blue) or less than -0.6 inches (red). The black star represents the chosen reference point (NOPK). ....	16
Figure 6 - Locations of select survey monuments chosen for deformation time-series analysis. The black star represents the chosen reference point (NOPK). ....	17
Figure 7 - The time-series of vertical deformation for the survey points identified in Figure 6. ....	18
Figure 8 - Cumulative LOS displacement from October 2010 – July 2024. The contours represent 1-inch intervals. ....	24
Figure 9 – The vertical displacement overplotted with faults as white lines (June 2023 – July 2024). The black star represents the chosen reference point (NOPK). ....	25
Figure 10 – The East-West displacement overplotted with faults as white lines (June 2023 – July 2024). The black star represents the chosen reference point (NOPK). ....	26
Figure 11 – The vertical displacement for the LA Basin (June 2023 – July 2024). The black star represents the chosen reference point (NOPK). ....	28
Figure 12 – The East-West mean displacement rate for the LA Basin (June 2023 – July 2024). The black star represents the chosen reference point (NOPK). ....	29
Figure 13 – The Cumulative displacement along the ascending LOS for the LA Basin (June 2023 – July 2024). The black star represents the chosen reference point (NOPK). ....	30
Figure 14 – Diagram showing the phase and amplitude of a radar wave .....	33
Figure 15 – Diagram illustrating various scattering types.....	33
Figure 16 – Surface deformation detected using InSAR.....	34
Figure 17 – Interferogram spanning the Bam earthquake on December 26, 2003 .....	35
Figure 18 – Phase unwrapping .....	35
Figure 19 – An area of low coherence (top left) and medium/high coherence (centre) across an example site. ....	36
Figure 20 – Descending viewing geometry .....	36
Figure 21 – A diagram showing how sloped surfaces create variations in pixel spacing. ....	37
Figure 22 – An example of radar layover and shadow.....	37

## Tables

Table 1 – The sensitivity vectors for InSAR results produced with Sentinel-1 data. ....	10
Table 2 – Uncertainty estimates. ....	12
Table 3 – Audit summary.....	12
Table 4 - InSAR derived annual vertical displacement values at the survey monuments. ....	20
Table 5 - InSAR derived annual East-West displacement values at the survey monuments. ....	22
Table 6 - InSAR derived annual ascending LOS displacement values at the survey monuments.....	23

## Copyrights

InSAR data, document, images © Viridien | Viridien Satellite Mapping 2024 unless otherwise specified.





## Acronyms

<b>AGMS</b>	Accumulated Ground Movement Study
<b>AOI</b>	Area of Interest
<b>APS</b>	Atmospheric Phase Screen
<b>Bperp</b>	Perpendicular Baseline
<b>CR</b>	Corner Reflector
<b>CSD</b>	Community Standards District
<b>DEM</b>	Digital Elevation Model
<b>DifSAR</b>	Differential Synthetic Aperture Radar Interferometry
<b>Envisat</b>	Environmental Satellite
<b>ERS</b>	European Remote Sensing Satellite
<b>ETM+</b>	Enhanced Thematic Mapper Plus
<b>FM O&amp;G</b>	Freeport-McMoRan Oil & Gas
<b>GIS</b>	Geographic Information System
<b>GPS</b>	Global Positioning System
<b>InSAR</b>	Interferometric Synthetic Aperture Radar
<b>IOF</b>	Inglewood Oil Field
<b>LA</b>	Los Angeles
<b>LiDAR</b>	Laser Imaging Detection and Ranging
<b>LOS</b>	Line-of-Sight
<b>PS</b>	Persistent Scatterer(s)
<b>PSI</b>	Persistent Scatterer InSAR
<b>RMS</b>	Root-mean-square
<b>SAR</b>	Synthetic Aperture Radar
<b>SCIGN</b>	Southern California Integrated GPS Network
<b>SNR</b>	Signal to Noise Ratio
<b>SPR</b>	Sentinel Peak Resources
<b>SRTM</b>	Shuttle Radar Technology Mission
<b>TSD</b>	Time-series DifSAR
<b>USGS</b>	United States Geological Survey
<b>UTM</b>	Universal Transverse Mercator
<b>WP</b>	Work Package



# 1 Background

This report presents surface deformation results derived using satellite InSAR, including details of the digital deliverables and an overview of InSAR processing necessary to fully understand the data.

This report will highlight the latest vertical and East-West horizontal displacement results from June 2023 to July 2024, as well as that of the ascending line-of-sight displacement, which offers long-term context from October 2010 through to July 2024.

## 1.1 Inglewood Oil Field

In October 2008, the LA County Board of Supervisors adopted the Baldwin Hills Community Standards District (CSD), which established new development standards and operating procedures for the Inglewood Oil Field (IOF). The aim of the CSD is to provide a means of implementing regulations, safeguards and controls for activities related to drilling for and production of oil and gas within the oil field. These regulations will ensure that oil field operations are conducted in harmony with adjacent land uses and to minimise the potential adverse impact of such operations.

The LA County planning document and standards require the oil field operator to develop an annual ground movement (subsidence and/or uplift/rebound) monitoring plan as part of an effort to increase field production. The ordinance requires that the operator monitor (survey) both vertical and horizontal ground movement throughout the field and that the survey results are analysed in relation to oil field activities such as production, steam and/or water injection (waterflooding).

In 2010 an Accumulated Ground Movement Study (AGMS) was conducted by Plains Exploration and Production (PXP) in accordance with the CSD. In 2013, PXP were acquired by Freeport-McMoRan Oil & Gas (FM O&G). The AGMS serves as a reference baseline for future annual monitoring surveys. Between 2010 and 2013, yearly DifSAR monitoring surveys were carried out.

In 2013 the scope of work was enhanced, involving a change in SAR data source from the RADARSAT-2 satellite to TerraSAR-X, and a consequent change in processing methodology, with the aim of maximising the temporal and spatial information across the IOF.

In 2015, further enhancements were made incorporating TerraSAR-X SAR data from 2010-2012 and 2015, resulting in a continuous dataset from October 2010 to December 2015. Additionally, TerraSAR-X SAR data from July 2014 to December 2015 was acquired from a different viewing angle, allowing the two SAR datasets to be combined to resolve vertical and East-West horizontal deformation. Effective January 1<sup>st</sup> 2017 Sentinel Peak Resources (SPR) acquired FM O&G's onshore California assets, including the IOF.

In 2017, the scope of work involved a change in SAR data source from the TerraSAR-X satellite to Sentinel-1, and a consequent change in processing methodology, with the aim of maximising spatial information across the IOF.

In December 2021, one of the satellites in the Sentinel constellation, Sentinel-1B, malfunctioned and the European Space Agency determined it could not be recovered. Sentinel-1A is still acquiring data across this site in both the ascending and descending orbits. However, the loss of Sentinel-1B increased the temporal revisit time from 6-days to 12-days. The sampling rate still provides robust coverage of the Area of Interest and Viridien does not propose altering the imaging acquisition plan for ongoing monitoring.

For this update, the Sentinel-1 data is appended to the TerraSAR-X data to create a continuous dataset in the ascending line-of-sight from October 2010 to July 2024, as well as vertical and East-West horizontal datasets from July 2014 to July 2024.

## 1.2 Los Angeles Basin

In addition to the requirements of work conducted for the IOF area of interest (AOI), this report includes an expansion of the area of analysis to include the wider LA Basin area. Although not part of the regulatory requirements, this places the displacement observed within the IOF AOI into a wider context, to aid interpretation of the results within a regional setting.



## 2 Area of interest

### 2.1 Inglewood Oil Field

The AOI is an approximately 5 x 5-mile area centred on Baldwin Hills, Los Angeles County, California (Figure 1). The site is surrounded by the urban infrastructure of the nearby Baldwin Hills community. The CSD boundary is an area of approximately 2.5 square miles centrally located within the AOI.

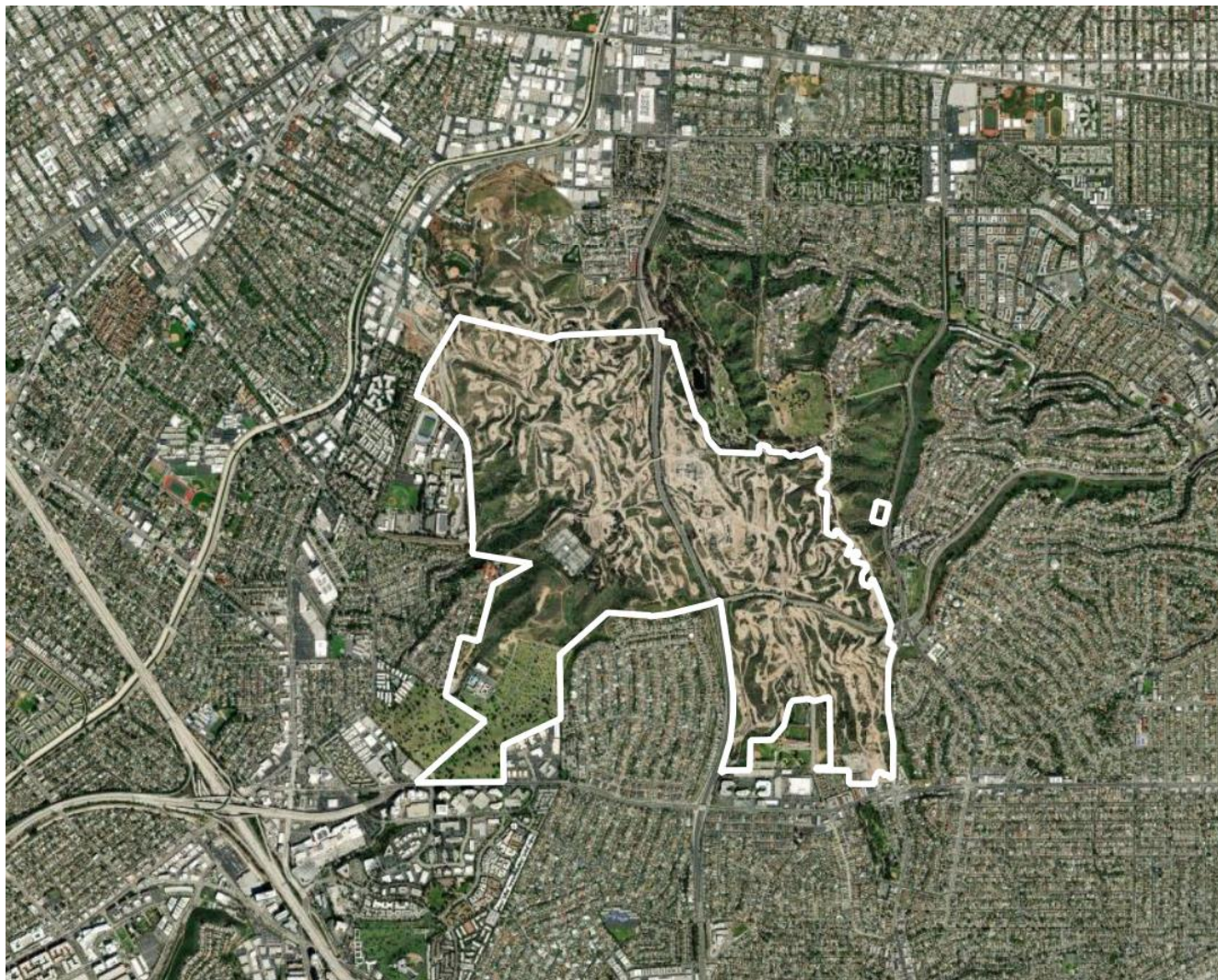


Figure 1 – Optical Satellite image of the Inglewood Oil Field AOI. White polygon = CSD boundary.

© Viridien 2024. Contains modified Copernicus Sentinel data 2024 Background image: © Esri, DigitalGlobe, GeoEye, Earthstar Geographics, CNES/Airbus DS, USDA, USGS, AeroGRID, IGN, and the GIS User Community.





## 2.2 Los Angeles Basin

The two SAR data footprints acquired for the monitoring of the IOF AOI each cover an area of approximately 150 x 150 miles over the LA Basin (Figure 2). In addition to the analysis performed on the smaller IOF AOI, a wide-area deformation result has been processed across the joint extents of the TerraSAR-X footprints as per the previous reporting period and the Sentinel-1 footprints acquired for this reporting period.

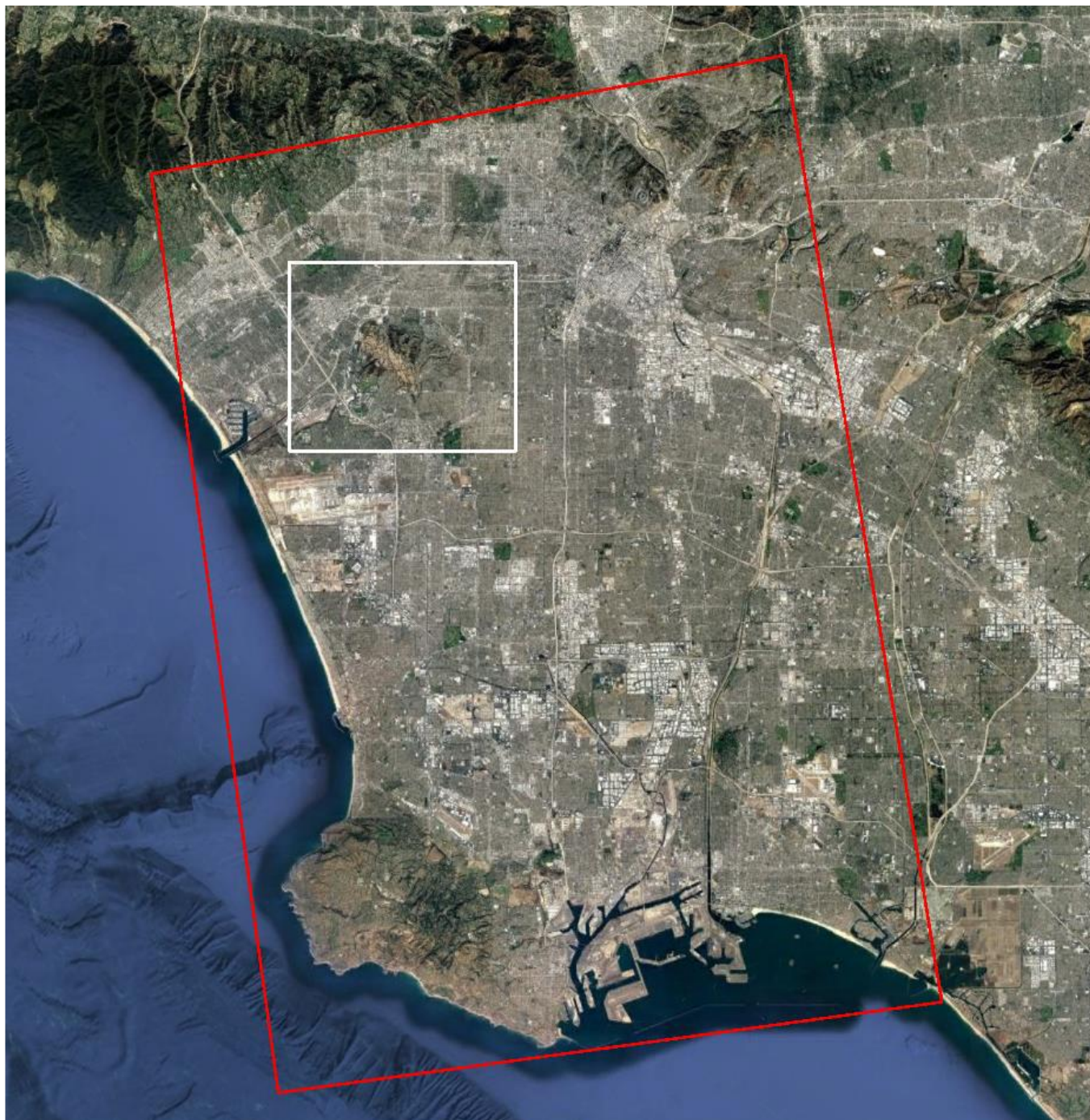


Figure 2 - Total area processed with LA Basin AOI in red and Inglewood Oil Field AOI in white.

© Viridien 2024. Contains modified Copernicus Sentinel data 2024 Background image: © Esri, DigitalGlobe, GeoEye, Earthstar Geographics, CNES/Airbus DS, USDA, USGS, AeroGRID, IGN, and the GIS User Community.



### 3 InSAR Data and Processing

#### 3.1 SAR Data

The processing utilised 664 SAR images acquired by the Sentinel-1 satellites between 27<sup>th</sup> March 2015 and 1<sup>st</sup> July 2024. All previous SAR data acquired by TerraSAR-X has also been incorporated into the analysis.

#### 3.2 InSAR Processing

InSAR processing of two SAR images separated in time provides a measure of the ground displacement which occurred over that time period (details of InSAR methodology can be found in Appendix A: (InSAR Technical Background)). This is termed an interferogram. Combining multiple interferograms, spanning different but overlapping time periods, it is possible to link these into a network. This forms a continuous time series of measurements, giving displacement measurements for each SAR image. It is also possible to use the large volume of data to mitigate a number of error sources, typically increasing the accuracy of the measurements down to sub-centimetric levels.

Distributed scatterers (DS) are comprised of multiple low or moderate responses within a SAR image pixel, typically corresponding to natural targets (e.g. ground surface, rocky outcrops etc.). Point scatterers (PS) are comprised of a single strong response within a SAR pixel, typically corresponding to man-made structures (e.g. buildings, artificial reflectors, pipelines etc.).

In this case, processing is a combination of DS from Sentinel-1 and PS from TerraSAR-X. The PS are mapped onto the DS locations (with averaging applied where applicable). The results provide average annual motion rates as well as multi-year motion histories via a time-series. InSAR is capable of mapping millimetric to decimetric annual motion rates, with millimetric precision.

##### 3.2.1 Elevation

Correcting for topography is an important step in InSAR processing. Initial corrections for the effects of topography within the processing used a LiDAR DEM (acquired in 2021) merged with the USGS 30 m Shuttle Radar Topography Mission (SRTM) DEM outside of the LiDAR acquisition area (which was primarily focused on the CSD).

##### 3.2.2 Line-of-sight (LOS)

InSAR measures displacement towards or away from the satellite, along an inclined line-of-sight (LOS). This inclined LOS means that InSAR does not measure the 3D (up, north and east) motion, but rather the combination expressed in the LOS. The Sentinel-1 data used in this work was acquired using both the ascending and descending orbits, imaging the AOI down a LOS from the west and the east respectively. The incidence angles and LOS bearings can be found in Table 1.

The sensitivity vectors below describe how 3D motion is translated into LOS. For example, 1 mm of vertical uplift would be measured as 0.83 mm in the Sentinel-1 ascending InSAR results, and 1 mm of eastward movement would be measured as - 0.54 mm. Interpreting InSAR results should be done with an appreciation of these sensitivity vectors.

Satellite	Incidence angle	Line of sight bearing	Unit Sensitivity Vectors		
			Up	North	East
Sentinel-1 (Ascending)	34°	77°	0.83	-0.13	-0.54
Sentinel-1 (Descending)	39°	283°	0.78	-0.14	0.61

Table 1 – The sensitivity vectors for InSAR results produced with Sentinel-1 data.

Further information on LOS geometry and the implications can be found in Section 9.2.5 in the Appendix.



### 3.3 Corrections

In this study, two corrections were adopted to account for atmospheric effects and inaccuracies in the modelled satellite orbits.

#### 3.3.1 Atmospheric Effects

Residual atmospheric influence can be a particular issue in areas with large contrasts in topographic relief. These signals are typically related to atmospheric stratification, where higher areas ‘poke up’ through low-level moist air into dryer air above. This gives a characteristic relationship between apparent deformation signals and topographic height, which allows calculation and subtraction of an empirical correction.

It is possible that lateral variations in atmospheric moisture can bias this empirical correction and leave residual artefacts in areas of topography. Time-series measurements in these areas are likely to contain higher levels of atmospheric influence and are also more likely to suffer from bias in the mean displacement rate due to seasonal and inter-year variations. During processing, such signals were noted across the Palos Verdes Hills and Santa Monica Mountains in many of the SAR epochs. Calculation of the empirical correction was adjusted to minimise residual influence; however, the correction is challenging to apply and has resulted in a reduction in coverage over the Palos Verdes Hills.

#### 3.3.2 GPS Trend Removal

Inaccuracies in models of the satellite orbits, and wide-scale gradients in atmospheric moisture, have the potential to result in biases within the InSAR results. Typically, these are small when using Sentinel-1 data due to the superior orbit control, however when present they take the form of approximately planar gradients.

Since these gradients affect the whole image, it is usually possible to use non-deforming areas to calculate and remove a very good empirical correction for these effects. However, in the LA Basin, most of the area is affected by deformation from a variety of sources, and it is not possible to identify sufficient stable areas.

To correct the result, an alternative approach has been used; records from SCIGN continuous GPS stations distributed across the footprint were utilised to calculate velocities for each location during the InSAR timespan. These velocities were considered relative to the North Park (NOPK) station used as reference for the InSAR processing, to remove the effects of wide-scale tectonic motion relative to continental North America. Velocities for each GPS station were calculated and subtracted from the measured InSAR displacement rates. A small planar gradient correction was then calculated based on a least-squares minimisation of these differences.

### 3.4 Uncertainties

InSAR data, just like data from any other measurement technique, has associated uncertainties. These uncertainties are assumed to be normally distributed and quantified using standard deviation. This means that the true value will be within one standard deviation of the measured value 68% of the time, two standard deviations 95% of the time, and three standard deviations 99.7% of the time. Any interpretation of the InSAR data should be performed with an appreciation for these uncertainties.

The SCIGN cGPS data detailed in Section 3.3.2 provides validation against an independent dataset; these measurements have their own uncertainties, however for well-maintained continuous GPS these are expected to be low, and this is considered the most reliable method to evaluate uncertainties of the InSAR results. InSAR mean displacement rates have been compared to calculated GPS velocities for each result and the standard deviation of the difference provides an estimate of the upper bound on the uncertainty in the InSAR results (which relies on an assumption the GPS is error free).

Time-series are more susceptible to short-term atmospheric artefacts and as such, the uncertainty associated with the displacement values is greater than for the mean displacement rates. For example, the time-series measurements will generally vary within the specified uncertainties so small-scale changes should not be over-interpreted.





Result	Period	Misfit to cGPS (one standard deviation)
Ascending LOS	Oct 2010 – Jul 2024	± 0.03 in
Vertical result	May 2014 – Jul 2024	± 0.04 in
	Jun 2023 – Jul 2024	± 0.16 in
Horizontal result	May 2014 – Jul 2024	± 0.02 in
	Jun 2023 – Jul 2024	± 0.10 in

Table 2 – Uncertainty estimates.

## 4 Audit Summary

General details	
Name of site	Baldwin Hills and LA Basin
Point(s) of contact (SPR)	David Budy - dbudy@sentinelpeakresources.com
Point(s) of contact (Viridien)	Ben Conway-Jones – ben.conway-jones@viridiengroup.com
Site details	
Location of site	Los Angeles, United States
Area of interest	Inglewood Oil Field
Audit details	
Data used	
• DEM data	LiDAR (2021) merged with SRTM
• SAR (radar) type & resolution	Sentinel-1 (~20 m resolution) TerraSAR-X (~3 m resolution)
• SAR (radar) date range	Ascending LOS: Oct 2010 to July 2024 Dual LOS: May 2014 to July 2024
InSAR processing technique	DifSAR and PS combination
Reference point location	Lat.: 33.9797 Lon.: -118.3480 (NOPK GPS station)
Measurement accuracy	See Table 2.
Measurement precision range	Millimetric
Key comments & observations	
• InSAR processing	Three InSAR results are presented. Firstly, a one-year dual-LOS result from 25/06/2023 to 01/07/2024. Secondly, a long-term dual-LOS result from 02/07/2014 to 01/07/2024. This result is not presented in the report, but data files are provided as .xyz deliverables and on the SatExplorer InSAR portal. Finally, a long-term single-LOS result from 07/10/2010 to 01/07/2024. Since only the ascending LOS is used, it is not possible to provide the vertical and horizontal components.
• InSAR results	In the one-year result, uplift up to 1.45 inches is observed within the CSD and subsidence is observed on the eastern edge of the CSD of -0.75 inches. The East-West displacement generally corresponds to these uplift and subsidence features.

Table 3 – Audit summary.



## 5 Inglewood Oil Field InSAR Results

This section presents three InSAR results generated from the input SAR data. There are 2023 – 2024 vertical deformation results and 2023 – 2024 East-West deformation results, which cover the temporal period 25<sup>th</sup> June 2023 to 1<sup>st</sup> July 2024. There is also a cumulative ascending LOS deformation result spanning 7<sup>th</sup> October 2010 to 1<sup>st</sup> July 2024. Additional information on the interpretation of the data and results can be found in Appendix A: (InSAR Technical Background).

This section is not designed to replace detailed analysis performed on the digital deliverables; however, it provides an overview of broad trends in the results. Any interpretation of the results should be carried out with an appreciation of the uncertainties associated with the data outlined in Section 3.4.

### 5.1 2023 – 2024 Vertical Results

The vertical displacement spanning the period 25<sup>th</sup> June 2023 to 1<sup>st</sup> July 2024 is shown in Figure 3.

Analysis of the 12-month vertical displacement over 2023 – 2024 shows an uplift trend in the center of the CSD and a subsidence trend on the eastern edge of the CSD, in contrast with the dominating subsidence trend seen in the previous report. It is important to note that these results are examined for a 12-month interval (summer-summer), rather than the 18-month report for 2019-2020 and winter-winter 12-month intervals prior to that.

This vertical uplift displacement from June 2023 to July 2024 reaches a maximum of approximately 1.75 inches. The vertical subsidence to the East reaches a maximum of -0.75 inches. We explore the displacement time series at select survey monument locations in Figure 6. Further away from the CSD, around the boundaries of the AOI, there are several low-magnitude wide-scale variations in displacement. These may relate to other natural or anthropogenic processes such as groundwater variations, groundwater abstraction and pumping, and oil field production activity. There is the possibility that some of these low-magnitude signals may represent residual atmospheric artefacts.



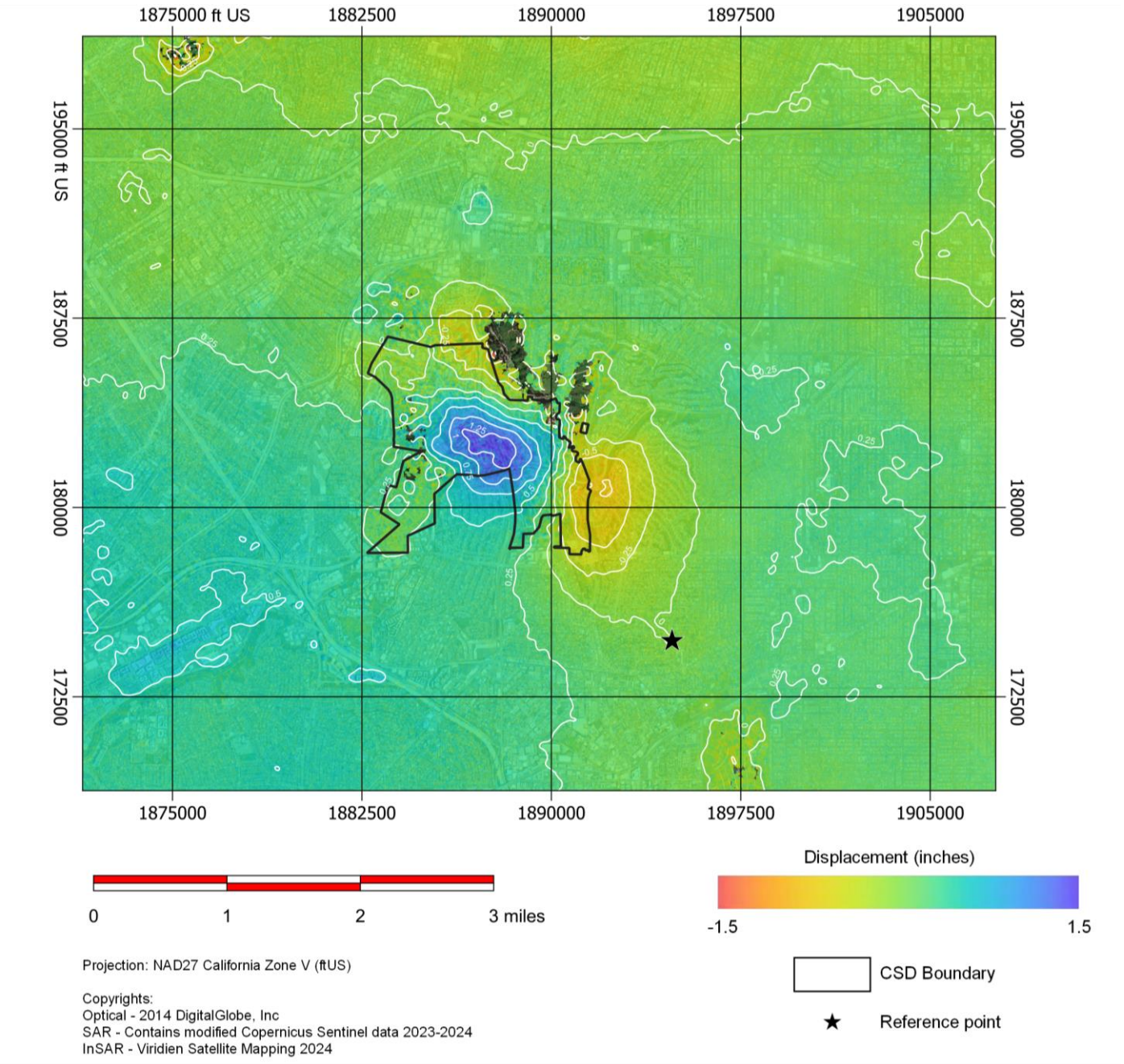


Figure 3 – Vertical displacement for IOF AOI with contours at 0.25-inch intervals (June 2023 – July 2024). The black star represents the chosen reference point (NOPK).



## 5.2 2023 – 2024 East-West Results

The East-West displacement spanning 25<sup>th</sup> June 2023 to 1<sup>st</sup> July 2024 is shown in Figure 4. Blue colours indicate displacement eastwards while orange and red colours indicate displacement westwards. Arrows representing the direction and magnitude of deformation have been included to assist interpretation.

From June 2023 to July 2024, East-West displacement generally corresponds with the deformation features seen in the vertical results. Specifically, contraction aligns with the centre of the subsidence feature on the eastern edge of the CSD and the outward movement aligns with the centre of the uplift feature within the CSD. The maximum rates are approximately 0.53 inches in the westerly direction and 0.96 inch in the easterly direction over the one year period.

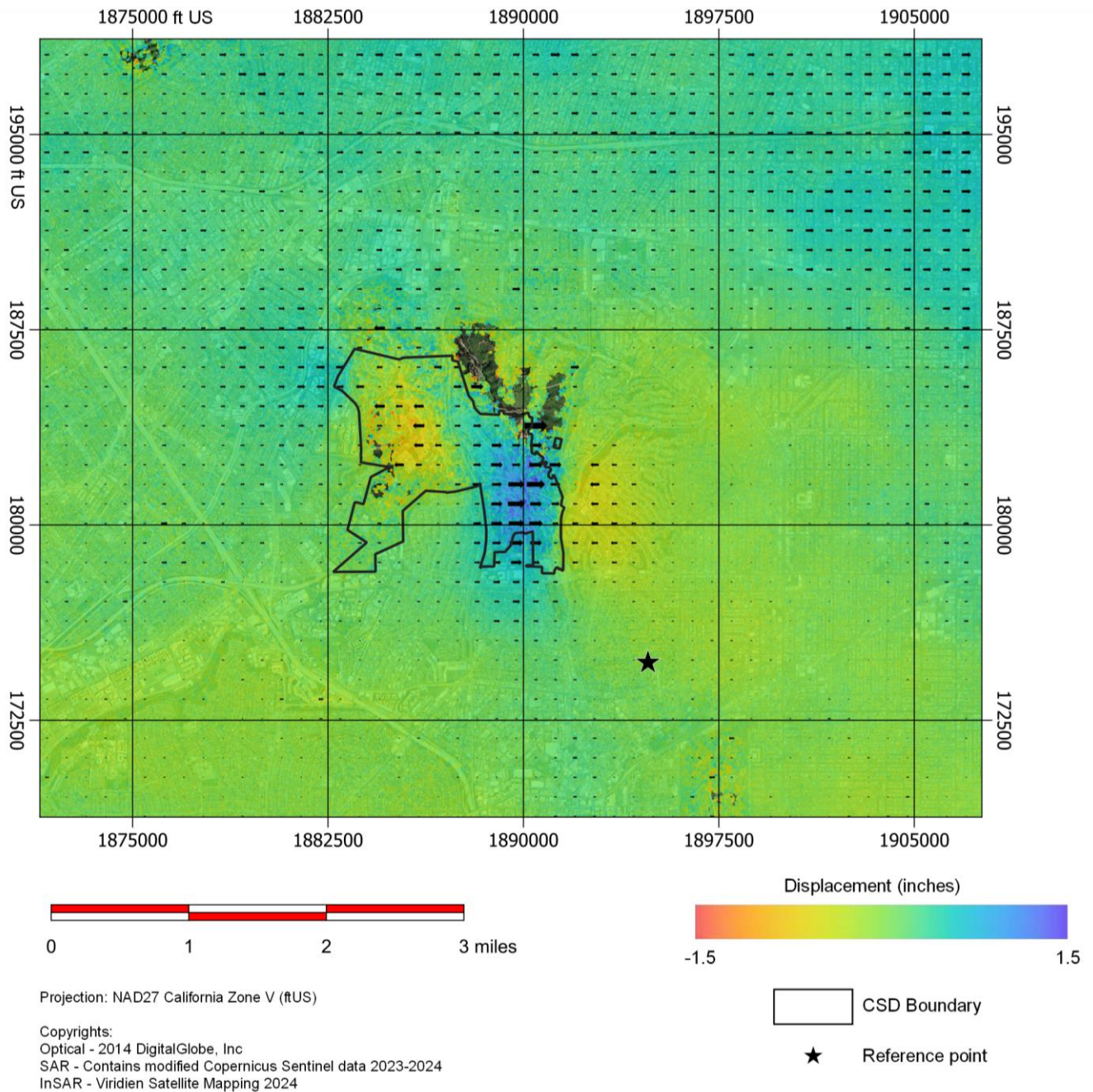


Figure 4 – East-West displacement with arrows indicating direction and magnitude of displacement (June 2023 – July 2024). The black star represents the chosen reference point (NOPK).





### 5.3 CSD Threshold

The CSD has set a deformation threshold of  $\pm 0.6$  inches. This threshold has been applied to the 2023 – 2024 vertical and East-West results, with the resulting graphic (Figure 5) depicting areas within the IOF AOI that exceed this threshold. Areas experiencing displacement more than -0.6 inches (subsidence or westerly displacement) are styled in red and areas experiencing displacement more than +0.6 inches (uplift or easterly displacement) are styled in blue.

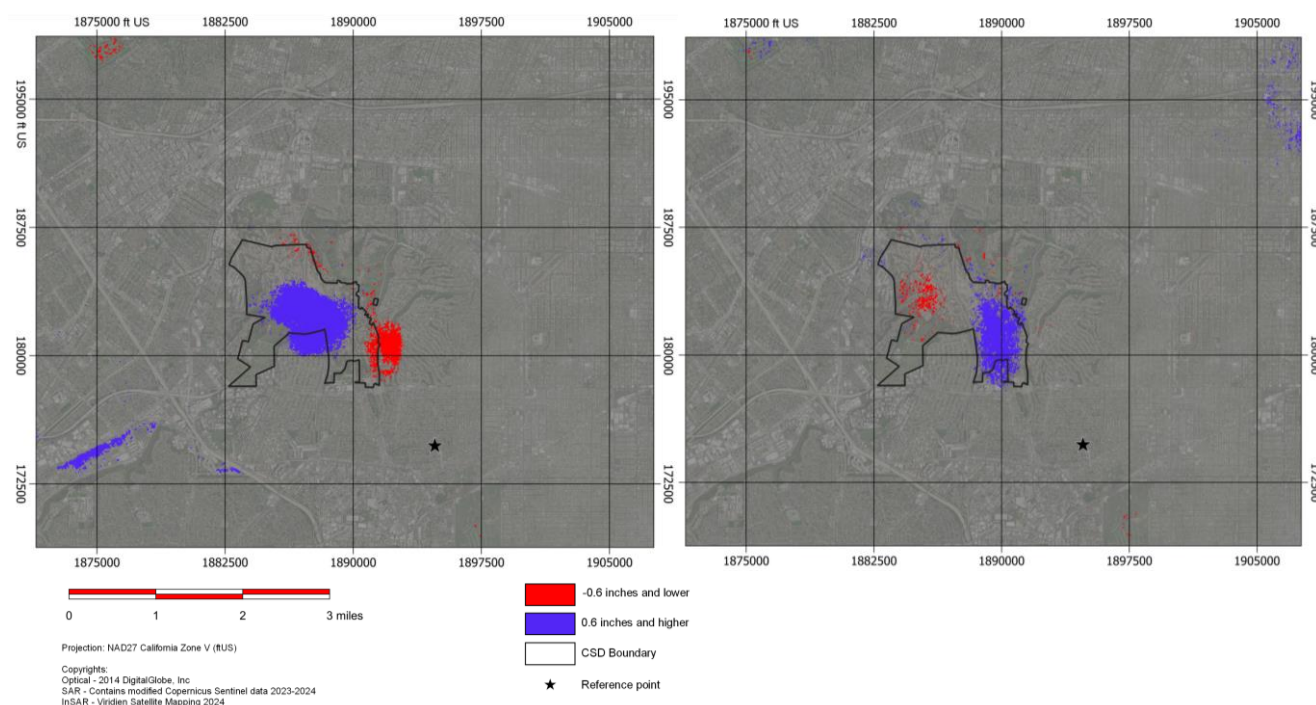


Figure 5 – The regions with vertical (left panel) or East-West (right panel) displacement magnitudes greater than 0.6 inches (blue) or less than -0.6 inches (red). The black star represents the chosen reference point (NOPK).



## 5.4 Time-Series Analysis

In addition to displacement rate maps, InSAR processing can provide a time-series for each SAR epoch with a displacement measurement for a given location. The time-series of six select survey monuments (identified in Figure 6) are shown in Figure 7. These time-series are generated from the average displacement in a 350 ft radius around each survey monument location.

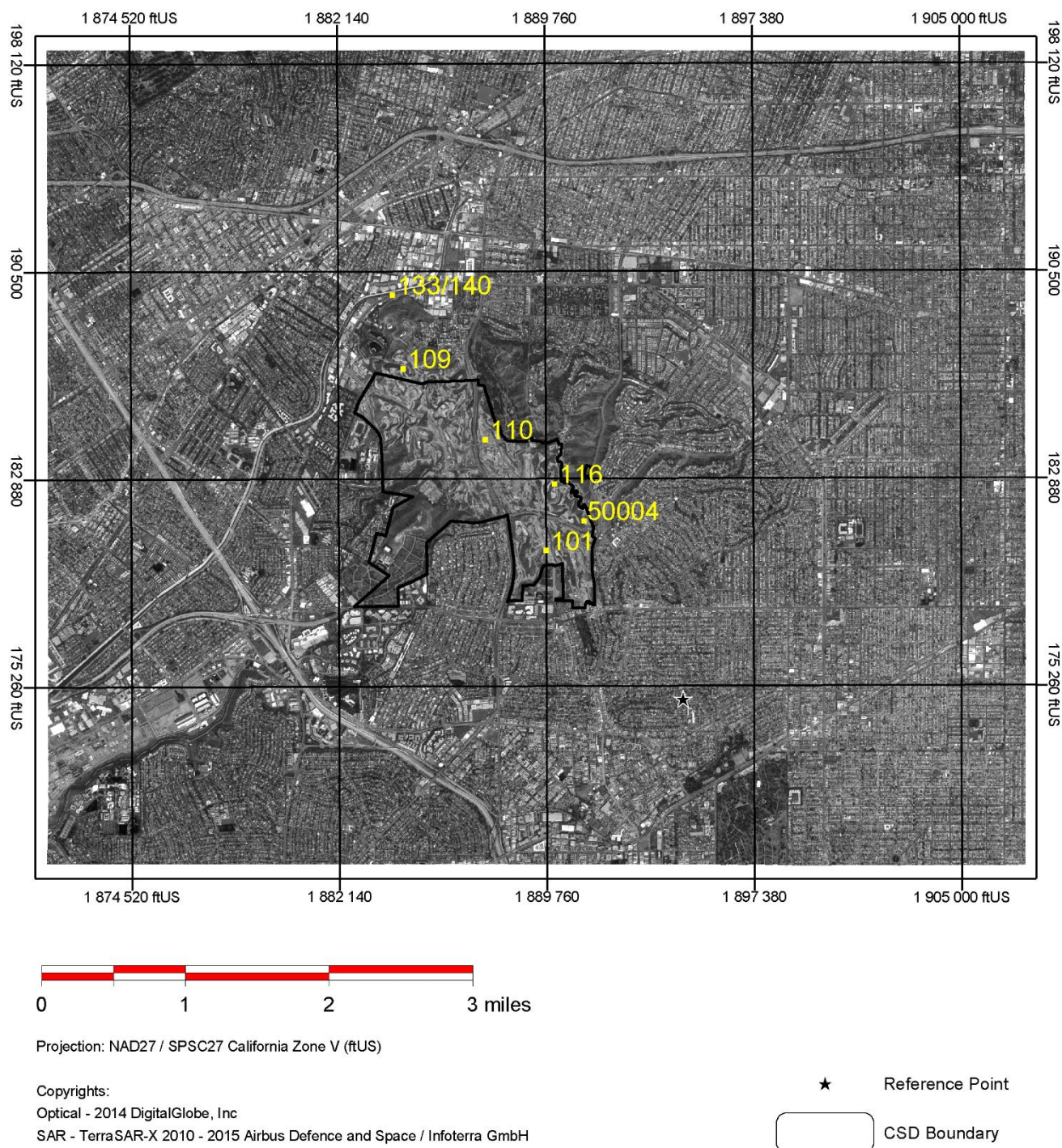


Figure 6 - Locations of select survey monuments chosen for deformation time-series analysis. The black star represents the chosen reference point (NOPK).

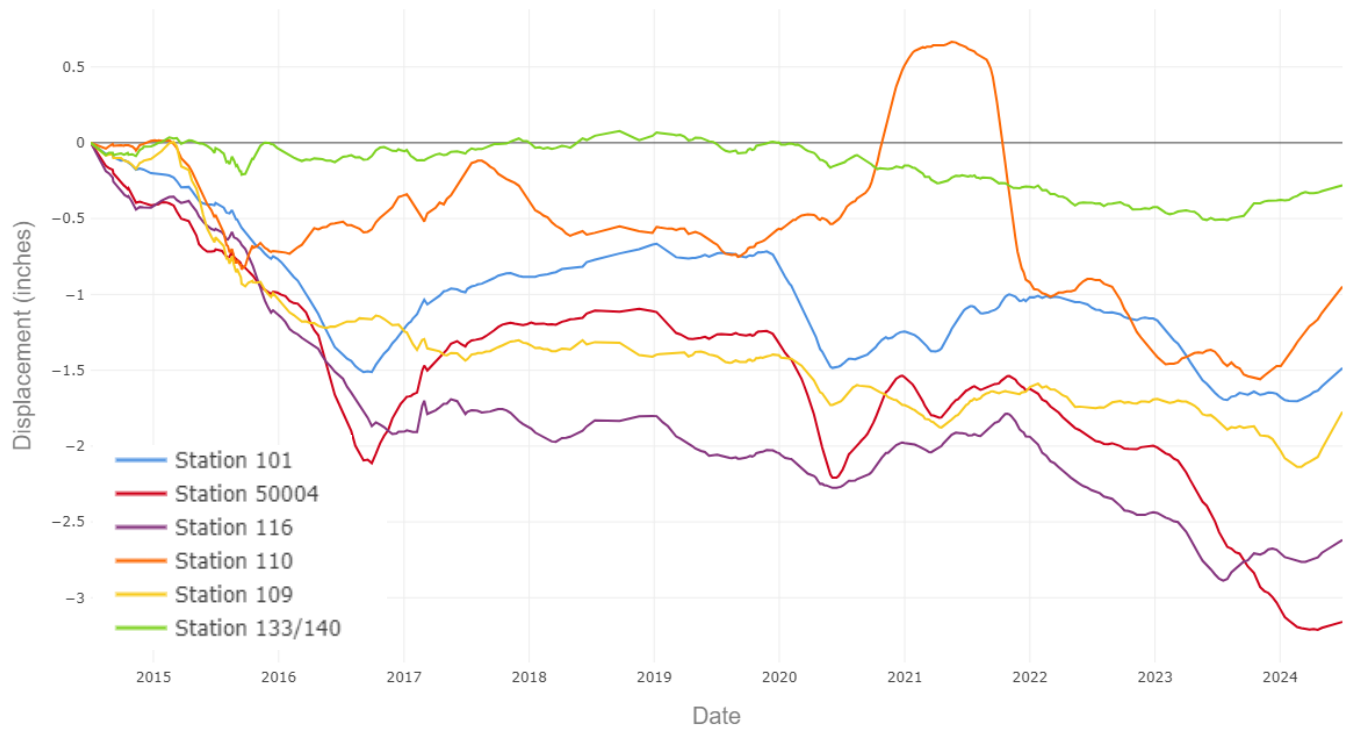


Figure 7 - The time-series of vertical deformation for the survey points identified in Figure 6.





## 5.5 Extraction of Point Measurements

InSAR data has been extracted at survey monuments by applying a radius of ~350 ft around each one and taking the average of the displacement, allowing a cross-comparison between survey results and InSAR. ***These values supersede those of the previous reports; any differences stem reprocessing of the time series data to improve redundancies.***

Annual vertical displacement at survey points derived from InSAR (inches)									
STATION ID	2015 Vertical	2016 Vertical	2017 Vertical	2018 Vertical	2019/2020 Vertical	2020/2021 Vertical	2021/2022 Vertical	2022/2023 Vertical	2023/2024 Vertical
101	-0.525	-0.230	0.193	0.167	-0.681	0.352	-0.016	-0.520	0.178
102	-0.212	-0.060	0.171	0.006	0.038	0.245	0.031	-0.168	-0.040
103	-0.159	-0.104	0.205	0.036	-0.113	0.277	-0.099	-0.106	-0.292
104	-0.235	0.051	0.148	0.042	-0.037	0.065	-0.430	-0.260	0.129
105	-0.171	0.043	0.290	0.047	-0.057	0.219	-0.040	0.073	-0.562
106	-0.317	-0.166	0.248	-0.080	-0.161	0.479	-0.177	-0.222	-0.612
107	-0.121	0.036	0.040	0.042	-0.039	0.177	0.043	-0.205	0.387
108	-0.590	0.219	-0.079	-0.063	0.124	0.150	-0.460	-0.288	-0.141
109	-0.958	-0.240	-0.055	-0.029	-0.346	-0.026	-0.020	-0.093	0.031
110	(null)	(null)	(null)	(null)	(null)	(null)	(null)	(null)	(null)
111	-0.038	0.296	-0.292	-0.096	-0.395	0.338	0.055	-0.220	-0.053
112	0.059	0.115	-0.203	-0.078	-0.195	0.083	0.092	-0.177	0.341
113	-0.103	-0.101	0.023	0.087	-0.199	-0.075	-0.002	-0.054	0.204
114	-0.099	-0.056	-0.075	0.051	-0.178	0.009	0.063	0.012	0.257
116	-0.731	-0.651	-0.226	0.105	-0.345	0.342	-0.370	-0.548	0.228
117	-0.647	-0.226	0.297	0.210	0.062	0.561	-0.774	-0.434	0.167
118	-0.222	0.019	0.118	0.092	-0.185	0.146	0.074	-0.252	0.373
120	0.175	0.085	-0.210	-0.019	-0.423	0.045	0.060	-0.152	0.197
121	-0.080	-0.070	-0.112	0.062	-0.476	0.029	0.115	-0.078	-0.024
122	-0.244	-0.121	-0.003	0.065	-0.306	-0.107	0.050	-0.044	0.140
123	-0.023	0.147	-0.158	0.004	0.069	0.443	-0.120	-0.236	0.591
126	-0.748	-0.243	0.100	0.267	-0.099	0.563	-0.497	-0.566	0.822
127	-0.075	-0.016	0.076	0.050	0.017	0.091	0.040	-0.115	0.261
128	-0.302	-0.067	0.448	-0.001	-0.356	0.447	-0.127	-0.034	-0.839
129	-0.107	0.042	0.318	0.019	-0.082	0.193	-0.045	-0.022	-0.457
130	-0.032	-0.030	0.061	-0.005	-0.078	0.070	-0.124	-0.127	-0.024
131	-0.068	-0.026	0.066	0.023	-0.099	-0.027	-0.219	-0.189	0.010
132	-0.104	0.012	0.031	0.045	-0.105	-0.052	-0.151	-0.164	0.117
133	-0.031	-0.030	0.086	0.103	-0.184	-0.081	-0.168	-0.105	0.234
134	-0.122	-0.103	-0.058	0.102	-0.182	-0.063	0.039	0.022	0.162
135	-0.055	-0.051	-0.034	0.105	-0.140	-0.032	0.019	0.017	0.236



Annual vertical displacement at survey points derived from InSAR (inches)									
136	-0.143	-0.142	-0.088	0.042	-0.220	0.009	-0.027	0.006	0.300
137	-0.128	-0.110	-0.098	-0.018	-0.139	0.005	0.004	0.017	0.378
138	-0.029	0.000	-0.018	-0.006	-0.064	0.085	-0.002	-0.101	0.295
139	-0.320	-0.409	-0.051	0.110	-0.009	0.180	-0.299	-0.270	0.075
201	-0.008	-0.033	0.068	0.072	-0.004	0.027	0.039	-0.012	0.234
202	-0.170	-0.124	-0.079	0.047	-0.204	-0.002	-0.075	0.063	0.357
203	-0.038	-0.082	0.091	0.053	-0.202	-0.018	-0.128	-0.082	0.219
204	-0.090	-0.102	-0.012	-0.010	-0.130	-0.101	-0.152	-0.097	0.122
205	-0.164	0.059	-0.079	-0.008	-0.066	-0.199	-0.184	0.137	0.168
206	-0.039	-0.084	0.106	0.066	-0.204	-0.029	-0.141	-0.105	0.240
50000	0.026	0.535	-0.395	-0.170	0.244	1.054	-0.666	-0.143	0.818
50002	-0.119	0.252	-0.312	0.144	0.086	0.784	-0.457	-0.284	1.139
50003	-0.871	-0.312	0.017	0.204	-0.695	0.263	0.041	-0.562	0.617
50004	-0.599	-0.594	0.306	0.049	-0.916	0.521	-0.322	-0.519	-0.662
50010	-0.165	0.033	0.114	0.046	-0.088	0.011	-0.328	-0.247	0.077
301	-0.241	-0.060	0.166	0.003	0.027	0.255	0.039	-0.142	-0.093
302	-0.822	-0.283	0.048	0.185	-0.696	0.268	0.059	-0.559	0.591
303	-0.587	-0.596	0.322	0.007	-0.925	0.512	-0.332	-0.565	-0.702
304	-0.726	-0.692	-0.238	0.125	-0.408	0.350	-0.349	-0.504	0.153
305	-0.113	0.004	0.033	0.039	-0.117	-0.061	-0.152	-0.170	0.122
306	-0.157	0.034	0.115	0.048	-0.074	0.040	-0.340	-0.250	0.094
307	-0.154	0.280	-0.385	0.189	-0.040	0.683	-0.389	-0.260	1.023
308	-0.005	0.578	-0.415	-0.186	0.212	1.084	-0.699	-0.215	0.654
309	0.039	0.296	-0.320	-0.072	-0.395	0.272	0.092	-0.215	0.005
310	0.054	0.118	-0.219	-0.109	-0.169	0.104	0.080	-0.172	0.344
311	-0.036	0.145	-0.389	-0.054	-0.615	0.038	0.047	-0.149	-0.050
312	0.070	-0.019	-0.136	0.030	-0.448	0.011	0.141	-0.152	0.073

Table 4 - InSAR derived annual vertical displacement values at the survey monuments.

Annual East-West displacement at survey points derived from InSAR (inches)									
STATION ID	2015 East/West	2016 East/West	2017 East/West	2018 East/West	2019/2020 East/West	2020/2021 East/West	2021/2022 East/West	2022/2023 East/West	2023/2024 East/West
101	0.082	0.286	-0.539	-0.061	0.100	-0.308	0.233	-0.226	1.022
102	0.087	0.071	-0.303	-0.085	-0.130	-0.185	-0.025	-0.255	0.672
103	-0.217	-0.030	0.050	0.128	-0.254	0.250	-0.173	-0.107	-0.271
104	-0.276	0.362	-0.158	0.001	0.110	0.283	-0.416	-0.179	-0.092
105	-0.157	0.127	0.258	0.064	-0.135	0.213	-0.098	0.073	-0.418



Annual East-West displacement at survey points derived from InSAR (inches)									
106	-0.166	-0.021	-0.004	-0.085	-0.200	0.238	-0.139	-0.290	-0.097
107	0.110	0.100	-0.401	-0.120	0.010	-0.165	-0.058	-0.001	0.322
108	-0.240	0.144	-0.434	-0.082	-0.070	-0.048	0.104	-0.068	-0.071
109	0.379	-0.161	-0.333	-0.005	-0.380	-0.542	0.270	0.078	0.080
110	0.169	0.418	-0.694	-0.219	0.097	0.308	-0.373	-0.104	0.390
111	0.235	-0.261	-0.294	-0.077	-0.595	-1.005	0.531	0.103	-0.241
112	-0.092	-0.177	-0.228	-0.107	-0.219	-0.422	0.132	-0.107	0.071
113	0.092	0.007	-0.323	-0.015	-0.113	-0.171	0.107	-0.077	0.229
114	-0.062	-0.029	-0.262	-0.016	-0.048	-0.300	-0.124	0.005	0.244
116	-0.129	0.141	-0.538	0.037	0.019	0.160	-0.178	-0.308	0.662
117	-0.116	0.520	-0.220	0.006	0.232	0.580	-0.555	-0.320	0.655
118	0.172	0.148	-0.432	-0.071	-0.008	-0.162	-0.014	-0.110	0.591
120	-0.091	-0.335	-0.172	-0.036	-0.276	-0.589	0.076	0.091	0.042
121	0.079	-0.147	-0.272	-0.044	-0.032	-0.507	0.080	-0.007	0.303
122	0.346	0.002	-0.277	-0.025	-0.075	-0.261	0.113	-0.056	0.258
123	0.215	0.155	-0.376	-0.233	0.022	-0.264	-0.022	0.085	0.003
126	0.216	0.501	-0.455	-0.025	0.145	0.354	-0.328	-0.247	0.637
127	0.044	0.044	-0.297	-0.076	-0.106	-0.144	-0.054	-0.111	0.412
128	-0.276	0.202	0.320	0.112	-0.357	0.340	-0.171	0.052	-0.332
129	-0.139	0.136	0.329	0.092	-0.257	0.241	-0.106	0.026	-0.468
130	-0.040	0.048	-0.085	0.112	-0.078	0.062	-0.164	-0.071	-0.117
131	-0.135	0.144	-0.117	0.050	-0.046	0.000	-0.200	-0.108	0.072
132	0.031	0.138	-0.185	0.023	-0.025	-0.043	-0.039	-0.079	0.034
133	0.071	0.037	-0.307	-0.010	-0.146	-0.144	0.133	-0.035	0.164
134	-0.029	-0.010	-0.294	-0.014	-0.050	-0.200	-0.010	-0.050	0.260
135	-0.027	0.004	-0.243	-0.033	-0.056	-0.224	-0.085	-0.074	0.206
136	-0.071	0.040	-0.246	-0.017	-0.059	-0.238	-0.109	-0.006	0.177
137	-0.125	-0.009	-0.229	-0.034	-0.105	-0.252	-0.086	0.007	0.150
138	-0.075	-0.008	-0.286	-0.065	-0.115	-0.256	-0.043	0.018	0.161
139	-0.223	0.040	-0.239	0.053	0.147	0.205	-0.316	-0.298	0.404
201	-0.102	-0.018	-0.157	-0.059	-0.099	-0.101	-0.090	-0.079	0.264
202	-0.038	0.112	-0.271	-0.009	-0.033	-0.209	-0.065	0.001	0.063
203	0.019	0.041	-0.312	0.044	-0.094	-0.121	0.071	-0.032	0.148
204	0.050	0.119	-0.196	0.029	-0.089	-0.046	-0.021	-0.180	0.107
205	0.021	0.123	-0.162	0.004	-0.005	-0.012	0.012	-0.140	-0.054
206	-0.002	0.045	-0.241	0.019	-0.077	-0.128	0.062	-0.033	0.133
50000	0.491	0.061	-0.407	-0.267	-0.350	-0.762	0.624	0.168	-0.279





Annual East-West displacement at survey points derived from InSAR (inches)									
50002	0.613	0.299	-0.476	-0.327	0.181	-0.106	-0.015	0.182	-0.090
50003	0.119	0.378	-0.740	-0.055	0.206	-0.226	0.083	-0.175	1.001
50004	-0.338	-0.155	-0.398	0.072	-0.384	0.258	-0.157	-0.383	0.472
50010	-0.245	0.251	-0.157	0.002	0.027	0.129	-0.310	-0.153	-0.039
301	0.079	0.033	-0.278	-0.120	-0.132	-0.174	-0.034	-0.255	0.657
302	0.119	0.369	-0.725	-0.044	0.219	-0.249	0.126	-0.177	1.049
303	-0.341	-0.134	-0.370	0.062	-0.395	0.269	-0.185	-0.393	0.477
304	-0.120	0.060	-0.613	-0.018	0.095	0.134	-0.181	-0.322	0.749
305	0.002	0.145	-0.187	0.022	-0.025	-0.024	-0.062	-0.068	0.030
306	-0.254	0.268	-0.155	0.013	0.033	0.165	-0.333	-0.164	-0.033
307	0.639	0.238	-0.421	-0.300	0.282	-0.101	-0.066	0.164	-0.053
308	0.486	0.028	-0.460	-0.251	-0.424	-0.853	0.695	0.138	-0.269
309	0.166	-0.295	-0.297	-0.031	-0.573	-1.013	0.506	0.093	-0.249
310	-0.114	-0.171	-0.209	-0.090	-0.215	-0.437	0.132	-0.140	0.060
311	-0.390	-0.417	-0.228	-0.096	-0.400	-0.840	0.206	0.027	-0.189
312	-0.129	-0.158	-0.194	-0.070	-0.200	-0.569	0.087	0.026	0.162

Table 5 - InSAR derived annual East-West displacement values at the survey monuments.

Annual displacement at survey points derived from InSAR (inches)					
STATION ID	2010 Vertical equivalent	2011 Vertical equivalent	2012 Vertical equivalent	2013 Vertical equivalent	2014 Vertical equivalent
101	-0.379	-0.899	-0.511	0.644	0.075
102	-0.183	-0.073	0.104	0.580	-0.128
103	0.019	0.200	-0.098	0.134	0.153
104	0.294	0.069	0.178	0.041	0.095
105	-0.209	0.076	-0.039	-0.017	0.224
106	-1.124	-0.003	-0.125	0.461	-0.016
107	0.068	-0.234	0.066	0.097	-0.079
108	(null)	0.102	0.011	0.224	0.314
109	0.233	0.078	0.316	0.237	-0.065
110	-0.405	-0.418	-0.339	-0.089	-0.078
111	0.135	-0.245	-0.217	0.167	0.156
112	0.270	0.066	-0.246	0.024	0.097
113	0.525	0.427	-0.098	0.202	0.015
114	0.594	0.291	-0.172	-0.039	-0.031
116	-0.094	-1.174	-1.088	0.541	-0.295
117	-0.353	-0.594	0.300	-0.017	-0.102
118	0.082	-0.393	0.009	0.294	-0.045
120	0.260	0.145	-0.491	0.033	0.340



Annual displacement at survey points derived from InSAR (inches)					
STATION ID	2010 Vertical equivalent	2011 Vertical equivalent	2012 Vertical equivalent	2013 Vertical equivalent	2014 Vertical equivalent
121	0.372	0.475	-0.678	-0.037	0.375
122	0.375	0.683	-0.393	0.131	0.163
123	0.269	-0.475	0.056	-0.242	-0.225
126	-0.521	-1.185	-0.147	-0.050	-0.177
127	-0.019	-0.056	0.035	0.252	-0.032
128	-0.459	0.050	-0.113	-0.002	0.125
129	0.067	0.148	-0.047	-0.158	0.207
130	0.072	0.079	-0.087	-0.044	0.089
131	0.201	0.173	0.030	0.039	0.111
132	0.334	0.153	0.120	0.112	0.105
133	0.539	0.257	0.030	0.196	0.036
134	0.760	0.384	-0.143	0.043	0.021
135	0.769	0.294	-0.100	0.040	0.003
136	0.688	0.234	-0.091	-0.068	-0.077
137	0.378	0.172	-0.140	-0.085	-0.227
138	0.158	0.074	0.008	0.028	-0.043
139	0.183	-0.202	-0.120	0.352	-0.010
201	-0.112	0.059	0.047	0.206	-0.078
202	0.822	0.194	-0.137	-0.082	-0.031
203	0.725	0.173	-0.029	0.155	-0.159
204	-0.096	0.186	-0.064	0.001	-0.003
205	-0.403	-0.013	-0.057	-0.268	-0.106
206	(null)	0.109	-0.033	0.177	-0.106
50000	0.579	-0.549	-0.236	-0.311	-0.532
50002	0.560	-0.998	-0.133	-0.712	-0.503
50003	-0.321	-1.355	-0.904	0.674	-0.036
50004	-1.571	-0.357	-0.589	0.919	0.067
50010	0.503	0.134	0.164	0.113	0.110
301	-0.231	-0.104	0.108	0.535	-0.102
302	-0.350	-1.315	-0.888	0.652	-0.028
303	-1.550	-0.388	-0.599	0.900	0.055
304	-0.614	-1.112	-1.037	0.570	-0.259
305	0.323	0.147	0.129	0.129	0.107
306	0.447	0.151	0.150	0.097	0.094
307	0.461	-0.975	-0.212	-0.750	-0.422
308	0.289	-0.647	-0.312	-0.091	-0.358
309	0.249	-0.189	-0.278	0.173	0.192
310	0.219	0.038	-0.272	0.067	0.066
311	0.444	0.180	-0.560	0.064	0.338
312	0.460	0.325	-0.647	-0.013	0.413

Table 6 - InSAR derived annual ascending LOS displacement values at the survey monuments



## 5.6 2010 – 2024 Ascending Results

This section presents the cumulative displacement that occurred between October 2010 and July 2024 (Figure 8) found by combining the ascending LOS time series results from TSX and Sentinel-1 satellites. Within the CSD, the highest-magnitude cumulative LOS displacement reaches -4.5 inches (predominantly subsidence) from October 2010 to July 2024. Displacement away from the satellite occurs within the southeast CSD, and with two features of displacement towards the satellite just outside of the CSD to the north and south. Outside of the CSD, broad areas of lower magnitude subsidence and uplift are visible, which may be due to aquifer activity. However, the cause of this adjacent deformation activity would require further study to parse mechanisms.

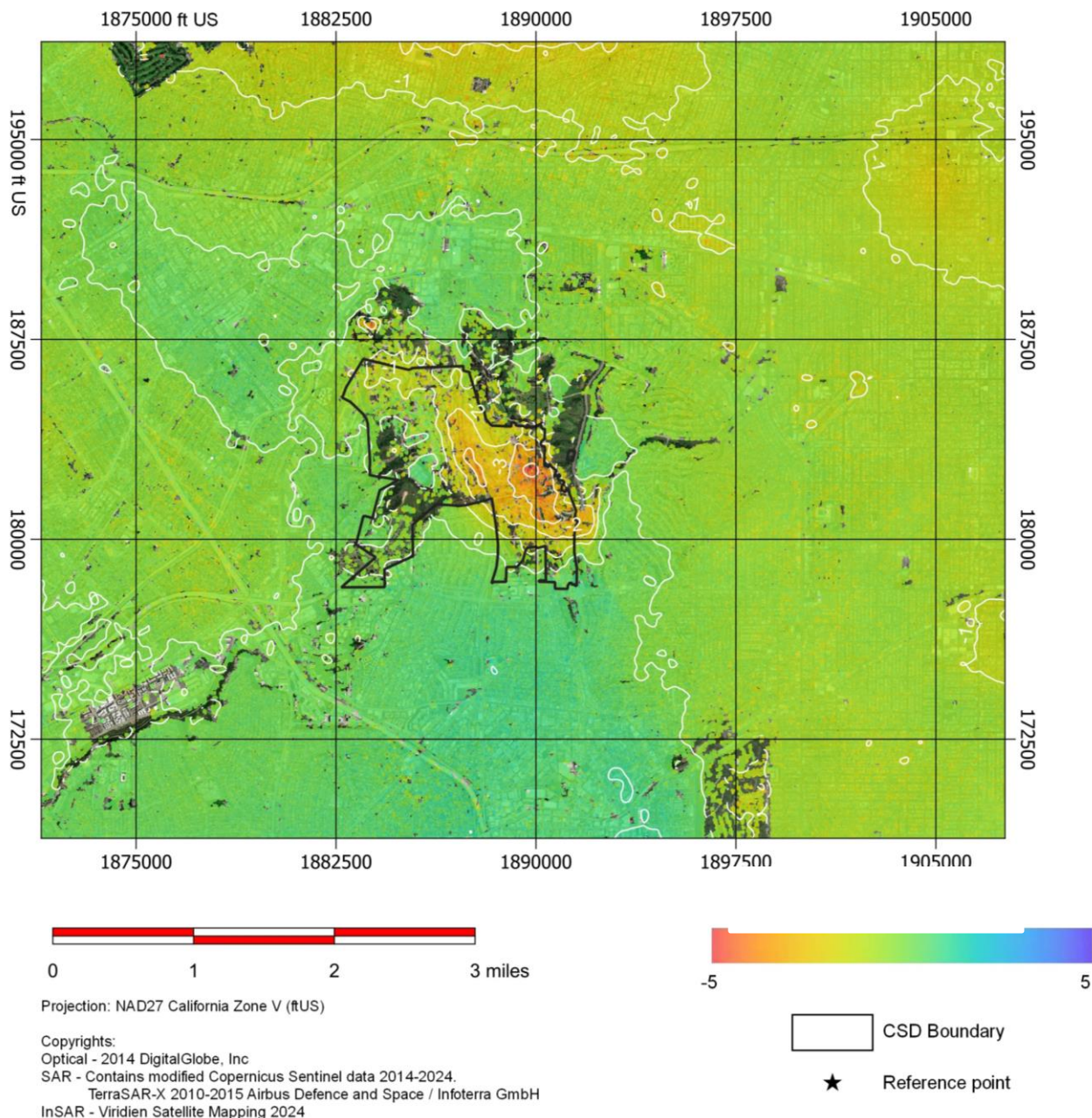


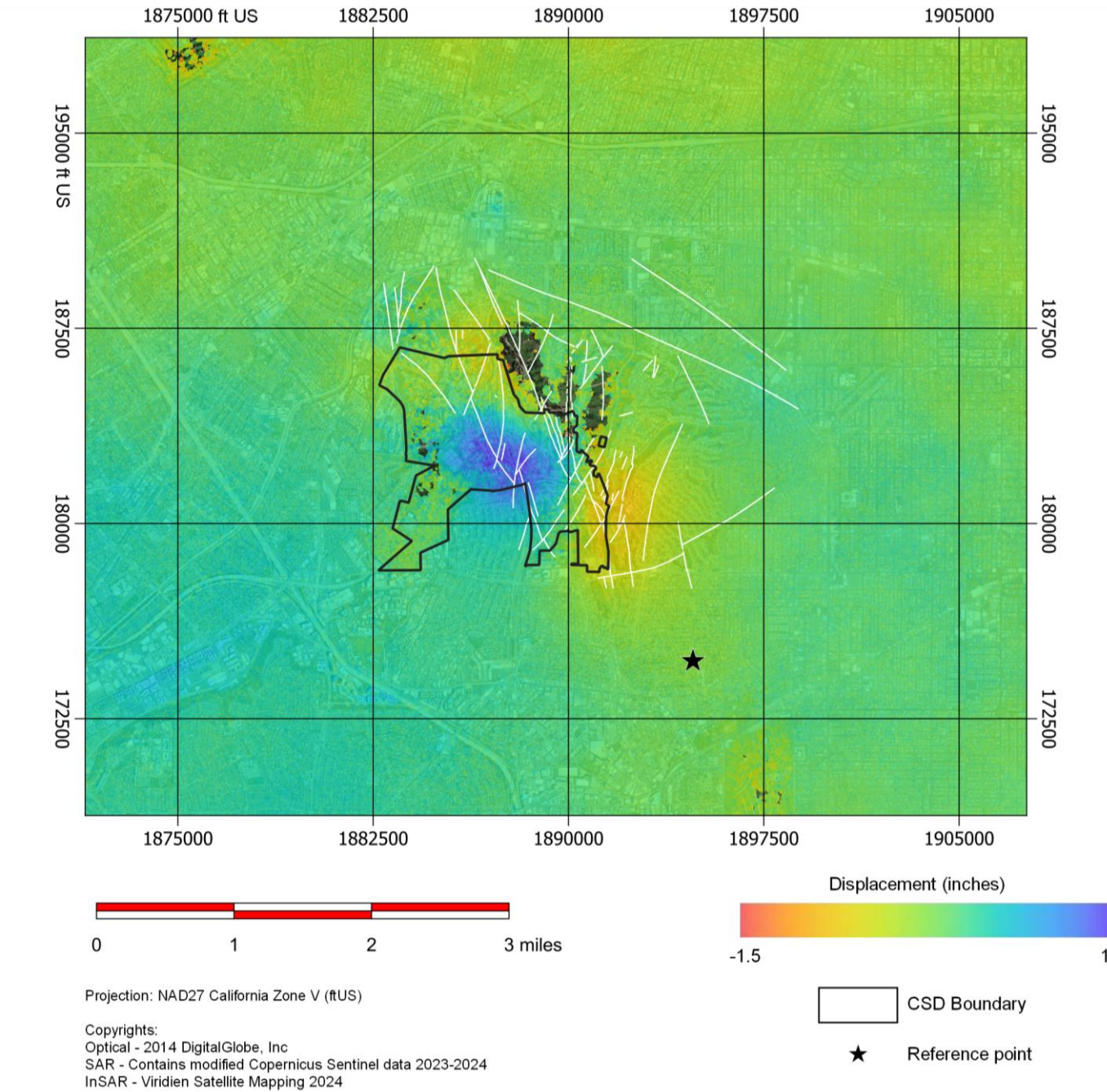
Figure 8 - Cumulative LOS displacement from October 2010 – July 2024. The contours represent 1-inch intervals.





5.7 Faulting

SPR supplied geological information for the IOF, including mapped and inferred faults associated with the Newport-Inglewood fault zone. The vertical displacement across 2023 – 2024 is mapped with inferred faults in Figure 9. The East-West displacement across 2023 – 2024 is mapped with inferred faults in Figure 10. There are no clearly visible discontinuities or abrupt changes in displacement gradient closely associated with mapped faults. However, the presence of displacement gradients in the vicinity of these faults means fault-related signals cannot be precluded, since such gradients could be caused by movement on faults below the surface, or detection could be limited by the spatial resolution of the InSAR data.



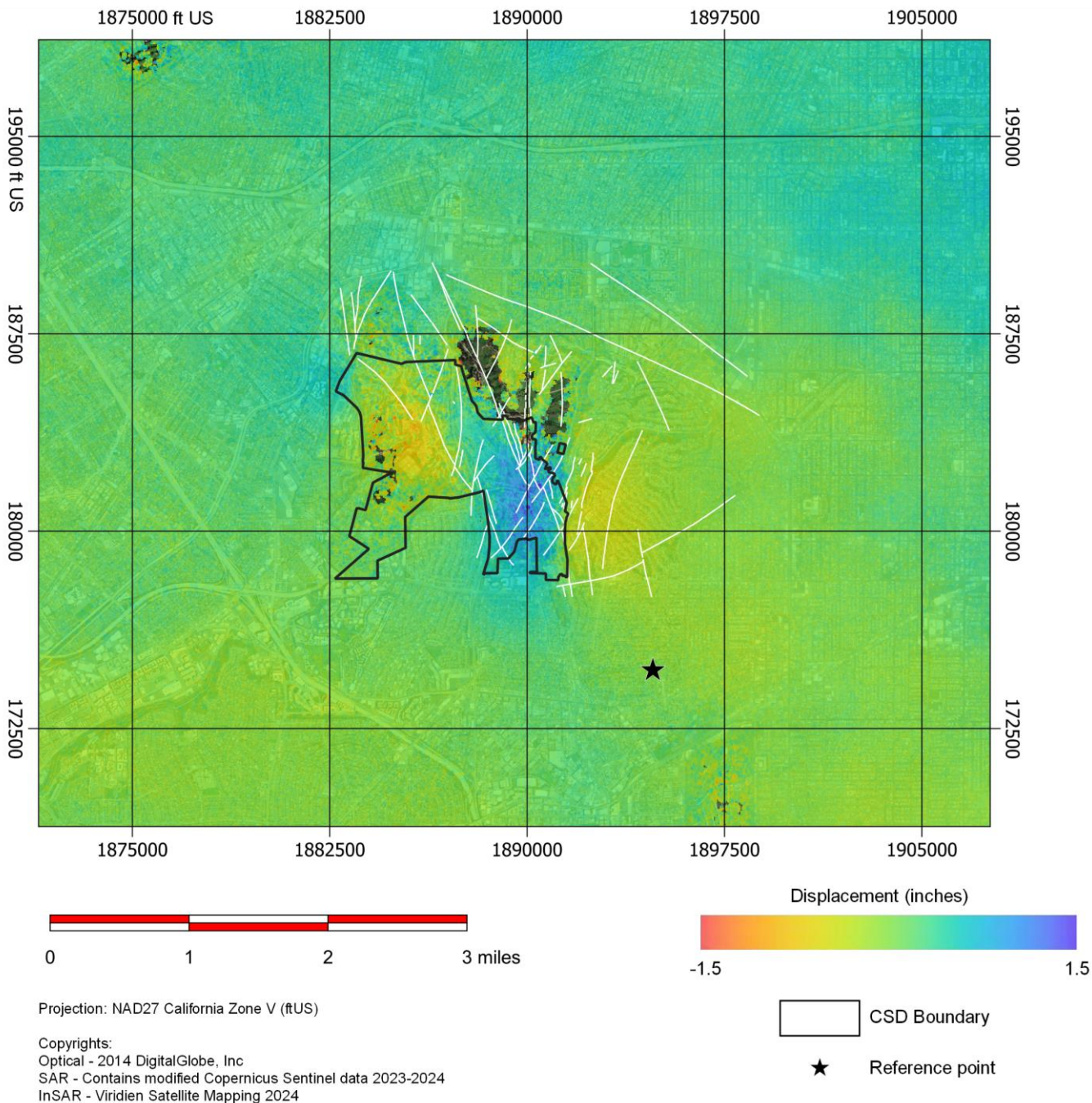


Figure 10 – The East-West displacement overplotted with faults as white lines (June 2023 – July 2024). The black star represents the chosen reference point (NOPK).





## 6 Los Angeles Basin InSAR Results

The Sentinel-1 footprints acquired to provide a deformation assessment of the IOF for the purposes of the Baldwin Hills CSD also cover the majority of the LA Basin. This wider dataset places the displacement signals seen within the IOF AOI into a wider context, and illustrates the complex interaction between the tectonic, hydrological, and anthropogenic sources of ground displacement in the region.

As outlined in Section 5, three results are provided:

- The 2023 – 2024 vertical displacement map (Figure 11)
- The 2023 – 2024 East-West displacement map (Figure 12)
- The 2010 – 2024 ascending LOS cumulative displacement map (Figure 13)

Several key areas around the LA Basin have been identified as areas of interest and were analysed within previous years' reports. A brief explanation of these areas has been included within this report to guide and aid any further analysis:

- InSAR continues to exhibit visible discontinuities present at various points along the trace of the Newport-Inglewood Fault, particularly towards the southern end. These appear to broadly coincide with the mapped traces of the en-echelon fault segments, separated by step-overs. The fault forms a hydrological barrier, with a sharp difference in displacement marking the boundary of the Santa Ana aquifer. The area to the east of the fault has long been noted in historical InSAR studies as an area of strong seasonal oscillations in ground displacement, because of groundwater variations in the aquifer.
- Oilfields in the Long Beach and Wilmington areas are in the latter stages of production, and are typically undergoing extensive enhanced recovery, including water injection.
- Beverly Hills has been highlighted as an area with several potential sources of deformation, including active oil fields and the intersection between the Santa Monica and Hollywood Faults and the northern extension of the Newport-Inglewood Fault. The location of, and relationship between, the different faults has been particularly controversial in recent years, with several high-profile development projects affected by this discussion amid renewed investigation of Alquist-Priolo zoning by the California Geological Survey.

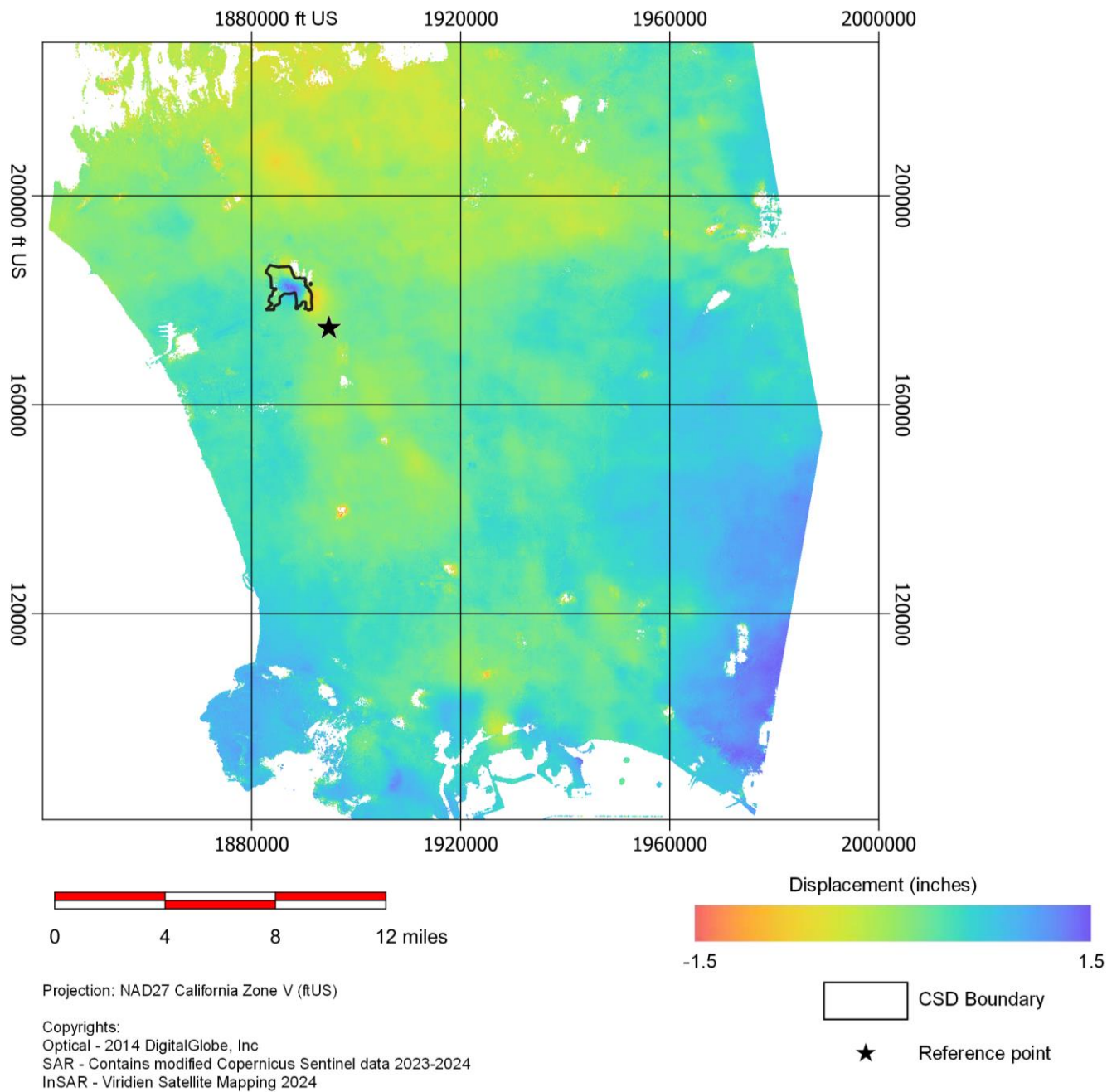


Figure 11 – The vertical displacement for the LA Basin (June 2023 – July 2024). The black star represents the chosen reference point (NOPK).



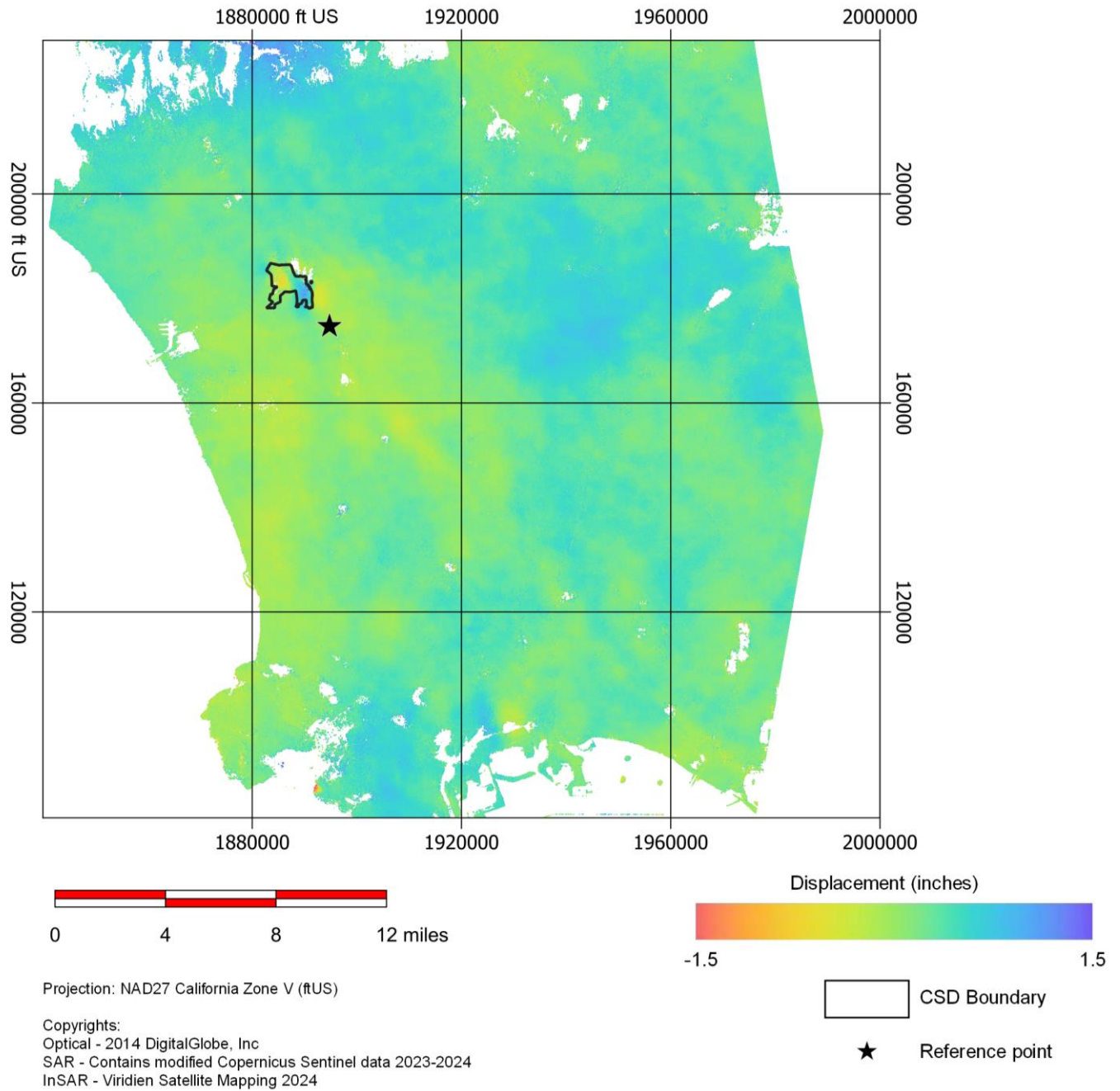


Figure 12 – The East-West mean displacement rate for the LA Basin (June 2023 – July 2024). The black star represents the chosen reference point (NOPK).

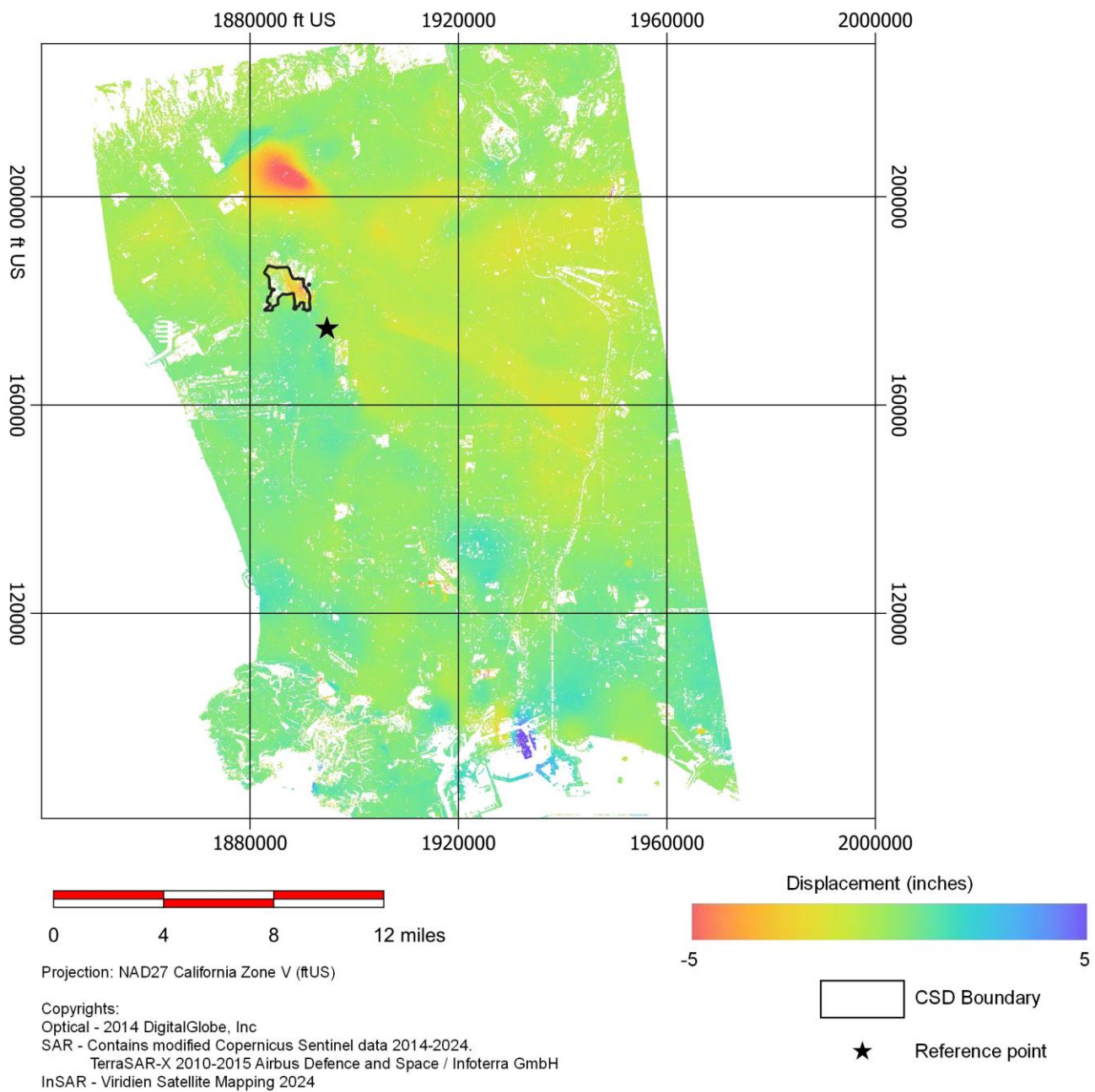


Figure 13 – The cumulative displacement along the ascending LOS for the LA Basin (June 2010 – July 2024). The black star represents the chosen reference point (NOPK).



## 7 Conclusions

### 7.1 Inglewood Oil Field

InSAR processing successfully added 63 Sentinel-1 images to the data stack, extending the time-series of measurements for the IOF by an additional period from 25<sup>th</sup> June 2023 to 1<sup>st</sup> July 2024. The data stack now totals 664 images between 27<sup>th</sup> March 2015 and 1<sup>st</sup> July 2024. All previous SAR data acquired by TerraSAR-X has also been incorporated into the long-term analysis.

Contours have been created which aim to assist with interpretation of the result, although it should be noted that the contouring process involves a degree of smoothing which can distort the appearance of the data. Arrows indicating magnitude and direction for the east-west result have been provided to assist with interpretation.

The period from June 2023 to July 2024 demonstrates:

- Uplift within the CSD reaching a maximum of approximately 1.45 inches
- Subsidence on the eastern edge of the CSD reaching a maximum of approximately -0.75 inches

These features are clear in the vertical displacement maps and are also indirectly seen in the East-West displacement maps. These results are a change from the trends seen in the previous report.

The cumulative ascending LOS displacement reaches an approximate maximum magnitude of -4.5 inches (predominantly subsidence) over the period from October 2010 to July 2024.

### 7.2 Los Angeles Basin

Over the greater Los Angeles Basin, the 2023 – 2024 interval shows complex fault constrained displacement is continuing near Beverly Hills and broad uplift trends are observed linked to Santa Ana aquifer (constrained by the Newport-Inglewood fault). Cumulatively from October 2010 to July 2024, the greatest displacements are similar to those observed in previous years, including the Santa Ana aquifer constrained along the Newport-Inglewood fault, Long Beach, Baldwin Hills and Beverly Hills. Continuous GPS data across the basin are incorporated again this year into the analysis, providing an independent validation of the InSAR results.

## 8 Deliverables

Our results are geo-referenced to high resolution optical imagery and subsequently re-projected to the client specified NAD27 datum with the State Plane California zone V (US Feet) projection (EPSG:26745). Grids are provided with 30 ft spacing over the Inglewood AOI and 600 ft spacing over the greater LA Basin, with displacement in inches. Viridien is providing the following deliverables:

- **XYZ\_deliverables**
  - Inglewood\_Vert\_2014\_2024\_NAD27\_inches\_30ft.xyz
  - Inglewood\_Vert\_2023\_2024\_NAD27\_inches\_30ft.xyz
  - Inglewood\_Horiz\_2014\_2024\_NAD27\_inches\_30ft.xyz
  - Inglewood\_Horiz\_2023\_2024\_NAD27\_inches\_30ft.xyz
  - Inglewood\_Asc\_2010\_2024\_NAD27\_inches\_30ft.xyz
  - LA\_Basin\_Vert\_2014\_2024\_NAD27\_inches\_600ft.xyz
  - LA\_Basin\_Vert\_2023\_2024\_NAD27\_inches\_600ft.xyz
  - LA\_Basin\_Horiz\_2014\_2024\_NAD27\_inches\_600ft.xyz
  - LA\_Basin\_Horiz\_2023\_2024\_NAD27\_inches\_600ft.xyz
  - LA\_Basin\_Asc\_2010\_2024\_NAD27\_inches\_600ft.xyz
- **Video\_deliverables**
  - SPR\_Vert\_2014-2024.mp4

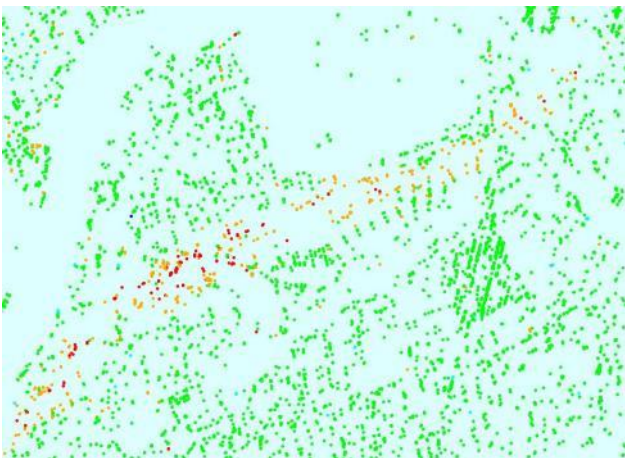


- SPR\_Vert\_2014-2024\_LA.mp4
- **Contour deliverables**
  - Inglewood\_Vert\_2023-2024\_NAD27\_contours.shp
- **SatExplorer Portal**
  - Rasters
    - 2023-2024 Vertical Displacement
    - 2023-2024 Horizontal Displacement
    - 2014-2024 Vertical Displacement
    - 2014-2024 Horizontal Displacement
    - 2010-2024 Ascending LOS Displacement
  - Timeseries Data
    - 2014-2024 Vertical Displacement
    - 2014-2024 Horizontal Displacement

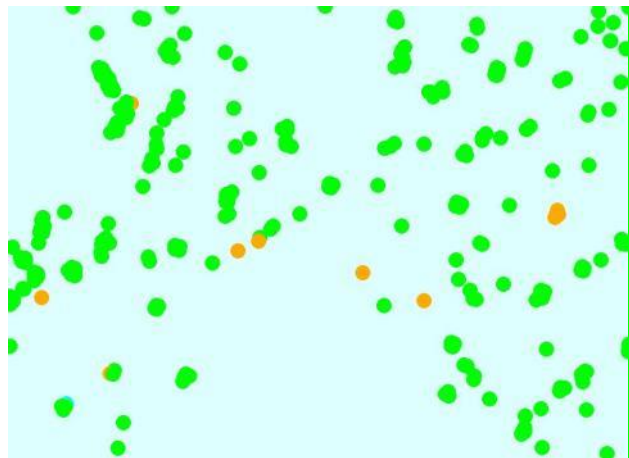
## 8.1 Interpretation

InSAR provides a complex dataset and users should consider the following information in any subsequent interpretations of the provided data:

- Deformation recorded for an individual or collection of DS points may represent motion of the surface, or of a feature on the ground, or most likely, a combination of the two. The deformation may be attributed to a variety of source factors.
- Users should consider the spatial and temporal consistency of motion exhibited by points when interpreting results. DS exhibiting significantly different levels of motion when compared to their surroundings are more likely to contain unresolved errors and be of lower accuracy than clusters exhibiting similar motion.



An example of a linear cluster of DS points all indicating similar deformation.



An example of isolated DS points showing different deformation compared to the surrounding PS points.

- If DS exhibit deformation, this does not mean that features across the study area are at risk. If DS are not moving away or towards the satellite, this does not mean they won't in the future.
- Analysis of displacement time-series may reveal episodic changes and or changes in acceleration of deformation. It is worth noting that displacement time-series may contain residual errors (such as uncompensated atmosphere) and are less precise than the mean displacement rate.

InSAR results should be analysed and interpreted alongside other complementary datasets.





## 9 Appendix A: (InSAR Technical Background)

### 9.1 SAR

SAR is a type of active remote sensing instrument that uses the microwave region of the electromagnetic spectrum. Although SAR instruments may be used in airborne or terrestrial contexts, for the applications considered here satellite-based SAR instruments predominate. SAR instruments transmit a series of radar pulses and record the reflections from the Earth's surface. This returned signal is then processed to form an image with each pixel containing the radar response of a particular location.

#### 9.1.1 Amplitude and Phase

A SAR signal can be imagined as a sine wave that contains amplitude and phase (Figure 14).

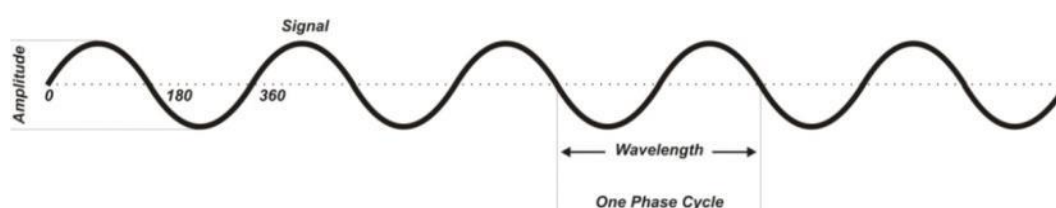


Figure 14 – Diagram showing the phase and amplitude of a radar wave

The amplitude is the strength of the radar response. This is typically affected by the backscatter characteristics of the surface. Smooth surfaces such as water typically yield low amplitude responses whereas rough surfaces reflect more of the radar signal back in the direction of the satellite yielding higher amplitude (Figure 15). Moisture content generally provokes significant changes in the dielectric properties of natural materials resulting in increased radar reflectivity i.e. electromagnetic wave penetration in an object is an inverse function of water content. SAR amplitude images are used for a wide variety of applications, including all-weather mapping, maritime monitoring, oil seep detection, and flood mapping.

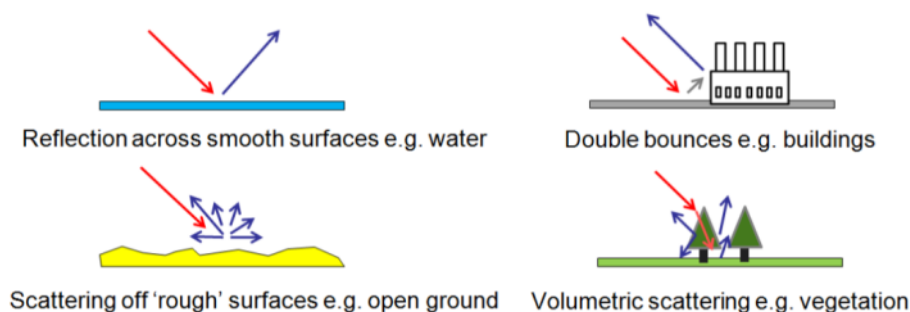


Figure 15 – Diagram illustrating various scattering types

Clockwise from top left: Smooth surfaces typically reflect the majority of the radar signal away from the satellite; Surfaces intersecting each other at 90° (for example buildings and infrastructure) can cause a double bounce, reflecting much of the signal back towards the satellite resulting in a bright response; Scattering from within dense vegetation canopies can cause complex reflection patterns with multiple bounces and a variable response; Rough surfaces scatter the radar wave in many directions, including a component back towards the satellite.

Distributed scatterers (DS) are comprised of multiple low or moderate responses within a SAR image pixel, typically corresponding to natural targets (e.g. ground surface, rocky outcrops etc.). Point scatterers (PS) are comprised of a single strong response within a SAR pixel, typically corresponding to man-made structures (e.g. buildings, artificial reflectors, pipelines etc.). InSAR processing techniques generally focus on deriving surface deformation from DS (such as DInSAR/DifSAR) and/or PS (such as PSI/PSInSAR™). For this study, processing focused upon analysing DS.





The phase is the fraction of a complete sine wave cycle (when the sine wave starts to repeat itself, one cycle of phase has occurred). Since the outgoing wave is produced by the SAR instrument, the phase is known, and can be compared to the phase of the return signal. The phase of a SAR signal depends on a complex interaction of surface properties, which vary from pixel to pixel, so a single SAR phase image appears to contain random noise.

## 9.2 Interferometry

Interferometry compares the phase values in different SAR images for the same point on ground, generating the interference between returned phase values to produce an interferogram.

If surface properties have stayed the same between the two SAR images the phase signals cancel out, leaving only the phase differences due to properties that have changed. Phase differences between SAR images appear in an interferogram as a series of 'fringes'. These fringes are directly related to the radar wavelength.

Differences in interferometric phase (phase shifts) can be caused by a number of factors, but the most important stems from changes in the path length (the distance to the ground and back) which is directly linked to topography and topographic change (i.e. deformation). The path length consists of a number of whole wavelengths plus some fraction of a wavelength. The total path length (i.e. the number of whole wavelengths) is not known, but the phase provides an extremely accurate measure of this extra fraction of a wavelength.

Satellite InSAR exploits the temporal separation between SAR data acquisitions, time periods in which deformation (movement towards or away from the SAR sensor) may have occurred (resulting in a phase shift). A pre-existing Digital Elevation Model (DEM) can be used to model and remove topographic contributions leaving behind the extra path difference that relates to surface deformation (together with some other contributions associated with atmosphere, satellite orbit and noise). Each 'fringe' in an interferogram is equivalent to a deformation magnitude of half the wavelength (since the wave travels the extra displaced distance on the way down to the ground and again on the way back up), along the inclined line-of-sight (LOS) viewing geometry of the satellite. Fringes can be thought of as contours of deformation, with more and tighter-spaced fringes representing greater and higher-gradient movement.

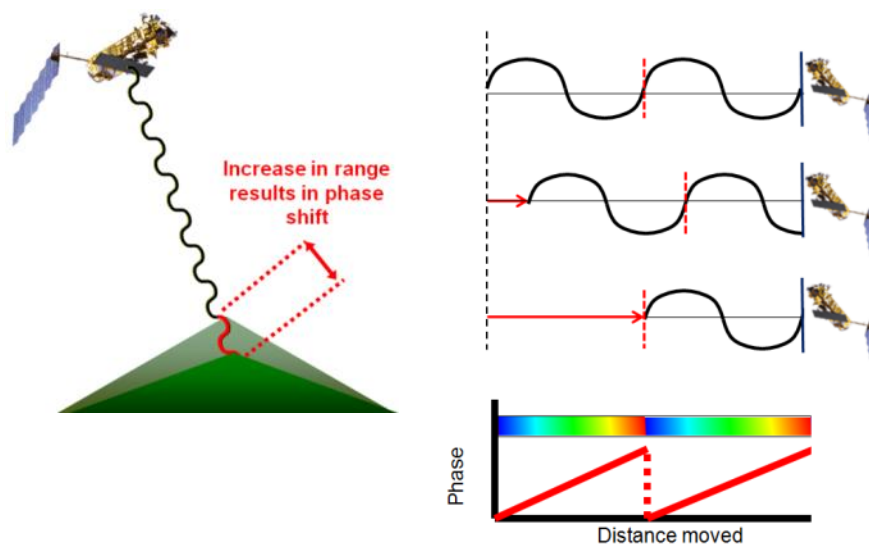


Figure 16 – Surface deformation detected using InSAR

Distributed scatterers (DS) are comprised of multiple low or moderate responses within a SAR image pixel, typically corresponding to natural targets (e.g. ground surface, rocky outcrops etc.). Point scatterers (PS) are comprised of a single strong response within a SAR pixel, typically corresponding to man-made structures (e.g. buildings, artificial reflectors, pipelines etc.). InSAR processing techniques generally focus on deriving surface deformation from DS (such as DInSAR/DifSAR) and/or PS (such as PSI/PSInSAR™). For this study, processing focused upon analysing DS.

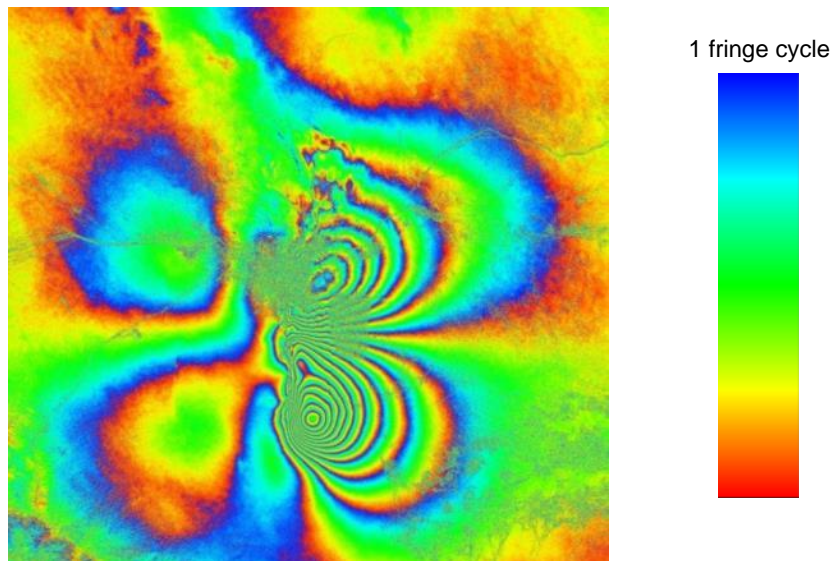


Figure 17 – Interferogram spanning the Bam earthquake on December 26, 2003

### 9.2.1 Unwrapping

As demonstrated in Figure 16, the phase only provides a measure of the residual fraction of a wavelength yet the total amount of deformation at a point also depends on how many complete cycles of phase have occurred, i.e. how many complete fringes are present between that point and a stable reference area. This is often referred to as the phase ambiguity. Where fringes are clearly resolved, they can be 'unwrapped' to produce a continuous deformation field. This involves finding the correct number of whole phase cycles that have occurred, relative to a chosen reference point, and can be considered analogous to 'summing the contours' (Figure 18).

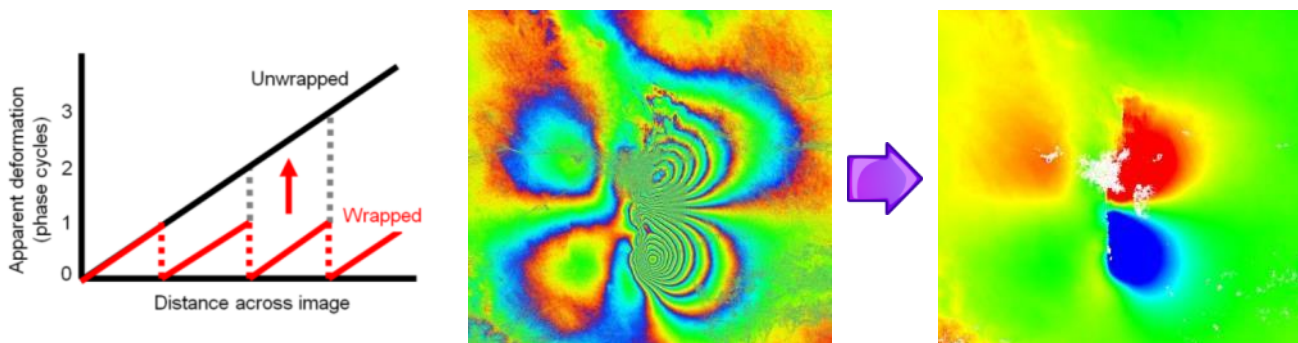


Figure 18 – Phase unwrapping

Graph showing apparent deformation (red) for a number of phase cycles/fringes, and the resulting unwrapped deformation once the phase ambiguities are taken into account (left). A 'wrapped' interferogram and unwrapped interferogram showing a continuous deformation field (centre & right).

### 9.2.2 Coherence

Coherence is a measure of the local spatial variability, for example over a 5x5 image pixel window, over the period spanned by an interferogram. Where variability of the ground surface is low, for example building roofs, deserts and arid areas, good quality measurements are obtained, and these areas are described as having high coherence. Where that variability is high, due to for example, vegetation growth, snow and/or excavations, poor quality measurements are obtained, and these areas are described as having low coherence.

High coherence areas exhibit spatial consistency of the measurements allowing gradual changes to be reliably interpreted. Low coherence areas exhibit random changes from pixel to pixel and it is not possible for those changes to be reliably



interpreted. Low coherence areas are usually masked during processing and excluded from results. Examples of low and high coherence can be seen in Figure 19.

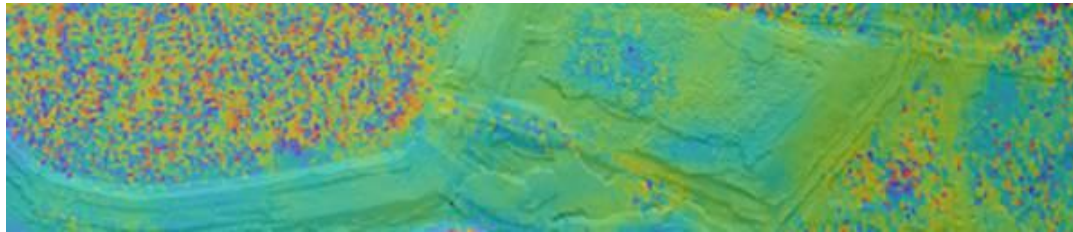


Figure 19 – An area of low coherence (top left) and medium/high coherence (centre) across an example site.

In areas of moderate coherence, filtering can be applied to increase the signal-to-noise ratio. For larger data stacks, this can take into account the temporal characteristics of the radar response to perform adaptive filtering, preserving smaller features and borders between different surface types.

Where coherence is very poor it is possible to deploy artificial radar reflectors, which act as coherent measurement points. The most common artificial reflectors are known as corner reflectors. When deployed correctly, these artificial points can provide coherent pixels between SAR images allowing for InSAR measurements to be taken and provided.

### 9.2.3 Atmosphere

SAR data can be acquired night or day and in all weather conditions, but atmospheric conditions can adversely affect InSAR results. Levels of water vapour in the atmosphere change over time and space, and this can cause variations in the atmospheric refractivity. Differences in refractivity between the two SAR image dates can result in the presence of atmospheric artefacts in interferograms.

### 9.2.4 Stable Reference Area

InSAR processing is undertaken relative to a reference area that is assumed to be stable. Each reference area is chosen based on a number of criteria that indicate it should provide a robust reference point for the dataset, and these therefore vary between the datasets. All measurements within the InSAR results are relative to the chosen 'stable' area. The location of each reference point is given within the results section.

### 9.2.5 Line-of-sight (LOS)

InSAR measures displacement towards or away from the satellite, along an inclined LOS. This inclined LOS means that InSAR does not measure the 3D (up, north and east) motion, but rather the combination expressed in the LOS. This is demonstrated in Figure 20.

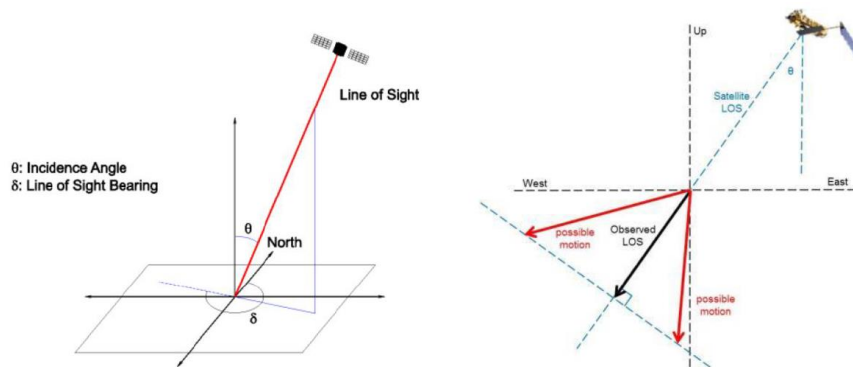


Figure 20 – Descending viewing geometry



This slanted geometry can also affect the pixel spacing and visibility of areas that slope towards or away from the LOS. Figure 21 shows how sloped topography that faces the LOS will be represented by fewer pixels in the radar image compared to the real-world length of the slope, and conversely slopes that face away from the LOS will be represented by more pixels in the radar image.

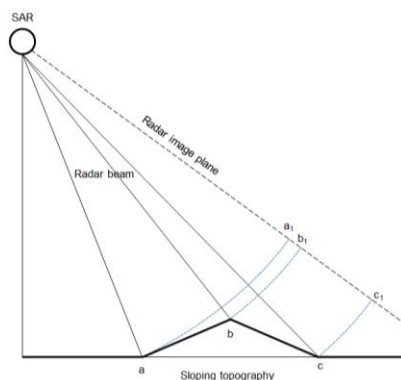


Figure 21 – A diagram showing how sloped surfaces create variations in pixel spacing.

Shadow occurs when the SAR satellite cannot see a slope due to steep slope angles, these appear dark in the radar imagery. Layover occurs when the SAR signal hits the top of a steep slope before it images the face of the slope, this leads to a confused bright signal, as can be seen in Figure 22, where it is not possible to generate an image. One way of mitigating this issue is to use a satellite looking in the opposing direction, so that areas of shadow in one line-of-sight should be visible in the other. In these results western facing slopes can lack measurement coverage due to this issue.

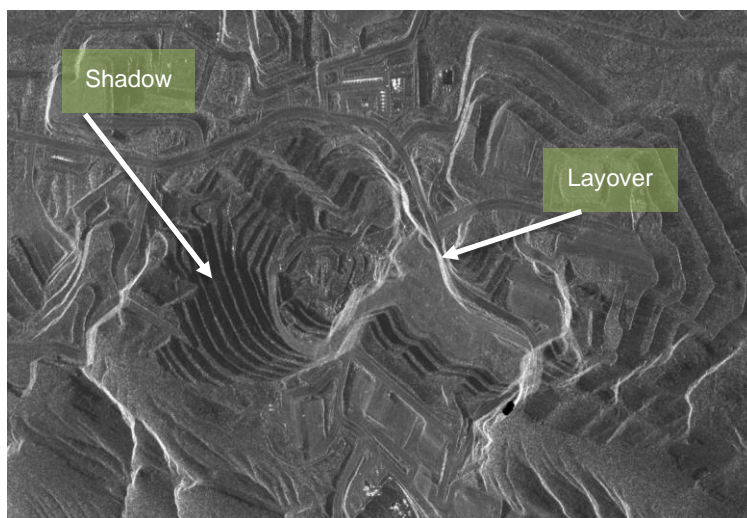


Figure 22 – An example of radar layover and shadow.